THE UNIVERSITY
of EDINBURGH

Investigating RNA silencing-mediated epigenetic modifications in virus-infected plants

Yue Fei

Doctor of Philosophy

The University of Edinburgh

2018

Table of contents

Declaration

The work presented in this thesis is the original work of the author. This thesis has been composed by the author and has not been submitted in whole or in part for any other degree.

Yue Fei

Acknowledgements

First and foremost, I would like to thank my PhD supervisor Dr Attila Molnar for his insightful advice and extensive lab training during my PhD. Attila always encourages me to think and act independently. He has been very supportive and offered me a research assistant job to finance my thesis-writing year. Also, I would like to thank my thesis committee Dr Elizabeth Bayne and Prof Andrew Hudson for their continued support and input.

My special thanks to all the present and past members of Molnar lab: Dr Douglas Pyott, Dr Debbie Frederickson Matika, Aron Ferenczi, Muriel Monteiro and Lindsay Williams. Also to Prof Karl Oparka and his lab member Dr Kirsten Knox, Dr Danaé Paultre, Karen Bell who share lab space with us. Everyone has been a pleasure to work with and made the lab a fun place to be.

I want to express my gratitude to the Chinese Scholarship Council and the University of Edinburgh for providing me the great opportunity to study in UK and funding my PhD project.

Finally, I am extremely grateful to my family for their constant support. My parents gave me the best condition they could provide to support me during my education since my childhood. My greatest thanks to Tianliang, who constantly supported me during all these years.

Abstract

Plant viruses can cause many plant diseases, which result in substantial damage to crop production. To overcome viral infections, plants evolved RNA silencing which can recognise viral RNAs during their replications and slice them into small RNA (sRNA) using antiviral nucleases called DICER or Dicer-like (DCL). The resulting virus-derived small interfering RNA (vsiRNA, 21-24 nucleotides) then guides effector nucleases, namely ARGONAUTE (AGO), to cleave viral RNAs in the cytoplasm in a nucleotide-specific manner. However, the activity of vsiRNA is not restricted to the control of viral RNA accumulation. Virus-derived sRNAs can regulate host gene expression if host mRNAs share sequence complementarity with vsiRNAs. Interestingly, vsiRNAs are also able to target and methylate homologous DNA sequences in the nucleus indicating that vsiRNAs have potential to regulate endogenous genes at transcriptional level by modifying the epigenetic status of gene promoter sequences. This mechanism is referred to as transcriptional gene silencing (TGS). Thus, RNA silencing opens up new strategies to stably and heritably alter gene expression in plants. However, the mechanisms and efficacy of plant virus-induced TGS are largely unknown.

The aim of my PhD was to investigate the molecular and environmental factors that are involved in virus-induced epigenetic modifications in the infected plants and in their progeny. First, I examined the required sequence complementary between sRNAs and their nuclear target sequence. I demonstrated for the first time that nuclear-imported vsiRNAs can induce RNA-directed DNA methylation (RdDM) and subsequently heritable virus-induced transcriptional gene silencing (ViTGS) even when they do not share 100% nucleotide sequence complementarity with the target DNA. This finding reveals a more dynamic interaction between viral RNAs and the host epigenome than previously thought. Secondly, I explored how environmental stimuli such as light and temperature can affect the efficacy of ViTGS. I found that ViTGS is greatly inhibited at high temperature. Using RNA-seq, I established that

inefficient ViTGS at high temperature is due to the limited production of secondary sRNAs that may limit the initiation, amplification and spreading of virus-induced DNA methylation to neighbouring cells and down generations. Lastly, I studied the link between the viral suppressors of RNA silencing (VSRs): viral proteins that can interfere with plant RNA silencing and ViTGS. I established that VSRs of certain viruses can impair TGS in infected tissues, suggesting that viruses may alter the epigenome and consequently plant gene expression in the infected plants and their progeny.

Collectively, my work reveals how viruses can re-program the epigenome of infected plants, and deepens our knowledge of how we can harness pathogens to modify the epigenome for plant breeding.

Abbreviations

AGO – ARGONAUTE

BPMV – bean pod mottle virus

BYV – beet yellows virus

CaLCuV – cabbage leaf curl virus

CaMV – Cauliflower Mosaic Virus

CMT3 – CHROMOMETHYLASE 3

CMV – Cucumber Mosaic Virus

CP – coat protein

CymRSV – Cymbidium Ringspot Virus

DCL – DICER-LIKE

DMRs – differential methylation regions

dpi – days pots inoculation

DRM2 – DOMAINS REARRANGED METHYLTRANSFERASE 2

dsRNA – double-stranded RNA

GFP – GREEN FLUORESCENT PROTEIN

HA – hemagglutinin

HcPro – helper component protease

hcsiRNA – heterochromatic siRNA

MET 1 – DNA METHYLTRANSFERASE 1

miRNA – microRNA

NBS-LRR – nucleotide-binding site leucine-rich repeat

nt – nucleotide

ORF – open reading frame

PCV – peanut clump virus

phasiRNA – phased short interfering RNA

Pol II – RNA polymerase II

PPR – Pentatricopeptide Repeat

PTGS – post-transcriptional gene silencing

PVX – Potato Virus X

PVY – Potato Virus Y

RdDM – RNA-directed DNA methylation

RDR – RNA dependent RNA polymerase

RISC – RNA induced silencing complex

RNAi – RNA interference

SA – Salicylic acid

SGS3 – SUPPRESSOR OF GENE SILENCING3

siRNA – short interfering RNA

SNS – single nucleotide substitutions

sRNA – small RNA

ssRNA – single-stranded RNA

tasiRNA – trans-acting short interfering RNA

TBSV – Tomato bushy stunt virus

TCV – Turnip Crinkle Virus

TE – transposable element

TGBp1 – TRIPLE GENE BOX PROTEIN1

TGS – transcriptional gene silencing

TNA – Total nucleic acid

TRV – Tobacco rattle virus

TVBMV – tobacco vein banding mosaic virus

TYLCV – Tomato yellow leaf curl virus

TYMV – turnip yellow mosaic virus

UTR – un-translated region

UV – ultraviolet

VIGS – virus-induced gene silencing

ViPTGS – virus-induced post-transcriptional gene silencing

ViTGS – virus-induced transcriptional gene silencing

vsiRNA – virus-derived siRNA

VSR – viral suppressors of RNA silencing

Chapter 1: General introduction

1.1 General features of RNA silencing

RNA silencing is an evolutionarily conserved mechanism of genetic regulation in eukaryotes, which plays a fundamental role in plant development, defence responses and epigenetic regulation (Baulcombe, 2004). The common feature of RNA silencing pathways involves the cleavage of a double stranded RNA (dsRNA) into short 21-24 nucleotide RNAs (sRNA) by an RNase III-like nuclease called Dicer or Dicer-like (DCL) (Bernstein *et al.*, 2001). These sRNA molecules are incorporated into ARGONAUTE (AGO) proteins, along with other factors, to form an RNA-induced silencing complex (RISC) and target homologous sequences through Watson-Crick base pairing. A subset of RNA silencing pathways additionally utilise RNA-dependent RNA polymerases (RDRs) to amplify the sRNA silencing signals (Voinnet, 2008). RNA silencing could lead to post-transcriptional gene silencing (PTGS) and transcriptional gene silencing (TGS). The former involves cleavage or translational inhibition of complementary RNA transcripts in the cytoplasm, while the latter is associated with RNA-directed DNA methylation (RdDM) of the target sequence in the nucleus (Matzke & Mosher, 2014). Broadly, sRNA can be divided into microRNA (miRNAs) and short-interfering RNA (siRNAs). The major distinction between these two classes of sRNA is that they are derived from different precursors. miRNAs derive from single-stranded RNA (ssRNA) precursors that fold into an imperfectly matching hairpin-like structure. By contrast, siRNAs derive from perfectly matching dsRNA precursors formed by the intermolecular hybridization of two complementary RNA strands (Axtell, 2013).

In plants, genes for the core components of RNA silencing are encoded by multigene families with conserved clades, and they play distinct roles in diverse RNA silencing pathways to control plant development, abiotic stress signalling and defence against

invading nucleic acids such as viruses or transposons (Voinnet, 2001, Baulcombe, 2004, Borsani *et al.*, 2005, Aravin *et al.*, 2007). *Arabidopsis* encodes four DCLs, six RDRs, and ten AGOs, which functionally combine in specific ways to create distinct but partially overlapping pathways commonly triggered by dsRNA. Depending on whether the dsRNA trigger derives from the host genome or outside the host genome, RNA silencing can be divided into two classes: endogenous and exogenous RNA silencing **(Figure 1.1 and Figure 1.4**).

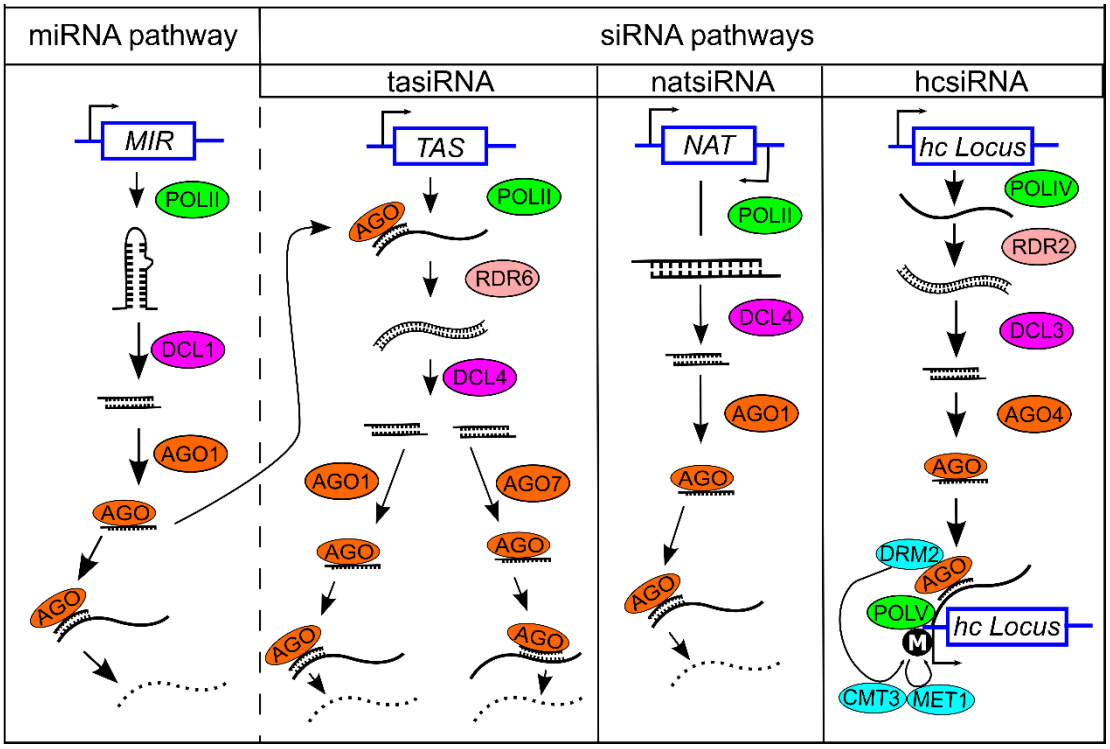

Figure 1.1 Summary of RNA silencing pathways initiated from endogenous loci in plants (Pyott & Molnar, 2015). DNA/RNA are represented by blue/black lines respectively, and white M indicates cytosine methylation. Dashed lines indicate sRNA generation by dsRNA cleavage, dotted lines represent RNA degradation.

1.2 Endogenous RNA silencing

1.2.1 micro RNA pathway

Plant miRNAs, which are typically 20-22 nucleotides in length, are *MIR* genes transcribed by RNA polymerase II (Pol II) into long noncoding transcripts **(Figure 1.1)**. These single-stranded long transcripts fold into hairpin-like structures, which can be recognised and processed predominantly by DCL1 to generate the mature miRNA/miRNA* duplex (Voinnet, 2009). The miRNA (guide strand) is loaded on the AGO1 and the miRNA* (passenger strand) is typically degraded. Once loaded, the RISC is guided by sequence complementarity to a target mRNA, leading to target cleavage and degradation or to repression of its translation (Brodersen *et al.*, 2008).

Plant miRNAs have perfect or near-perfect complementary to their targets, which tolerate up to five mismatches. High complementarity at 5'and central region of the miRNA is critical for plant miRNA/target pairing and slicing (Mallory *et al.*, 2004, Brodersen & Voinnet, 2009). Plant miRNA targeting normally leads to transcript cleavage and is predominantly found in the coding region. By contrast, base-pairing requirements of animal miRNAs are more tolerant: they solely depend on "seed" pairing (the first 2 to 7 nucleotides of the 5' end of the miRNA) (Bartel, 2009). Most animal miRNA targeting in 3' untranslated regions (UTRs) leads to translational inhibition and only rarely slicing (Brodersen & Voinnet, 2009).

Most plant miRNAs are 21 nt long and are usually associated with PTGS. However, a subtype of 23-25 nt long miRNAs in both *Arabidopsis* and rice processed by DCL3 can enter into the heterochromatic siRNA effector pathway and direct chromatin modifications at their target genes (heterochromatic siRNAs are discussed in detail in the heterochromatic siRNA section below) (Vazquez *et al.*, 2008, Chellappan *et al.*, 2010, Wu *et al.*, 2010). miRNA directed DNA methylation can occur in *cis* and *trans*, and can spread from its target site to repress adjacent regulatory features and affect

gene expression (Khraiwesh *et al.*, 2010). Plant miRNA was initially identified as a result of its essential roles in development (Reinhart *et al.*, 2002, Vaucheret *et al.*, 2004). Many further studies established that miRNAs also regulate other biological functions including hormonal control, immune responses, and stresses adaptation (Sunkar *et al.*, 2007, Pedersen & David, 2008)

1.2.2 Secondary siRNA pathway

In plants, some miRNAs can trigger the production of secondary siRNAs, which in turn can silence other genes *in trans*. Depending on their precursor mRNAs, secondary siRNAs have been classified into different subclasses, such as *trans*-acting siRNAs (tasiRNAs) and phased siRNAs (phasiRNAs) (Axtell, 2013) **(Figure 1.1)**.

The biogenesis of tasiRNAs involves Pol II transcription of long noncoding tasiRNA precursors from *TAS* loci. After a 22 nt miRNA-guided AGO1 transcript cleavage, the cleaved target transcripts are then stabilized by SUPPRESSOR OF GENE SILENCING3 (SGS3) and converted into dsRNA by RDR6 (Peragine *et al.*, 2004, Vazquez *et al.*, 2004, Allen *et al.*, 2005, Chen *et al.*, 2010, Cuperus *et al.*, 2010). The resulting dsRNA products are then processed by various DCLs into 21-22 nt tasiRNAs and loaded onto AGO1 or AGO7 to induce PTGS of complementary target mRNA in the cytoplasm (Vazquez *et al.*, 2004, Yoshikawa *et al.*, 2005, Howell *et al.*, 2007, Montgomery *et al.*, 2008, Jouannet *et al.*, 2012). In addition, some 21 nt tasiRNAs processed by DCL1 are incorporated into AGO4 or AGO6 to guide *de novo* DNA methylation of *TAS* genes (Wu *et al.*, 2012).

Many of the known tasiRNAs are phased. The term “phased” indicates that the sRNAs are generated precisely in a head-to-tail arrangement, starting from a specific nucleotide. This is due to sequential processing of the dsRNA by DCL4 (Allen *et al.*, 2005, Song *et al.*, 2012, Fei *et al.*, 2013). These precisely phased secondary siRNAs are known as phasiRNAs. Interestingly, phasiRNAs are generated not only from

noncoding *TAS* loci but also from protein-coding transcripts (Chen *et al.*, 2007, Howell *et al.*, 2007). Many studies have identified that phasiRNAs are involved in regulation of numerous protein-coding genes and gene families, including the *NB-LRR*, *MYB*, and *PPR* families (Howell *et al.*, 2007, Zhai *et al.*, 2011, Xia *et al.*, 2012). Specially, NB-LRR-containing disease-resistance genes encode innate immunity receptors, and phasiRNAs produced from NB-LRRs seem to be beneficial for plant-microorganism interactions and plant immunity (Zhai *et al.*, 2011).

The mechanism of miRNA-induced triggering of phasiRNA biogenesis has been studies extensively in recent years. As mentioned above, transcripts that are cleaved by AGO1 in association with 22 nt miRNAs results in biogenesis of tasiRNA from *TAS* loci (Chen *et al.*, 2010, Cuperus *et al.*, 2010). However, recent studies suggested that miRNA duplexes with a single 22 nt strand (either the guide or passenger strand), or a 21 nt miRNA duplex with asymmetric bulges, results in structural changes to AGO1 that recruits RDR6 prior to the expulsion of the miRNA* strand from AGO1 complex and cleavage of the target transcript (Manavella *et al.*, 2012, McHale *et al.*, 2013). Furthermore, the latest study analysed the function of AGO1 slicer activity in tasiRNA biogenesis using *ago1* slicer-deficient mutants. The results suggested that AGO1 cleavage of the *TAS* transcript is important in the phasing of tasiRNAs, but not for recruitment of SGS3/RDR6 and production of secondary siRNAs derived from the *TAS* transcript (Arribas-Hernández *et al.*, 2016).

Secondary siRNAs are relatively rare in wild-type *Arabidopsis*, which has only four families of *TA*S genes comprising eight loci (Fei *et al.*, 2013). This is probably due to the structure of the *Arabidopsis* genome, which is unusually small and nearly devoid of functional transposable elements. By contrast, other plant genomes, such as those of rice and maize, contain thousands of tasiRNA- and phasiRNA- generating loci (Fei *et al.*, 2013). The recent studies of sRNAs in non-*Arabidopsis* species have greatly increased the knowledge of novel sRNAs and novel functions for existing sRNAs (Xia *et al.*, 2012, Zhai *et al.*, 2015).

1.2.3 Heterochromatic siRNA pathway

Heterochromatic siRNAs (hcsiRNAs) are derived from transposable elements (TEs) and pericentromeric repeats **(Figure 1.1)**. Most of hcsiRNAs are 24 nt in length. In numerous flowering plant species, 24-nt sRNAs are the most abundant sRNAs (Axtell, 2013). The function of hcsiRNAs is to ensure genome integrity, by maintenance of the DNA methylation status of transposable elements through RdDM (Matzke & Mosher, 2014).

The current model for the biogenesis of hcsiRNA begins with transcription of heterochromatic loci by plant-specific RNA polymerases Pol IV, followed by dsRNA synthesis via RDR2 and processing by DCL3 (Law & Jacobsen, 2010, Matzke & Mosher, 2014). The resulting siRNA duplexes are exported to the cytoplasm and incorporated into AGO4-clade AGOs forming the complexes. The AGO4-bound heterochromatic siRNAs are imported back to the nucleus to target nascent transcripts transcribed by Pol V. The DNA methyltransferase DOMAINS REARRANGED METHYLTRANSFERASE 2 (DRM2) is recruited to establish *de novo* DNA methylation at cytosine in all sequence contexts (CG, CHG and CHH, where H is A, C, or T) (Matzke & Mosher, 2014). This is known as the canonical RdDM pathway **(Figure 1.2)**. DNA methylation at symmetrical CG and CHG nucleotide groups is maintained during subsequent rounds of DNA replication through the action of DNA METHYLTRANSFERASE 1 (MET1) and CHROMOMETHYLASE 3 (CMT3), respectively.

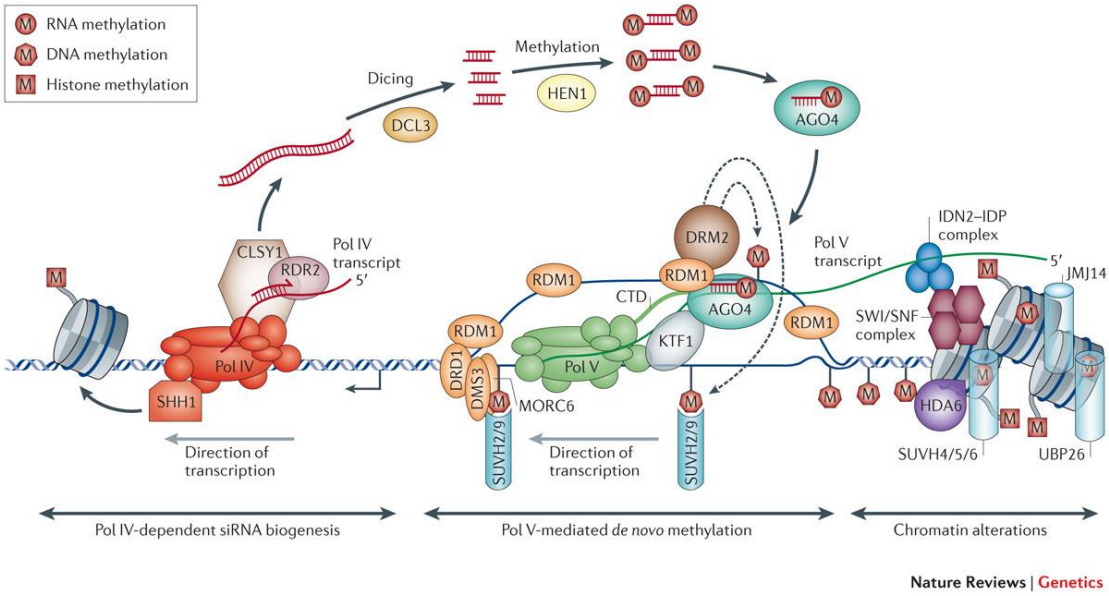

Figure 1.2 Canonical RdDM pathway. A transcription fork model for RdDM is shown (Matzke & Mosher, 2014). In Pol IV-dependent siRNA biogenesis (left panel), Pol IV transcribes an ssRNA that is copied into a dsRNA by RDR2. The dsRNA is processed by DCL3 into 24-nt siRNAs that are methylated by HEN1 and incorporated into AGO4. In Pol V-mediated methylation (middle panel), Pol V transcribes a scaffold RNA that base-pairs with AGO4-bound siRNAs. AGO4 is recruited through interactions with the AGO hook regions in the largest subunit of Pol V and with KTF1. RDM1 links AGO4 and DRM2, which catalyses *de nove* methylation of DNA. Pol V recruitment is potentially aided by SUVH2 or SUVH9, both of which bind to methylated DNA. Nucleosome positioning (right panel) is adjusted by the SWI/SNF complex, which interacts with the IDN2–IDP complex that binds to Pol V scaffold RNAs.

Besides the canonical RdDM pathway (Pol IV-RDR2-DCL3), several additional sRNA pathways can direct RdDM and are referred to as non-canonical RdDM mechanism (Cuerda-Gil & Slotkin, 2016) **(Figure 1.3)**. Many of the non-canonical RdDM mechanisms start with Pol II transcription and mRNA substrates, several of these mechanisms have been implicated in the initiation of virus, transgene and TE silencing (Bond & Baulcombe, 2015, Fultz *et al.*, 2015). For instance, in a Pol II-RDR6 pathway, Pol II transcription of transposons followed by RDR6 amplification of the transcripts

into dsRNAs produces 21-22 nt siRNAs that initially induce PTGS of the transposon mRNAs (Pontier *et al.*, 2012, Nuthikattu *et al.*, 2013). In addition, these transposon-derived siRNAs can also interact with AGO4 or AGO6 to initiate the *de novo* methylation of the transposon (Pontier *et al.*, 2012, Nuthikattu *et al.*, 2013, McCue *et al.*, 2015). This subsequently feeds into canonical RdDM pathway to maintain and reinforce the silencing of the transposons (Nuthikattu *et al.*, 2013). Furthermore, when the RDR6-dependent dsRNAs reach saturation for DCL2 and DCL4, they become accessible for DCL3 to generate 24 nt hcsiRNAs. Then, the 24 nt hcsiRNAs trigger canonical RdDM to silence transposons (Marí-Ordóñez *et al.*, 2013). Moreover, recent publications have identified a new class of hcsiRNAs in *Arabidopsis* that are generated independent of DCLs and are involved in DNA methylation (D. L. Yang *et al.*, 2016, Ye *et al.*, 2016). These Dicer-independent siRNAs are incorporated into the AGO4 protein, and subsequently trimmed down at their 3' end to produce a group of 20-60 nt ladder siRNAs by exosome-core complex exonucleases. The authors suggest that this pathway functions to initiate TE silencing (Ye *et al.*, 2016).

The 24 nt hcsiRNAs RNAs regulate important epigenetic mechanisms, such as imprinting and paramutation. In plants with larger genomes, hcsiRNAs have essential roles during reproductive transitions such as meiosis, gametogenesis and embryogenesis, and they are probably associated with the more repetitive nature of the genome (Borges & Martienssen, 2015).

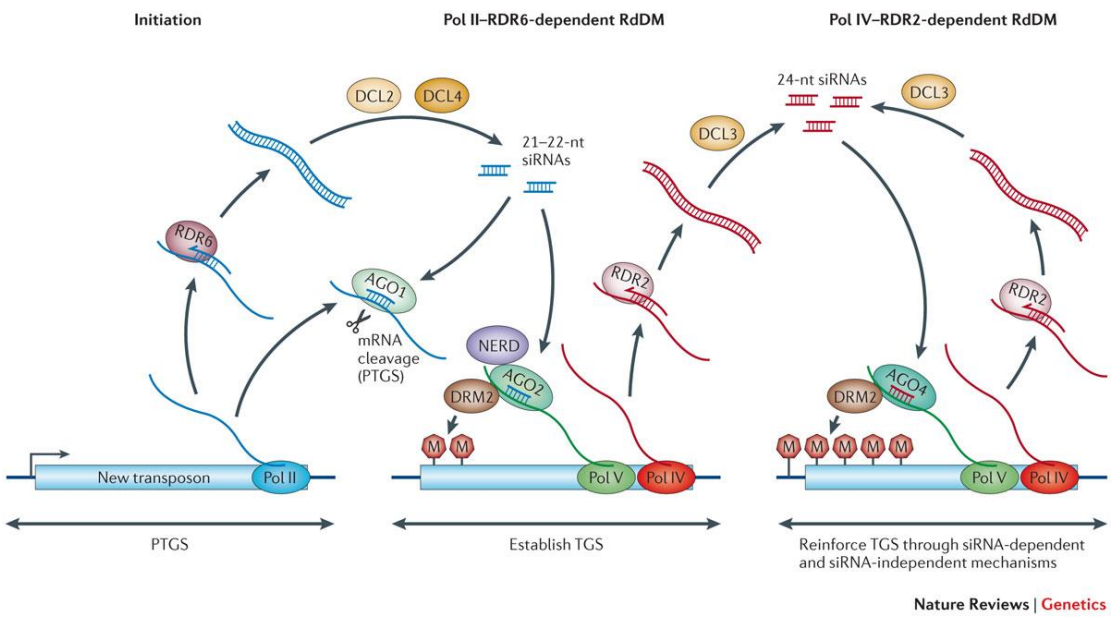

Figure 1.3 Non-canonical Pol II–RDR6-dependent RdDM pathway (Matzke & Mosher, 2014). This pathway provides a means to establish RdDM and eventually ensure stable TGS of a newly acquired transposon that is originally a target of PTGS. In PTGS (left panel), a newly inserted transposon is initially active and transcribed by Pol II. Some of the transcripts are copied by RDR6 to produce dsRNAs, which are processed by DCL2 and DCL4 into 21–22-nt siRNAs. These siRNAs are loaded onto AGO1 and guide cleavage of transposon transcripts in a typical PTGS pathway. In a deviation from the canonical RdDM pathway (middle panel), some of the 21–22-nt siRNAs can also trigger low levels of DNA methylation in a manner that is dependent on DRM2, Pol V and AGO2, which interacts with NERD through its AGO hook motif. The sparsely methylated DNA recruits Pol IV, which initiates the canonical RdDM pathway by transcribing an ssRNA. The ssRNA is copied by RDR2 into a dsRNA that is processed by DCL3 into 24-nt siRNAs. Following incorporation into AGO4 (right panel), the 24-nt siRNAs base-pair with Pol V scaffold transcripts, which results in DRM2 recruitment and dense methylation. siRNAs are continuously produced from the methylated template by Pol IV pathway components, which reinforces TGS that can be maintained in an siRNA-independent manner by MET1, CMT3 and DDM1.

1.3 Exogenous RNA silencing

1.3.1 Transgene-induced siRNA pathway

In transgene-induced RNA silencing, the host RNA-dependent RNA polymerase can recognise the 'aberrant' RNA transcribed by the transgene and subsequently copy the ssRNA template into the dsRNA (Baulcombe, 2004) **(Figure 1.4)**. The aberrant RNAs lack features of normal RNAs, and they may be misfolded, lacking 5' cap or 3' poly-adenosine tail (Herr *et al.*, 2006). The dsRNA is processed by DCL4 or DCL2 into 21 nt and 22 nt siRNAs (Fusaro *et al.*, 2006, Parent *et al.*, 2015). Then, the siRNAs are loaded into different AGO proteins, mostly AGO1 to regulate expression of the transgenic RNA through PTGS (Mallory & Vaucheret, 2009). Moreover, the dsRNA can be processed into 24 nt siRNAs, which can mediate transcriptional gene silencing of transgenes in *Arabidopsis* (Chan, 2004).

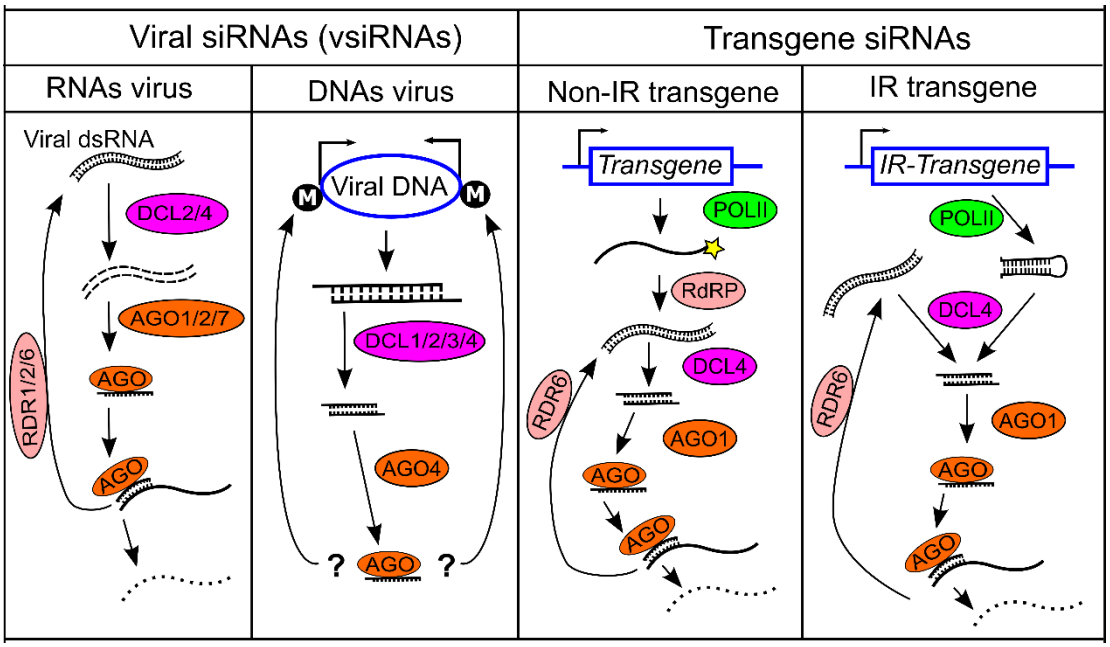

Figure 1.4 Summary of RNA silencing pathways initiated by exogenous DNA or RNA (Pyott & Molnar, 2015). DNA/RNA are represented by blue/black lines respectively, yellow star represents structural aberrancy, and white M indicates cytosine methylation. Dashed lines indicate sRNA generation by dsRNA cleavage, dotted lines represent RNA degradation.

Both DCL2 and DCL4 have been studied intensively and display some functional redundancy in virus and transgene silencing (Dunoyer *et al.*, 2005, Deleris *et al.*, 2006, Mlotshwa *et al.*, 2008). However, several studies have suggested that DCL4 and DCL2 possess unique function in siRNA biogenesis and transitivity in PTGS. DCL4 outcompetes DCL2, resulting in a much higher abundance of 21 nt siRNAs than 22 nt siRNA being produced from dsRNA (Deleris *et al.*, 2006, Mlotshwa *et al.*, 2008). However, DCL2 plays crucial role in transitivity and secondary siRNA production (Parent *et al.*, 2015, Taochy *et al.*, 2017, Chen *et al.*, 2018). DCL2-dependent 22 nt siRNAs efficiently recruit RDR6 and facilitate biogenesis of secondary siRNAs (Parent *et al.*, 2015, Taochy *et al.*, 2017). Recent studies in *Arabidopsis* have shown that *dcl2* mutations suppresses the accumulation of secondary siRNAs, whereas *dcl4* mutations promote DCL2 activity and transitive biogenesis of secondary siRNAs (Parent *et al.*, 2015, Taochy *et al.*, 2017). Most recently, grafting experiments in both *Arabidopsis* and *Nicotiana benthamiana* have shown that DCL2 was required for systemic spreading of PTGS (Taochy *et al.*, 2017, Chen *et al.*, 2018).

Based on the mechanism of transgene-induced RNA silencing, transgenes can be engineered to trigger silencing with high efficiency by introducing inverted repeats (IR) into transgenic sequences. In the case of IR transgenes, dsRNA is automatically formed from a single transcript folding back on itself making silencing highly efficient because the dsRNA molecule is directly processed by DCL2 and DCL4 into siRNA molecules (Waterhouse & Helliwell, 2003). Those siRNAs can lead to TGS and PTGS of target gene. This is known as RNA interference (RNAi). RNAi provides a powerful tool for functional genomics due to its targeted nature, ability to silence genes to the equivalent of null mutants and applicability to any transformable species.

1.3.2 virus-derived siRNA pathway

The other class of exogenous sRNAs is virus-derived siRNAs (vsiRNAs) **(Figure 1.4)**. vsiRNAs are one of the earliest discovered sRNAs and are responsible for RNA silencing-mediated antiviral immunity (Hamilton & Baulcombe, 1999). The biogenesis of vsiRNAs is analogous to that of endogenous sRNAs, which require diverse essential components including DCLs, RDRs, and AGOs.

Antiviral RNA silencing can be triggered by dsRNA derived from viruses. For RNA viruses, the dsRNAs are generated from the secondary structures in viral transcripts and double stranded replication intermediates (RIs) encoded by viral RNA-dependent RNA polymerases (Molnar *et al.*, 2005, Baulcombe & Dean, 2014). The production of vsiRNAs (21-22 nt) from plant RNA viruses is mainly catalysed by DCL4 and DCL2 (Deleris *et al.*, 2006). The vsiRNAs are then incorporated into AGO1 and AGO2 to target complementary viral RNA through PTGS in cytoplasm. Some cleavage products serve as templates for host RDR1 or RDR6 to synthesize abundant *de novo* dsRNAs that are processed by DCLs into secondary siRNAs that enhance antiviral RNA silencing (Garcia-Ruiz *et al.*, 2010, Wang *et al.*, 2010).

In the case of plant DNA viruses, viruses accumulate in the nuclei of infected plant cells and use host Pol II to make transcripts. The overlapping bidirectional read-through transcripts from DNA virus genome as well as the transcript secondary structures can form the dsRNAs (Pooggin, 2013). Unlike RNA viruses, all four DCLs appear to work in concert to generate 21-nt (DCL4 and DCL1), 22-nt (DCL2) and 24-nt (DCL3) vsiRNAs in DNA virus infected tissues (Blevins *et al.*, 2006, Aregger *et al.*, 2012). These vsiRNA are associated with AGO proteins to form RISC to mediate TGS of viral DNA by DNA methylation (Wassenegger *et al.*, 1994, Raja *et al.*, 2010).

An important feature of vsiRNAs is that they are able to move through plasmodesmata over short distances (cell-to-cell movement) and through phloem (systemic movement)

(Dunoyer *et al.*, 2013). This allows vsiRNAs to reach systemic tissue with, and even before, the invading virus which primes antiviral silencing in cells. Consequently, replication or movement of the pathogen into those cells is delayed or precluded.

1.4 Viral counter-defence of RNA Silencing

RNA silencing is the major antiviral defence in plant. To counteract this antiviral defence, most plant viruses have evolved silencing suppressor proteins targeting different steps of the antiviral silencing pathway. Broadly, the action of viral suppressors of RNA silencing (VSR) can be classified into three categories: (1) binding to long dsRNA resulting in inhibition of Dicer processing; (2) binding and sequestration of siRNA duplexes preventing RISC assembly; and (3) direct targeting of effectors or processing factors leading to their inhibition or destabilization.

Targeting long dsRNA is one of the strategies used by VSRs to block the silencing initiation step of antiviral silencing. Some viral proteins have been shown to bind the dsRNA *in vitro* in a size-independent manner and inhibit the processing of the dsRNA to siRNAs, such as P14 of *Pothos latent aureusvirus*, 2b of *Cucumber mosaic virus* (CMV) (Merai *et al.*, 2005, 2006, Goto *et al.*, 2007). However, the inhibition of viral RNA recognition and the subsequent dicing by plant Dicer effectors is not a frequent strategy of known VSRs.

The most common strategy of VSRs inhibiting RNA silencing is binding and sequestration of siRNA duplexes, which prevents the RISC assembly (Lakatos *et al.*, 2006). The best-known example of this mode of action was illustrated by P19 of tombusviruses. Crystallographic studies have shown that P19 forms a head-to-tail homodimer, which acts like a molecular calliper, measuring the length of siRNA duplexes and selectively binding to 21-bp siRNA duplexes with high affinity (Vargason *et al.*, 2003, Ye *et al.*, 2003). P19 can sequester both siRNAs and miRNAs, preventing their incorporation into AGO1-containing RISCs (Schott *et al.*, 2012).

Based on the P19 precedent, several VSRs were subsequently shown to suppress RNA silencing through siRNA duplexes binding and preventing siRNA loading into AGO1. These VSRs include *Potyviral* HcPro, *Turnip crinkle virus* (TCV) P38, *Beet yellows virus* (BYV) P21 and *Peanut clump virus* (PCV) P15 (Lakatos *et al.*, 2006, Merai *et al.*, 2006, Schott *et al.*, 2012, Garcia-Ruiz *et al.*, 2015). In a recent study, co-immunoprecipitation and sRNA profiling revealed that HcPro can associate with vsiRNAs during TuMV infection, suggesting that HcPro could suppress antiviral silencing by sequestering vsiRNAs and preventing their loading into AGO1 (Garcia-Ruiz *et al.*, 2015).

Interaction with the effectors of the antiviral silencing pathway is the third mode of VSR action. AGO1 inactivation is regarded as a general mechanism of RNA silencing suppression. TCV P38 protein and *Sweet potato mild mottle virus* P1 protein interact directly with AGO1 via a glycine/tryptophan hook motif (Azevedo *et al.*, 2010, Giner *et al.*, 2010). Moreover, the CMV 2b protein inhibits AGO1 activity through a physical interaction, which leads to inhibition of AGO1 slicing activity in a RISC *in vitro* reconstituted assay (Zhang *et al.*, 2006). Furthermore, a few studies have identified that VSRs can also directly target other components of the antiviral silencing pathway, leading to their inhibition or stabilization. For instance, the VSR P6 of *Cauliflower mosaic virus* (CaMV) has been shown to interact physically with the dsRNA-binding protein DRB4, a cofactor required for DCL-4 dependent vsiRNA processing (Haas *et al.*, 2008). VSRs can also suppress the RDR capabilities to block the secondary sRNA amplifications. The V2 protein of the DNA virus *Tomato yellow leaf curl virus* (TYLCV) directly interacts with the RDR6 cofactor SGS3 to suppress silencing amplification and virus resistance (Glick *et al.*, 2008). Similarly, Potato virus X (PVX) TRIPLE GENE BOX PROTEIN1 (TGBp1), also known as P25, was also shown to inhibit RDR6/SGS3-dependent dsRNA synthesis *in planta* (Okano *et al.*, 2014).

VSRs regulate the multiple layers of the complex defence, counter-defence and

counter-counter-defence arms race between host and pathogen. They are recognised as the major contributors to the development of viral symptoms. It is suggested that VSRs are not only blocking RNA silencing but also serve as central hub regulators to dynamic interconnections between antiviral silencing, protein-based immunity, hormone signalling, RNA metabolism and subcellular organization (Pumplin & Voinnet, 2013).

1.5 Virus-induced gene silencing

Based on the plant antiviral silencing mechanism, virus-induced gene silencing (VIGS) has been developed as a method for silencing endogenous target genes in plants (Ruiz *et al.*, 1998). To silence a gene of interest, a fragment of the host gene sequence is cloned into a modified virus vector and is infected into the plants. This recombinant virus can trigger the plant antiviral RNA silencing pathway, resulting in the production of vsiRNAs. The processed vsiRNAs can mediate PTGS by targeting the corresponding homologous mRNA in the cytoplasm. Apart from PTGS, vsiRNAs can also cause TGS by directing the RdDM machinery to induce methylation of the corresponding DNA sequence in the nucleus. Methylation of cytosine residues in the promoter of the gene can interfere with transcription, resulting in transcriptional gene silencing of the target gene. Intriguingly, this virus-induced TGS is heritable in plants. It has been shown that a recombinant CMV-based vector carrying endogenous promoter sequences could induce heritable gene silencing in petunia and tomato plants (Kanazawa et al. 2011). This observation suggests that vsiRNAs have the potential to regulate endogenous genes at a transcriptional level by modifying the epigenetic status of their promoter sequences. Moreover, virus infection can initiate novel and persistent epigenetic changes that may influence pathogenesis, stress-responses and development.

VIGS is one of the most widely used tools for gene function studies in plants (Burch-Smith *et al.*, 2004). VIGS can easily and rapidly silence genes in a broad range of plant species (Zhang *et al.*, 2010, Senthil-Kumar & Mysore, 2011, Yuan *et al.*, 2011, Hajeri

et al., 2014, Liu *et al.*, 2016). Moreover, it can be used to study the function of genes where mutations are embryo-lethal or result in a severely deformed plant (Senthil-Kumar *et al.*, 2008). VIGS can also be used to silence genes with multiple copies or multiple family members. With all these advantages, VIGS has been used to perform both forward and reverse genetics to identify plant genes involved in various plant development processes.

Many plant RNA and DNA viruses have been modified as VIGS vectors for expressing foreign proteins and to induce sequence-specific PTGS for studying gene functions. There are 25 commonly used VIGS vectors that have gene silencing ability in plants **(Table 1.1)**. Among these, four vectors have already been implicated in TGS (Potato virus X, Tobacco rattle virus, Cucumber mosaic virus and Apple latent spherical virus), whereas very little is known about the pervasiveness and efficiency of virus-induced TGS (ViTGS).

Table 1.1 List of VIGS vectors

Genus	VIGS vectors
Bromovirus	Brome mosaic virus (BMV)
Carlavirus	Poplar mosaic virus (PopMV)
Cheravirus	Apple latent spherical virus (ALSV)
Citrivirus	Citrus leaf blotch virus (CLBV)
Closterovirus	Citrus tristeza virus (CTV), Grapevine leafroll-associated virus-2 (GLRaV-2)
Comovirus	Bean pod mottle virus (BPMV), Cowpea mosaic virus (CPMV)
Cucumovirus	Cucumber mosaic virus (CMV)
Hordeivirus	Barley stripe mosaic virus (BSMV)
Potexvirus	Alternanthera mosaic virus (AltMV), Bamboo mosaic virus (BaMV), Pepino mosaic virus (PepMV), Potato virus X (PVX), Plantago asiatica mosaic virus, Foxtail mosaic virus (FoMV)
Potyvirus	Pea seed-borne mosaic virus (PSbMV), Plum pox virus (PPV), Potato virus A (PVA)
Tobamovirus	Tobacco mosaic virus (TMV), Sunn-hemp mosaic virus (SHMV)
Tobravirus	Pea early browning virus (PEBV), Tobacco rattle virus (TRV)
Tombusvirus	Tomato bushy stunt virus (TBSV)
Tymovirus	Turnip yellow mosaic virus (TYMV)

Chapter 2: Materials and methods

2.1 Plant material and growth conditions

Nicotiana benthamiana plants line 16c (Ruiz *et al.*, 1998) harbouring the GFP transgene under the control of the CaMV 35S promoter were grown in Levington F2+S professional growth compost in a controlled growth chamber at 22℃ with 16-h light and 8-h dark periods.

In chapter 4, *N. benthamiana* 16c plants were grown at 22℃ for three weeks. After virus inoculation, plants were transferred to SANYO/Panasonic growth chambers at constant temperature of 15℃, 22℃, and 29℃ under 16/8 h light/dark cycles. Light intensity levels (high light 150 µmol/$m^{-2}s^{-1}$, medium light 75 µmol/$m^{-2}s^{-1}$, and low light 35 µmol/$m^{-2}s^{-1}$) were adjusted using neutral density light filters (Blacklights Ltd., Neutral density filters #210 and #299).

In chapter 5, seeds of *Arabidopsis thaliana* were imbibed and stratified in 1.5 mL Eppendorf tubes in darkness at 4℃ and then directly planted onto soil. The plants were grown in a controlled growth chamber at 22℃ with 16-h light and 8-h dark periods.

2.2 Cloning and Constructs

2.2.1 Construction of the TRV-based VIGS vectors

20 µM of 120 nt oligonucleotides matching the CaMV 35S promoter (nt -208 to -89) (Otagaki *et al.*, 2011), the GFP5 coding sequence (nt +364 to +483) (Ruiz *et al.*, 1998) and their derivatives harbouring single-nucleotide substitution at regular intervals were mixed with the corresponding reverse complement oligonucleotides (**Table 2.1**) in 1× NEB Buffer 3 (New England Biolabs, NEB) in a 25 µL reaction volume. To anneal the oligonucleotides, the mixtures were incubated at 98℃ for 5 min and then slowly cooled down (-0.3℃/s) to room temperature. 1 µL of dsDNA was phosphorylated with T4 Polynucleotide Kinase (1 U/µL; NEB) in 1× T4 DNA ligase buffer (NEB) and subsequently ligated into the SmaI site of Tobacco Rattle Virus (TRV) vector pTRV2

(Senthil-Kumar & Mysore, 2014) to generate TRV-35S, TRV-35S-1M_A, TRV-35S-1M_B, TRV-35S-2M, TRV-35S-4M, TRV-GFP and TRV-GFP-2M.

2.2.2 Construction of the TBSV-based VIGS vectors

A 120 nt fragment of the 35S promoter (nt -208 to -89) was amplified by RT-PCR using the oligonucleotide primers listed in **Table 2.1**. The PCR products were digested with the XhoI restriction enzyme, and then were cloned in sense and antisense orientations into the Tomato bushy stunt virus (TBSV) vectors (Pignatta *et al.,* 2007) to generate TBSV-35S and TBSV-35S-A. The same procedure was followed to clone a 120 nt coding sequence of the GFP gene (nt +364 to +483) in sense and antisense orientations into the TBSV to generate TBSV-GFP-S and TBSV-GFP-A. To investigate the effect of P19 on TGS and PTGS, the same inducer sequences were cloned into the silencing suppressor mutant version of TBSV (delete P19) to generate TBSV-35S-△P19, TBSV-35S-A-△P19, TBSV-GFP-S-△P19 and TBSV-GFP-A-△P19.

2.2.3 Construction of the TuMV-based VIGS vectors

The CaMV 35S promoter (nt -208 to -89) was cloned into the TuMV vector through NcoI restriction site to create TuMV-35S-S. Two nucleotides (CA) were added at the 5’ of antisense sequence of 35S promoter (nt -206 to -89), and the antisense 35S promoter sequence was ligated into the NcoI site of TuMV vector to generate the TuMV-35S-A.

To test the effect of target regions on TuMV-VIGS, three target regions from GFP coding sequence (nt +1 to +120), (nt +366 to +485) and (nt +671 to +790) were cloned into TuMV, respectively. These 120-nt insertions were cloned in sense and antisense orientations into the TuMV to generate TuMV-5’GFP-S, TuMV-5’GFP-A, TuMV-GFP-S, TuMV-GFP-A, TuMV-3’GFP-S and TuMV-3’GFP-A.

2.2.4 Construction of the pDE vectors

pDE expression vector was modified from pDe-Cas9-△ccd binary vector. First, the BASTA (herbicide phosphinothricin) cassette was deleted from pDe-Cas9-△ccd by

HindIII restriction digestion to create pDe-Cas9-△ccd-△ppt. Then, Cas9 sequence was removed from pDe-Cas9-△ccd-△ppt by AscI restriction digestion.

For generating pDE-silencing inducer constructs, the 120-nt 35S promoter sequence (nt -208 to -89) and the 120-nt GFP coding sequence (nt +364 to +483) were PCR amplified using the oligonucleotide primers listed in **Table 2.1**, and subsequently ligated into the AscI opened vector pDe-Cas9-△ccd-△ppt to create pDE-35S and pDE-GFP, respectively.

For generating pDE-silencing suppressor constructs, each VSR (Chapman *et al.*, 2004) was PCR amplified with HA epitope-tagged and cloned into the pDe-Cas9-△ccd-△ppt vector to create pDE-2b, pDE-P19, pDE-P21 and pDE-HcPro, respectively.

2.3 Bacterial transformations

2.3.1 Transformation of Escherichia coli cells with recombinant DNA

The recombinant DNA was transferred into DH5alpha *E. coli* competent cells using heat shock transformation. *E. coli* competent cells from -80℃ were thawed on ice and 2.5 μL of the recombinant DNA were added into 50 μL competent cells. Mixtures were kept on ice for 30 mins. Heat shock was given at 42℃ for 1 minute. After heat shock, the tube was placed on ice to cool down. 450 μL LB medium was added, and then was incubated in a shaker at 37℃ at 200 rpm for one hour. The cells were divided into 100 μL and 350 μL portions and plated on LB agar with the appropriate antibiotics. The plates were incubated at 37℃ overnight. Colonies were checked the next day by colony PCR.

2.3.2 Transformation of Agrobacterium tumefaciens cells with plasmid vectors by electroporation

50 μL electro-competent *Agrobacterium* cells (strain GV3101:pMP90 + pSOUP) were thawed on ice and 2.5 μL of plasmid DNA was added and mixed carefully. Cells were left to incubate on ice for 5 minutes and transferred into a pre-chilled electroporation cuvette. The cells were transformed with plasmid DNA using cell electroporator (Eppendorf) with volts setting at 1800V. Then 450 μL of liquid YEP medium was added and the mixture was incubated in a shaker at 28℃ and 200 rpm for 2-3 hours.

The cells were divided into 100 μL and 350 μL portions and plated on YEP agar with the appropriate antibiotics. The plates were incubated at 28℃ for 2 days.

2.4 Plant transformation

2.4.1 Stable transformation of Arabidopsis thaliana

Agrobacterium tumefaciens (strain GV3101:pMP90 + pSOUP) cells were transformed with the relevant plasmid by electroporation. The transformed cultures were grown in the 5 mL of YEP liquid medium containing the selective antibiotics at 28℃ in a shaker at 200 rpm overnight. 1 mL of overnight culture was inoculated into 50 mL of YEP medium (in a 250-mL flask) with the appropriate antibiotics and 150 uM acetosyringone. The culture was incubated at 28℃ in a shaker at 200 rpm for 20-24 hours. Cells were pelleted by centrifugation at 5000 rpm for 15 minutes. Pelleted cells were resuspended in an equal volume of infiltration medium (1/2 MS, 5% (w/v) sucrose, 0.02% Silwet L-77, 150 μM acetosyringeone, and 3 mM MES pH5.5). Plant inflorescences were dipped into an *Agrobacterium* suspension for two minutes, then placed into clear plastic bags and shaded for 24 hours. This process was repeated 7 days later. T_1 seeds were collected and sowed on soil. 7 days after germination, seedlings were sprayed with a 120 mg/L solution of BASTA using a hand-held spray bottle. The BASTA spray treatment was repeated at 14 and 21 days after germination. BASTA resistant plants were transplanted into individual pots.

2.4.2 Agrobacterium-mediated transient expression in Nicotiana benthamiana

Agrobacterium cells were grown as described above and resuspended in infiltration medium (10 mM MES pH 5.6, 10 mM $MgCl_2$, and 150 μM acetosyringeone). The OD_{600} was measured for each culture, and cultures were diluted to an OD_{600} ~1.0. Then the cultures were incubated at room temperature for 2 hours. The cells were syringe infiltrated into the abaxial surface of 3 fully expanded leaves of 4-week-old *N. benthamiana* 16c plants.

2.5 Sap collection and rub inoculation

2.5.1 Induction of recombinant viruses into N. benthamiana by agroinfiltration

For TRV infections, separate cultures containing TRV RNA1 and modified TRV RNA2 were mixed in a 1:1 ratio. The culture was then infiltrated into young leaves of wild-type *N. benthamiana* using a 1 mL syringe without a needle. The inoculated plants were placed into a tray and covered with lid, which was removed 2 days after infection. The same procedure was followed to agroinfiltrate *N. benthamiana* with TuMV constructs.

Sap was collected from systemic leaves of infected plants 5 to 12 days post infiltration (dpi). Approximately 0.5 g of leaves were harvested and ground with three volumes of 1 mM sodium phosphate buffer (pH 7.0) in chilled mortar. Then it was transferred to a fresh eppendorf tube and the plant debris was pelleted by centrifugation at maximum speed for 10 minutes. The abaxial leaf surface of 4-week-old *N. benthamiana* 16c plants were dusted with aluminium oxide powder and 10 µL of viral sap was applied by rub inoculations. Three leaves were inoculated on each plant with the corresponding virus sap.

2.5.2 In vitro transcription of TBSV

For generate TBSV sap, all TBSV plasmids were linearized at the 3' end with SmaI and used for *in vitro* transcription. Digested DNA was purified from 1% agarose gels using the QIAquick Gel Purification Kit (Qiagen). The transcription reaction mixture was prepared at room temperature, since DNA may precipitate in the presence of spermidine at 4℃. The reaction mixture was consisted of 10 µL 5× T7 transcription buffer (Promega), 10 mM DTT, 2.5 mM of each rNTP, 5 µg linearized DNA, 50 units RNaseOUT Recombinant Ribonuclease Inhibitor (40 U/µL; Invitrogen), and 50 units T7 RNA Polymerase (20 U/µL; Thermo Scientific) in a total volume of 50 µL. Reactions were incubated at 37℃ for 2 hours. The transcription products were analysed by 1% agarose gel electrophoresis. 2 µL products were mixed with 2× RNA loading dye, denatured by heating at 65℃ for 5 min, then loaded on the gel. 10 µL of

transcription product was used to rub inoculate the abaxial leaf surface of 4-week-old *N. benthamiana* plant dusted with aluminium oxide powder. Three leaves were inoculated on each plant and three plants were inoculated with the corresponding virus transcript. The sap was collected from systemic leaves of the inoculated *N. benthamiana* plants at 9 dpi.

2.6 Imaging of GFP fluorescence

GFP expression was monitored under UV light using a handheld mercury UV lamp (UVP, B-100AP Lamp 100W 365nm). Photographs were taken by a Canon G16 camera. Exposure settings were f/5.6, ranging from 0.5 to 5 seconds, depending on the intensity of GFP fluorescence and distance from the plant.

2.7 Plant DNA/RNA purification

Total nucleic acids (TNA) were purified from plant tissue by phenol/chloroform extraction using a method adapted from (White & Kaper, 1989). Plant tissue was collected in 1.5 mL Eppendorf tubes containing two metal ball-bearings and frozen in liquid nitrogen. Plant tissue was ground in pre-chilled blocks in a Qaigen Tissue Lyzer (Qaigen). 600 µL of Tris-buffered water-saturated phenol (pH 8.0) and 600 µL of TNA extraction buffer (100 mM Glycine, 100 mM NaCl, 2% SDS, 10 mM EDTA, pH 9.5) was added to the powdered plant tissue. The samples were vortexed and then centrifuged at 13, 000 rpm for 10 minutes. The supernatant was transferred to a fresh tube containing 600 µL of phenol:chloroform:isoamyl alcohol (25:24:1) and repeat the phenol:chloroform:isoamyl alcohol extraction step. The 500 µL of supernatant was then transferred to a new tube containing 500 µL of chloroform:isoamyl alcohol (24:1) and mixed/centrifuged as before. The 400 µL of supernatant was then transferred to a siliconized tube and precipitated in 1 mL absolute ethanol and 20 µL 4 M sodium acetate (pH 5.2). Samples were mixed by inverting the tubes and then incubated at -20°C for 30 minutes. TNA was pelleted by centrifugation at 13, 000 rpm for 30 minutes at 4°C. The pellet was washed with 1 mL 80% ethanol. The ethanol was poured off and aspirated with a pipette tip and tubes were left open on ice for 30 minutes to allow

residual ethanol to evaporate. The dried TNA pellets were resuspended in 50 µL of RNase-free water. The concentration of the TNA was determined using a Nanodrop. The RNA quality was checked by mixing 2 µL of sample with 2× RNA loading dye, heating the samples at 65℃ for 5 minutes, and separating the TNA on a 1.2 % agarose gel.

2.8 DNase treatment and cDNA synthesis

3 µg of TNA was treated with Turbo DNase (Ambion) to remove DNA according to the manufacturer's instruction. The RNA was precipitated with ethanol, then dissolved in 15 µL of RNase-free water. cDNA was synthesised from 1 µg of RNA using random hexamer primers and SuperScript II (Life Technologies). cDNA was diluted 1:10 with water for subsequent applications.

2.9 PCR

For cloning, Q5 Hi-Fidelity DNA polymerase (NEB) was used for PCR amplifications. PCR reagents were added according to the manufacturer's guidelines. PCR cycles were carried out for 2 min at 98℃, followed by 35 cycles of 98℃ for 10 s, 50-60℃ (Primer Tm+3℃) for 20 s, 72℃ for 20 s/kb of target DNA product and 72℃ for 2 min. PCR products were separated on a 1% agarose gel containing SYBR safe gel stain (Invitrogen). Gels were run in 1× TBE buffer and imaged in a digital gel imager (UVP).

For colony PCR, *Taq* DNA polymerase (NEB) was used and instead of DNA template, a tiny amount of a bacterial colony was added with a pipette tip to the PCR mix. The PCR cycling conditions were as follows: 2 min at 95℃, followed by 35 cycles of 95℃ for 30 s, 50-60℃ (Primer Tm -5℃) for 30 s, 72℃ for 30 s/kb of target DNA product and 72℃ for 10 min. Then, the PCR products were analysed by agarose gel electrophoresis.

2.10 Quantitative RT-PCR (qRT-PCR)

Quantitative RT-PCR analysis was carried out with SYBR Green I Master Mix on a LightCycler®480 instrument (Roche) using virus- and housekeeping gene-specific primers **(Table 2.1)**. 10 µL reactions were used, containing 5 µL SYBR green master

mix, 2 µL of 1 µM forward primer, 2 µL of 1 µM reverse primer, and 1 µL of 1:10 diluted cDNA. Three technical replicates were performed for each gene per sample analysed. The following cycling conditions were used for all reactions: 95℃ 5 min > (95℃ 10s > 60℃ 10s > 72℃ 15s) x 45.

2.11 Northern Blotting

10 µg of total TNA was mixed with 2× RNA loading dye (10 mM EDTA, 0.10% bromophenol blue and 0.10% xylene cyanol in 100% (v/v) deionized formamide), heated at 65℃ for 5 minutes, and loaded on a 0.75 mm 15% (w/v) denaturing polyacrylamide gel (7M Urea). The gel was pre-run at 100 V for 30 minutes and the wells were rinsed with 0.5× TBE running buffer. The RNA samples were separated by running the gel at 100 V until the bromophenol blue (bottom dye) reached the bottom of the gel. The small RNAs run between the bromophenol blue and xylene cyanol in a 15% denaturing polyacrylamide gel. After electrophoresis, the separated RNA was blotted to Hybond N+ membrane (GE Healthcare) using capillary blotting. After overnight blotting, the RNA was crosslinked to the membrane with UV at 120000 µJoules (Statagene, UV Stratalinker 2400). Oligonucleotide Probes were end-labelled with $^{32}\gamma$-ATP by T4 polynucleotide kinase (Thermo Scientific). All probes were purified through a Microspin G-25 column (GE Healthcare) according to the manufacturer's instructions. 2 µL of 0.5 M EDTA was added to the labelled probe and the probe was denatured at 90℃ for 5 minutes before adding it to the hybridisation buffer. The membrane was cut slightly above the xylene cyanol dye. The upper part of the membrane was hybridised with a U6 probe as loading control, and the bottom part with a small RNA-specific probe. Membranes were washed in hybridisation buffer at 40℃ for 30 minutes, and then hybridised with a $^{32}\gamma$-ATP-labelled probe in hybridisation buffer at 40℃ overnight. After overnight hybridisation, the membranes were washed twice in 2X SSC, 0.1% SDS at 40℃ for 10 minutes. The two parts of the cut membrane were aligned and wrapped together in Saran wrap and exposed to a phosphor imaging plate. The radioactive signals were detected by scanning the

phosphor plate in a Typhoon scanner (GE healthcare, Typhoon FLA 7000). Oligonucleotides used for Northern blotting are listed in **Table 2.1**.

2.12 Sequencing

2.12.1 Sanger sequencing

PCR products for sequencing were purified using the following SAP/EXO reaction: 5 µL PCR product, 0.66 µL shrimp alkaline phosphatase (NEB), 0.06 µL ExonucleaseI (NEB), 4.28 µL water. The reaction was incubated at 37℃ for 30 minutes and terminated by incubating at 80℃ for 10 minutes.

The purified PCR product was sequenced by Big Dye v3.1 (Applied Biosystems). The sequencing reaction was performed in a total volume of 10 µL per reaction volume. 1µL Big Dye was mixed with 2 µL buffer, supplied with the kit, 1.6 µL of the sequencing primer (2 µM), 5 µL of the SAP/EXO purified PCR product, and the volume was adjusted to 10 µL with H_2O. For the sequencing reaction, the thermal cycling conditions were as follows: 96℃ 45s > (96℃ 10s > 50℃ 5s > 60℃ 4min) x 25. The samples were submitted to Edinburgh Genomics for sequencing.

2.12.2 Bisulfite sequencing

RNA was removed from TNA by RNaseA digestion. After phenol/chloroform extraction, ethanol precipitation and re-suspension in sterile distilled water (Ambion), the DNA was quantified by Qubit using the dsDNA high-sensitivity (HS) assay kit (Life Technologies). Approximately 400ng of DNA was treated with bisulfite reagent according to the EZ DNA Methylation-Gold Kit (Zymo Research). Approximately 50 ng of DNA was amplified by *Taq* DNA polymerase (NEB) using gene-specific oligonucleotides **(Table 2.1)**. PCR cycles were as follows: 95℃ 180s > (95℃ 30s > 62℃ 30s > 62℃ 90s) x 40. The resulting PCR products were gel purified (Qiagen) and subsequently ligated into the pGEM-T Easy vector (Promega). DH5alpha *E. coli* competent cells were transformed with the recombinant DNA and then spread on LB-agar plates supplemented with 50 µg/mL carbenicillin. Eight to 16 clones from each sample were sequenced by BigDye v3.1. Bisulfite-converted sequences were aligned

to the corresponding sequences using Clustal Omega (http://www.ebi.ac.uk/Tools/msa/clustalo/). DNA methylation patterns were analysed by the CyMate software (Hetzl *et al.*, 2007).

2.12.3 Small RNA sequencing and bioinformatics analysis

Small RNA libraries were prepared from 3 µg of TNA using the Illumina TruSeq Small RNA Library Prep Kit and sequenced on the Illumina HiSeq 2500 platform with 50-base single end reads at Edinburgh Genomics (Edinburgh, UK). Sequence analysis was performed using the Geneious software (version 11.1.4 http://www.geneious.com). Briefly, after removing the adaptor sequences, size-selected reads between 21-24 nt were mapped either to recombinant TRV RNA2 or to the transgenic *N. benthamiana* 16c T-DNA+partialTn5393 locus (GenBank Accession No. KY464890) and its derivatives, where target sequences were modified according to the mutations that were introduced to the TRV trigger (TRV-35S-2M and TRV-GFP-2M). Only perfectly matching small RNAs were included in our analyses.

2.13 Oligonucleotides

Oligonucleotides were ordered from Sigma-Aldrich Ltd and re-suspension in sterile distilled water to obtain a 100 µM stock solution. All oligonucleotides used for cloning, bisulfite sequencing, qPCR and radioactive probes are listed in the following table **(Table 2.1)**.

Table 2.1 List of oligonucleotides used in this study

Oligonucleotide name	Sequence	Description
35S -208_F	CATCGTTGAAGATGCCTCTG	TRV-VIGS
35S -89_R	ATATCACATCAATCCACTTGCTTTG	TRV-VIGS
35S-1M_A_F	CATCGTTGAGGATGCCTCTGCCGACAGTGATCCCAAAGATGGACCCCCATCCACGAGGAGCATCGTGGAGAAAGAAGACGTTCCAACCATGTCTTCAAAGCAAGTGGATCGATGTGATAT	TRV-VIGS
35S-1M_A_R	ATATCACATCGATCCACTTGCTTTGAAGACATGGTTGGAACGTCTTCTTTCTCCACGATGCTCCTCGTGGATGGGGGTCCATCTTTGGGATCACTGTCGGCAGAGGCATCCTCAACGATG	TRV-VIGS
35S-1M_B_F	CATCGTTGAAGATGCCTCTACCGACAGTGGTCCCAAAGACGGACCCCCACCCACGAGGAACATCGTGGAAAAAGAAGACATTCCAACCACGTCTTCAAAACAAGTGGATTGATGTGATAC	TRV-VIGS
35S-1M_B_R	TATCACATCAATCCACTTGTTTTGAAGACGTGGTTGGAATGTCTTCTTTTTCCACGATGTTCCTCGTGGGTGGGGGTCCGTCTTTGGGACCACTGTCGGTAGAGGCATCTTCAACGATG	TRV-VIGS
35S-2M_F	CATCGTTGAGGATGCCTCTACCGACAGTGATCCCAAAGACGGACCCCCATCCACGAGGAACATCGTGGAGAAAGAAGACATTCCAACCATGTCTTCAAAACAAGTGGATCGATGTGATAC	TRV-VIGS
35S-2M_R	GTATCACATCGATCCACTTGTTTTGAAGACATGGTTGGAATGTCTTCTTTCTCCACGATGTTCCTCGTGGATGGGGGTCCGTCTTTGGGATCACTGTCGGTAGAGGCATCCTCAACGATG	TRV-VIGS
35S-4M_F	CATCATTGAGGATGTCTCTACCGATAGTGATCCCGAAGACGGACTCCCATCCACAAGGAACATCATGGAGAAAGGAGACATTCCGACCATGTCTCCAAAACAAGCGGATCGATGCGATAC	TRV-VIGS
35S-4M_R	GTATCGCATCGATCCGCTTGTTTTGGAGACATGGTCGGAATGTCTCCTTTCTCCATGATGTTCCTTGTGGATGGGAGTCCGTCTTCGGGATCACTATCGGTAGAGACATCCTCAATGATG	TRV-VIGS
GFP +364_F	AAGGACGACGGGAACTACAAG	TRV-VIGS
GFP +426_R	CTTGTGGCCGAGGATGTTTC	TRV-VIGS
GFP-2M_F	AAGGACGACAGGAACTACAGGACACGTGCCGAAGTCAAGCTTGAGGGAGGCACCCTCGTTAACAGGATCAAGCTTAAGGAAATCGATTTTAAGGAGGACAGAAACATCCCCGGCCACAAA	TRV-VIGS
GFP-2M_R	TTTGTGGCCGGGGATGTTTCTGTCCTCCTTAAAATCGATTTCCTTAAGCTTGATCCTGTTAACGAGGGTGCCTCCCTCAAGCTTGACTTCGGCACGTGTCCTGTAGTTCCTGTCGTCCTT	TRV-VIGS
TBSV-35S_F	GCGCTCGAGTTCACTTATCTAGCATCGTTGAAGATGCCTCTGC	TBSV-VIGS
TBSV-35S_R	CGCCTCGAGATATCACATCAATCCACTTGC	TBSV-VIGS
TBSV-35S-A_F	GCGCTCGAGTTCACTTATCTAGATATCACATCAATCCACTTGC	TBSV-VIGS
TBSV-35S-A_R	ATACTCGAGCATCGTTGAAGATGCCTCTGC	TBSV-VIGS

TBSV-GFP_F	GCGCTCGAGTTCACTTATCTAGAAGGACGACGGGAACTACAAG	TBSV-VIGS
TBSV-GFP_R	TATCTCGAGCTTGTGGCCGAGGATGTTTCCG	TBSV-VIGS
TBSV-GFP-A_F	ATACTCGAGTTCACTTATCTAGCTTGTGGCCGAGGATGTTTCCG	TBSV-VIGS
TBSV-GFP-A_R	TATCTCGAGAAGGACGACGGGAACTACAAG	TBSV-VIGS
TuMV-35S_F	ATACCATGGCATCGTTGAAGATGCCTCTG	TuMV-VIGS
TuMV-35S_R	GCGCCATGGATATCACATCAATCCACTTGC	TuMV-VIGS
TuMV-35S-A_F	GCGCCATGGCAATATCACATCAATCCACTTGC	TuMV-VIGS
TuMV-35S-A_R	ATACCATGGTCGTTGAAGATGCCTCTGC	TuMV-VIGS
TuMV-5'GFP_F	GCGCCATGGGGATCCAAGGAGATATAAC	TuMV-VIGS
TuMV-5'GFP_R	GCGCCATGGGGACAACTCCAGTGAAAAGTT	TuMV-VIGS
TuMV-GFP_F	ATACCATGGGGACGACGGGAACTACAAGACA	TuMV-VIGS
TuMV-GFP_R	ATACCATGGAACTTGTGGCCGAGGATGTTTCC	TuMV-VIGS
TuMV-3'GFP_F	GCGCCATGGCACAATCTGCCCTTTCGAAAG	TuMV-VIGS
TuMV-3'GFP_R	GCGCCATGGAAAGCTCATCATGTTTGTATAGTTC	TuMV-VIGS
2b-HA_F	ATAGGCGCGCCATGGATGTGTTGACAGTAG	pDE clones
P19-HA_F	ATAGGCGCGCCATGGAACGAGCTATACAAG	pDE clones
P21-HA_F	CGCGGCGCGCCATGAAGTTTTTCTTTAATG	pDE clones
HA_R	ATAGGCGCGCCTTAAGCGTAGTCTGGGAC	pDE clones
P1-HcPro_F	ATAGGCGCGCCATGGCAGCAGTTACATTC	pDE clones
P1-HcPro_R	ATAGGCGCGCCCTAGAGTGCGTAATCTGG	pDE clones
35S-120-AscI_F	ATAGGCGCGCCCATCGTTGAAGATGCCTC	pDE clones
35S-120-AscI_R	CGCGGCGCGCCATATCACATCAATCCAC	pDE clones
GFP-120-AscI_F	ATAGGCGCGCCAAGGACGACGGGAACTA	pDE clones
GFP-120-AscI_R	ATAGGCGCGCCCTTGTGGCCGAGGATG	pDE clones
35S_short_BS_F	GAAAAGGAAGGTGGTTTTTATAAATGTTATTATTGT	BS-PCR
35S_short_BS_R	CTTRCAAAAAATAATAAAATTATRCATCATCCCTTACA	BS-PCR
M13_F	CGCCAGGGTTTTCCCAGTCACGAC	Colony PCR
M13_R	AGCGGATAACAATTTCACACAGGA	Colony PCR
Nb-act_F	GAAGATACTCACAGAAAGAGG	qPCR
Nb-act_R2	GGAGCTAATGCAGTAATTTCC	qPCR
CMV_F	AATCTCAGACTGTTCCGCTTC	qPCR
CMV_R	GATGGACAACCCGTTCACCAC	qPCR
mGFP5+148_F	ACTGGAAAACTACCTGTTCC	qPCR
mGFP5+344_R	TCAAACTTGACTTCAGCACG	qPCR
NbEF1a_F	CTTCTTGAGGCTCTTGACCAG	qPCR

NbEF1a_R	TGAGAGGTGTGGCAATCGAG	qPCR
TRV-CP-713_F	TGGGTTACTAGCGGCACTGA	qPCR
TRV-CP-856_R	GCTCGTCTCTTGAACGCTGA	qPCR
GFP-87F	CACTGGAGTTGTCCCAATTC	qPCR
GFP-304R	GCCGCTTCATATGATCTGG	qPCR
35S-1:60	CATCGTTGAAGATGCCTCTGCCGACAGTGGTCCCAAAGATGGACCCCCACCCACGAGGAG	Northern Blot Probe
35S-61:120	CATCGTGGAAAAAGAAGACGTTCCAACCACGTCTTCAAAGCAAGTGGATTGATGTGATAT	Northern Blot Probe
GFP-1:60	AAGGACGACGGGAACTACAAGACACGTGCTGAAGTCAAGTTTGAGGGAGACACCCTCGTC	Northern Blot Probe
GFP-61:120	AACAGGATCGAGCTTAAGGGAATCGATTTCAAGGAGGACGGAAACATCCTCGGCCACAAG	Northern Blot Probe
U6	GCTAATCTTCTCTGTATCGTTCC	Northern Blot Probe
miR159	TAGAGCTCCCTTCAATCCAAA	Northern Blot Probe

Restriction sites used for cloning are underlined

Chapter 3: Non-perfectly matching small RNAs can induce stable and heritable epigenetic modification

3.1 Introduction

sRNAs play a fundamental role in gene regulation in eukaryotes. They are generated from the cleavage of partially or perfectly matched dsRNA by DCL nucleases and are subsequently loaded into AGO proteins. AGO proteins are guided by the sRNAs to nucleic acid targets by base-pair complementarity. Thus, sRNAs act as molecular postcodes. If the target is mRNA, its cleavage, destabilization, or translational inhibition results in PTGS. If the target is DNA, the AGO-sRNA complex induces epigenetic change through cytosine methylation of DNA (Molnar *et al.*, 2011). This process is known as RdDM. RdDM in nuclear promoter regions often result in TGS thus cytosine methylation plays an important role in regulating gene expression.

RdDM is mediated by DCL3-generated 24 nt sRNAs derived from repeat sequences including transposons and transgenes. The 24 nt sRNAs guide AGO effector proteins (AGO4, 6, 9) to nascent transcripts produced by Pol V which act as scaffolds. Subsequent recruitment of DRM2 catalyses *de novo* DNA methylation at the target locus (Wierzbicki *et al.*, 2009, Havecker *et al.*, 2010). Maintenance of DNA methylation on newly synthesised DNA involves MET1 and CMT3 (Law & Jacobsen, 2010), which reproduce CG and CHG methylation, respectively.

The 24 nt sRNAs play an important role both in inter- and intra-genomic interactions including hybrid vigour (Shivaprasad *et al.*, 2012) and genome imbalance in triploid endosperm of Arabidopsis seeds (Lu *et al.*, 2012). Transposon-derived sRNAs have been involved in driving the evolution of gene expression in plants (Wang *et al.*, 2013). Importantly, recent experiments demonstrated that 24 nt sRNAs are mobile in plants and can direct TGS in recipient tissues including meristems (Molnar *et al.*, 2010, Melnyk *et al.*, 2011). Since meristems give rise to new organs including flowers,

mobile 24 nt sRNAs can initiate epigenetic changes that may persist and yield heritable (trans-generational) phenotypes. Despite their importance, there is no information about how the sRNAs recognise their nuclear target loci.

PTGS, which is mediated by 21-22 nt sRNAs, can operate with up to five mismatches between the sRNA and its target RNA (Amarzguioui, 2003, Brodersen & Voinnet, 2009, Carthew & Sontheimer, 2009). However, TGS has been widely assumed to only occur via 24 nt sRNAs with high degree of homology to the target sequence. Studies have been shown that transgene induced-TGS cannot occur between CaMV 35S promoter-driven transgenes and figwort mosaic virus (FMV) 34S promoter-driven transgenes, and the homology between 34S and 35S promoter is 63% with never more than six contiguous identical nucleotides (Thierry & Vaucheret, 1996). This result indicates that a high degree of sequence similarity is required between target sequences for TGS. Moreover, using a methylation acceptor sites (MAS)-free version of the CaMV 35S promoter by mutating CG and CHG sequence, the study showed that the modified CaMV 35S promoter can still trigger transgene-TGS despite a reduction of the homology to a wildtype 35S locus to 91% (Diéguez *et al.*, 1998).

In this chapter, we show that initiation of trans-generational RdDM does not require 100% sequence complementarity between the sRNAs and their nuclear target sequence. In addition, we demonstrate that promoter-targeted RdDM is not associated with secondary sRNA production in vegetative tissues.

3.2 Results

3.2.1 Construction of TRV-based silencing vectors

To set up a system where we could examine gene silencing, we used GFP driven constitutively by the CaMV 35S promoter as a reporter gene in transgenic *Nicotiana benthamiana* plants 16c (Ruiz *et al.*, 1998). A 120 bp segment of either the 35S promoter or GFP coding sequence were targeted to induce TGS and PTGS, respectively. To bypass the variance in transgene-derived sRNAs due to transgene rearrangements and positional effects, we delivered the sRNA precursors via recombinant RNA viruses. Our rationale was that the nuclear and the antiviral silencing pathways overlap and RNA virus-derived sRNAs can induce TGS with high efficiency (Jones *et al.*, 2001).

In this study, TRV was chosen as an inducer of gene silencing virus. TRV-based VIGS vectors are widely used in a broad host range with high silencing efficiency. TRV has a bipartite positive RNA genome consisting of RNA1 and RNA2 **(Figure 3.1A)**. TRV RNA1 is essential for viral movement and replication, which encodes 134- and 194-kDa replicase proteins, a 29-kDa movement protein and a 16-kDa cysteine-rich protein. The TRV RNA2 genome varies among different isolates of this virus and has genes encoding the coat protein and non-structural proteins (MacFarlane, 1999). The TRV vector induces mild symptoms in infected plants, which makes it suitable as a VIGS vector. In previous publications, a recombinant TRV carrying the full 35S promoter sequence, and a CMV harbouring a shorter 120 bp segment of 35S, had been shown to trigger sequence-specific DNA methylation and heritable TGS (Jones *et al.*, 1999, 2001, Otagaki *et al.*, 2011).

To systematically investigate the specificity and activity of TGS-inducing sRNAs, we designed sRNAs with mismatches to their target sequence. As a template for sRNA production, we used a recombinant TRV containing a 120 bp segment of the 35S

promoter (TRV-35S). We then created a series of variants carrying single-nucleotide substitutions (SNSs) at every 20, 10 or 5 nucleotides within this segment. The sRNAs produced from these vector variants would have at least one (TRV-35S-1M), two (TRV-35S-2M) or four (TRV-35S-4M) mismatches to the 35S target segment, respectively **(Figure 3.1A and B)**. To test the effect of the relative position of the SNSs, we produced two versions of TRV-35S-1M where the SNSs were shifted by 10 nt relative to each other (TRV-35S-1M_A, TRV-35S-1M_B) **(Figure 3.1B)**.

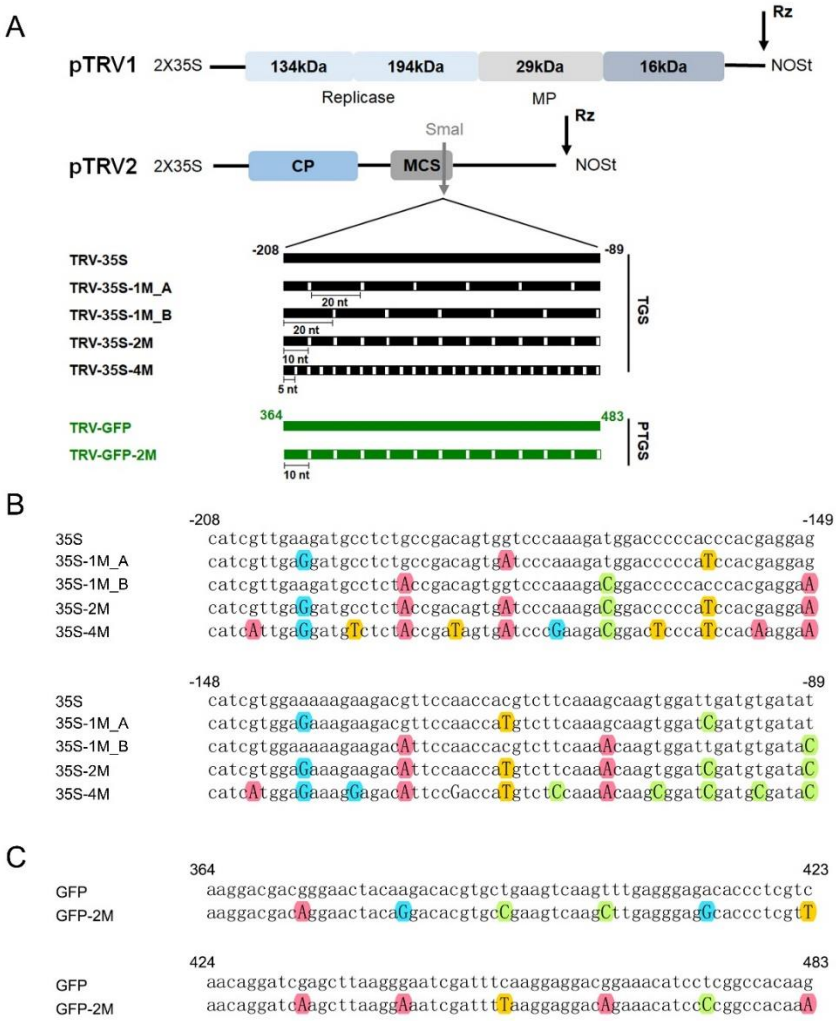

Figure 3.1 TRV-based VIGS vectors used in this study. (A) Schematic diagram of the TRV VIGS vectors pTRV1 and pTRV2. A 120 nt fragment of the CaMV 35S promoter (-208 to -89 relative to the transcription start site, black lines) or a 120 nt fragment of the GFP coding sequence (+364 to +483, green lines) was cloned into pTRV2 to induce TGS and PTGS, respectively. Single nucleotide substitutions (SNSs; white boxes) were introduced into the 120 nt fragments at regular intervals of 20, 10 or 5 nucleotides, which produced sRNAs with 1, 2 or 4 mismatches, respectively. SNSs were introduced from position 10 in TRV-35S-1M_A and from position 20 in TRV-35S-1M_B. pTRV1 was used along with pTRV2 to generate functional TRV particles. Rz, self-cleaving ribozyme; MCS, multiple cloning sites; CP, coat protein; MP, movement protein; NOSt, NOS terminator. (B) Sequence alignment of the 120 nt fragment from CaMV 35S and its derivatives from Figure 3.1A. Substituted A, C, G, T nucleotides are highlighted with red, green, blue and yellow colored circles, respectively. (C) Sequence alignment of the 120 nt fragment from mGFP5 and its derivative from Figure 3.1A.

3.2.2 Non-perfectly matching sRNAs can induce strong TGS in virus-infected plants

We infected 16c plants with wild type and recombinant TRVs and monitored GFP expression after infection under UV light. We found that the unmodified 35S segment was sufficient to induce strong GFP silencing in TRV-35S infected plants (seen in **Figure 3.2A** as red chlorophyll fluorescence in the absence of GFP expression), as reported for CMV (Otagaki *et al.*, 2011). Intriguingly, SNSs in the sRNAs did not prevent silencing. Plants infected with TRV-35S-1M_A, TRV-35S-1M_B and TRV-35S-2M showed similar levels of GFP silencing as plants inoculated with the non-mutated TRV-35S vector, while TRV-35S-4M caused an intermediate level of GFP silencing **(Figure 3.2A**). The relative positions of the SNSs in TRV-35S-1M_A and TRV-35S-1M_B had no effect on silencing. Taken together, SNSs in sRNAs occurring at 10 nt intervals begin to reduce TGS activity, but SNSs at 5 nt intervals still do not abolish it.

To further investigate the impact of virus infection on GFP expression, we isolated RNA from leaves infected systemically 2 weeks post inoculation and assessed GFP and viral RNA accumulation by qRT-PCR. In agreement with the phenotypic data, GFP silencing was associated with reduced GFP mRNA levels. We detected at least 50 times less GFP mRNA in TRV-35S, TRV-35S-1M and in TRV-35S-2M infected tissues compared to wild type TRV **(Figure 3.2B)**. The lower level of silencing induced by TRV-35S-4M **(Figure 3.2B)** was not due to reduced infection or stability of the virus because TRV-35S-4M samples contained at least twice as much viral RNA as tissues infected with other recombinant TRVs **(Figure 3.2C)**. From these experiments, we concluded that 35S promoter-targeting sRNAs do not require 100% sequence complementarity to induce TGS.

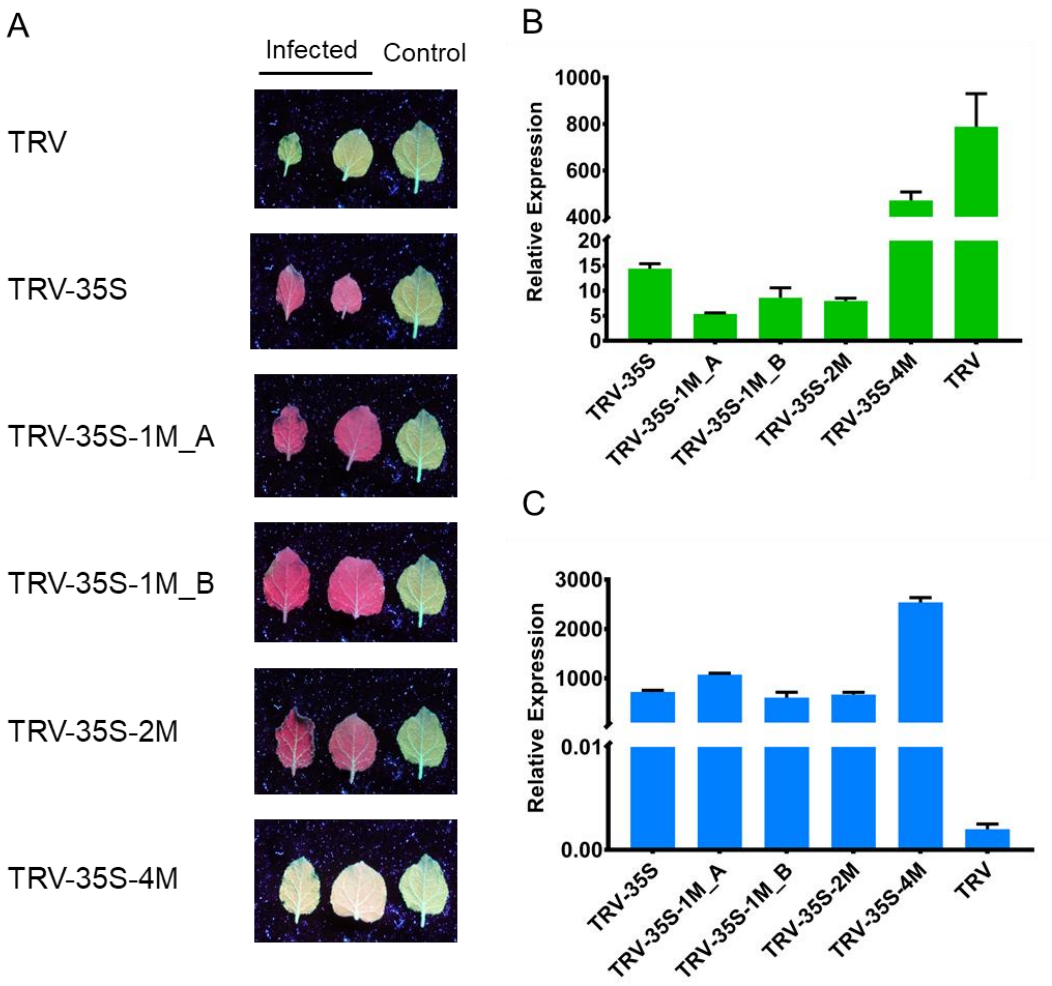

Figure 3.2 Non-perfectly matching small RNAs can induce strong transcriptional gene silencing in virus-infected plants. (A) Phenotypes of leaves of *N. benthamiana* 16c plants systemically infected with recombinant TRV as indicated in Figure 3.1A and B. Leaves were collected from independent plants. Photographs were taken under UV light at 18 dpi. GFP silencing reveals red fluorescence of chlorophyll. An uninfected 16c leaf is shown as a control (right). (B) Analysis of GFP expression in TRV-infected plants. RNA was extracted from the systemically infected leaves 18 dpi. After cDNA synthesis, GFP transcript levels were estimated by qPCR and normalized relative to Actin. Error bars indicate standard deviation of three technical replicates. (C) Measuring virus accumulation in TRV-infected plants. The same RNA samples as used as in Figure 3.2B were amplified using specific TRV primers (Table 2.1).

3.2.3 Non-perfectly matching small RNAs can induce high-levels of DNA methylation in virus-infected plants and their progeny

To investigate the effect of mismatches on sRNA-mediated DNA methylation, we isolated DNA from tissues infected with TRV, TRV-35S, TRV-35S-1M_A and B, TRV-35S-2M and TRV-35S-4M **(Figure 3.2A)** and used bisulfite sequencing to assess the level and context of cytosine methylation at the 35S target sequence. As expected, wild type TRV did not induce DNA methylation **(Figure 3.3)**. In contrast, infection with TRV-35S was associated with a high level of cytosine methylation, further supporting that the 120 nt 35S promoter sequence was a potent activator of RdDM. TRV-35S-1M, TRV-35S-2M and TRV-35S-4M, which produced mismatched sRNAs, were also able to direct DNA methylation of the nuclear target promoter **(Figure 3.3)**. Together with the phenotypic data **(Figure 3.2A)**, this shows that sRNAs with one or two mismatches can induce strong silencing via RdDM. Strikingly, mismatched sRNAs had reduced capacity to direct CHH methylation. Interestingly, sRNA with four mismatches that greatly impaired the targeting ability of AGO were still capable of initiating low levels of RdDM, especially at CHG sites **(Figure 3.3)**.

To test the effect of mismatched sRNAs on transgenerational epigenetic gene silencing, we analysed the virus-free progeny of 16c plants infected with wild type and recombinant TRVs. We found that silencing of the reporter gene with TRV-35S, TRV-35S-1M and TRV-35S-2M was passed to the next generation **(Figure 3.4A)**, suggesting that non-perfectly matching sRNAs were able to induce heritable TGS. Indeed, GFP expression **(Figure 3.4B)** and promoter DNA methylation **(Figure 3.4C)** showed a strong inverse correlation in the progeny and reduced GPF expression was always accompanied by high levels of DNA methylation. Our data also revealed that symmetric cytosine methylation (CG and CHG) was frequently inherited regardless of the number of mismatches in the sRNA inducer of TGS. Overall, these experiments provide direct evidence that transgenerational RdDM does not require 100% sequence complementarity between the sRNAs and the target DNA sequence.

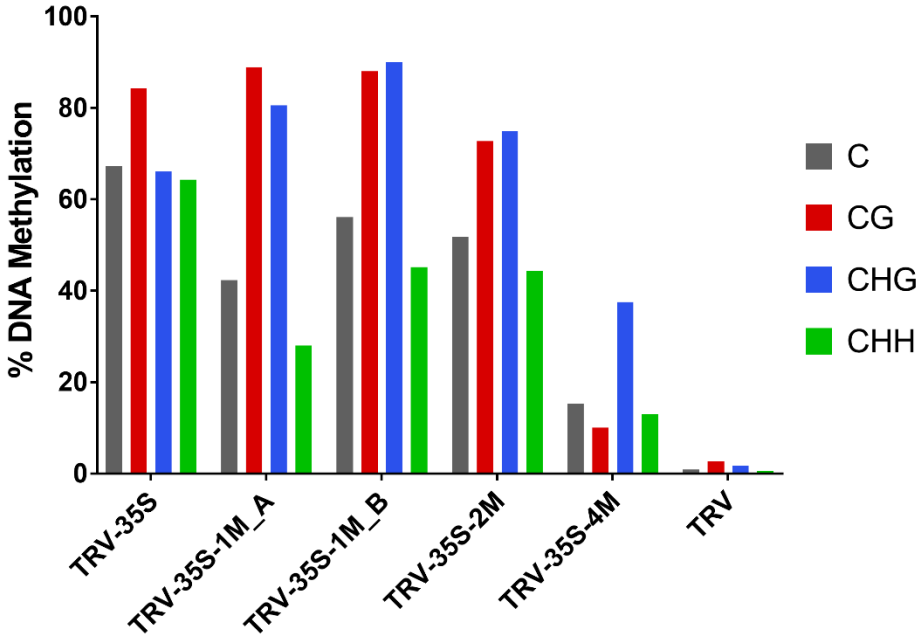

Figure 3.3 Non-perfectly matching small RNAs can induce high-levels of DNA methylation in virus-infected plants. Analysis of DNA methylation of the target CaMV 35S promoter (from -208 to -89) by bisulfite sequencing in TRV-infected *N. benthamiana* 16c plants at 18 dpi. DNA methylation patterns were analysed by CyMate. Levels of CG, CHG and CHH methylation are shown as red, blue and green bars, respectively, and total methylated cytosine as gray bars.

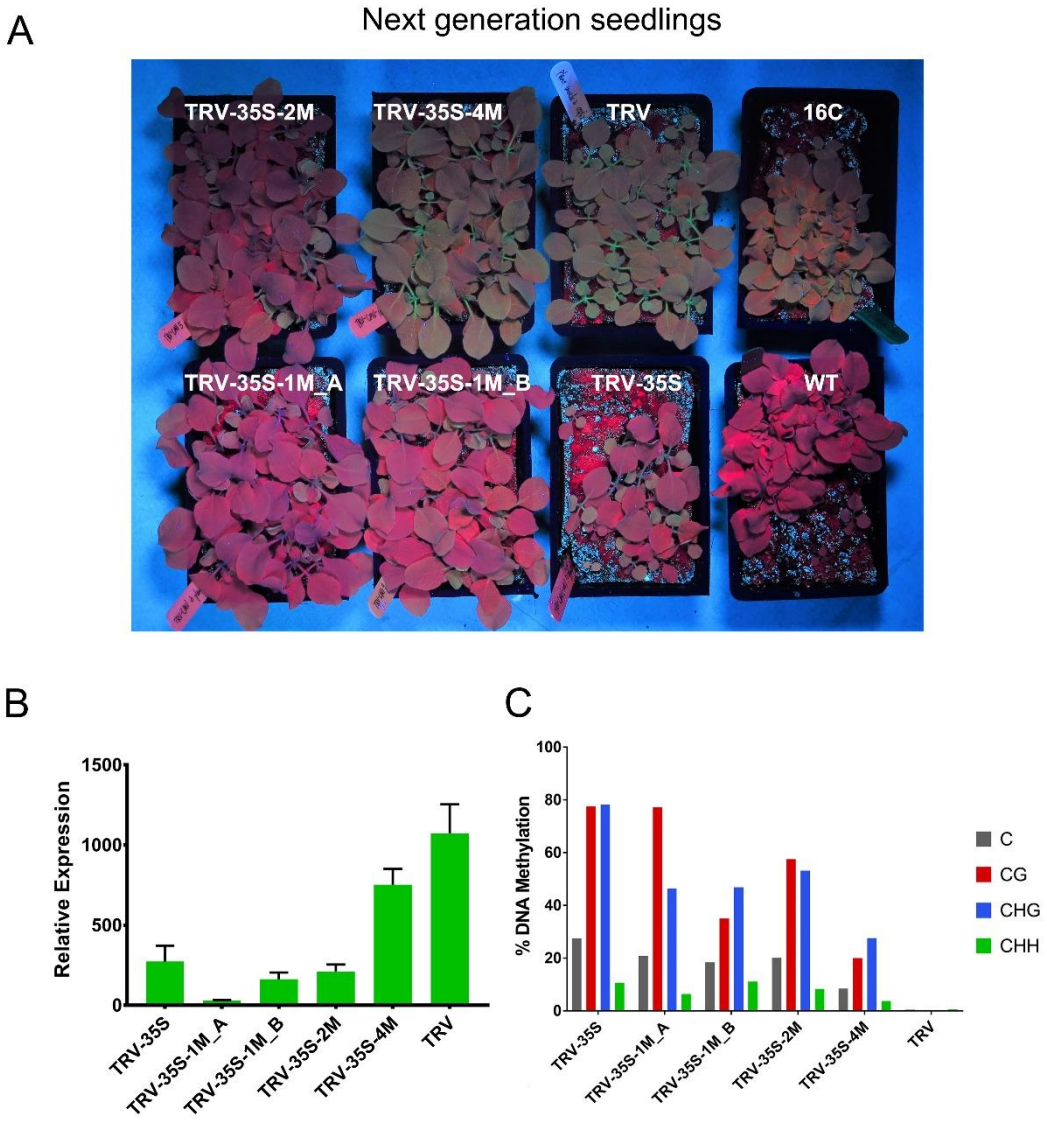

Figure 3.4 Non-perfectly matching small RNAs can induce transgenerational epigenetic gene silencing. (A) Progeny of at least three recombinant-TRV-infected *N. benthamiana* 16c plants were grown together and photographed under UV light at 20 days after germination. Wild type *N. benthamiana* and uninfected 16c plants are shown as controls. (B) Analysis of GFP expression in the progeny of TRV-infected plants. RNA was extracted from the seedlings shown in Figure 3.4A. After cDNA synthesis, GFP accumulation was measured by qPCR and the expression level was normalized to Actin. Error bars indicate standard deviation of three technical replicates. (C) Analysis of DNA methylation of the target CaMV 35S promoter (from -208 to -89) in the progeny of TRV-infected plants. DNA was extracted from seedlings shown in Figure 3.4A. DNA methylation patterns were analyzed and are shown as in Figure 3.3.

3.3 Discussion

We demonstrate that the initiation step of RdDM can tolerate mismatches between the inducing sRNAs and the nuclear target sequence. So, what kind of nucleic acid do sRNAs target in the nucleus? According to the current model (Wendte & Pikaard, 2017) based mainly on RdDM-mediated silencing of transposons in *Arabidopsis*, sRNAs guide AGO proteins to nascent scaffold transcripts, recruiting DRM2, which methylates the previously unmodified cytosine residues in any sequence context (CG, CHG or CHH). The scaffold RNA can be transcribed either by the plant-specific Pol V (Wierzbicki *et al.*, 2008, 2009, 2012) or less frequently by Pol II (Creasey *et al.*, 2014). Despite the wide accepted the "nascent transcript" model, the other models involving AGO4/siRNA-DNA interaction at RdDM loci have been proposed (Lahmy *et al.*, 2016). As Pol V elongates, AGO4 would interact with Pol V lncRNAs, generating a metastable multimeric complex. This complex would serve as an intermediate for the transfer of AGO4 to the DNA template. Following the interaction with the complementary ssDNA, AGO4-siRNA complexes would recruit DRM2 to the opposite siRNA-like DNA strand for DNA methylation.

Since Pol V recruitment requires DNA methylation (Johnson *et al.*, 2014) and 16c plants lack cytosine methylation at the 35S locus **(Figure 3.3)**, it is unlikely that Pol V transcripts are involved in the initiation step of virus-induced RdDM. Instead, we propose that Pol II transcripts could be the primary RNA targets in RdDM. The observation of bidirectional Pol II transcription around promoters (Bond & Baulcombe, 2015) is consistent with this hypothesis. Once DRM2 is recruited and the corresponding cytosine residues are methylated, CG and CHG methylation can be maintained throughout cell division by MET1 and CMT3, respectively, even without the sRNA trigger. Indeed, this methylation pattern could be detected in the virus-free progeny of plants infected with recombinant TRV-35S vectors **(Figure 3.4C)**, or using CMV (Otagaki *et al.*, 2011).

TRV-induced RdDM is correlated with the accumulation of 21-24 nt sRNAs suggesting that all DCLs can act on the precursor of sRNAs. Recent work showed that VIGS-RdDM was enhanced in *dcl*2,4 double mutants lacking most 22 nt and some 21 nt sRNAs (Bond & Baulcombe, 2015), suggesting that TRV-mediated epigenetic silencing requires DCL3-generated 24 nt sRNAs and the associated AGO4. However, AGO1-bound 21 nt sRNAs have been implicated in transposon silencing (Creasey *et al.*, 2014), therefore we cannot exclude the possibility that 21-22 nt sRNAs has a role in the early establishment of RdDM. Further work is required to identify the specific nucleases and chromatin modifying complexes associated with virus-induced RdDM and to test whether the targeting rule for sRNA-mediated RdDM differ between endogenous genes and transposons.

Chapter 4: Studying the effects of temperature and light intensity on virus induced gene silencing in plants

4.1 Introduction

It has long been recognised that environmental factors such as temperature dramatically affects plant-virus interactions (Chellappan *et al.*, 2005). In virus-infected plants, high temperature is frequently associated with attenuated symptoms (heat masking) and with low virus content (Johnson, 1922). By contrast, low temperature is often associated with rapid spread of virus disease and the development of severe symptoms (Gerik, 1990). For example, CymRSV-induced symptom severity was found to be higher at low temperature, and decreased with rising temperature which was associated with elevated levels of virus-derived siRNAs (Szittya *et al.*, 2003) indicating that plant-virus interaction is controlled by RNA silencing, and the RNA silencing-mediated defence response is temperature dependent.

In addition to temperature, other environmental factors such as light also play a key role in host susceptibility to viruses. It has been observed that plants infected in low light or prior to a dark period developed more viral lesions than those placed under high light or inoculated during a light period (Helms, 1965, Cheo, 1971). In a recent study it was found that both light deficiency and photosystem impairment increased the susceptibility of *N. benthamiana* to TuMV infection (Manfre *et al.*, 2011).

Virus-induced gene silencing (VIGS) has been shown as a powerful tool for studying gene function and plant microbe-interactions. Since VIGS can also induce sequence-specific RdDM of target promoters (Jones *et al.*, 2001, Kanazawa *et al.*, 2011), VIGS vectors could be used to modify the epigenetic status of target promoters and subsequently the transcriptional activity of target genes. However, there is no information about how environmental factors can affect VIGS and RdDM.

To build up a comprehensive picture about the effects of environmental factors on VIGS, we combined two environmental factors, namely temperature and light, and evaluated their influence on the efficacy of VIGS. We chose GFP as a reporter of gene silencing and TRV as a virus vector to study the effect of the above environmental cues on VIGS and RdDM.

4.2 Results

To investigate how temperature and light affect VIGS, we chose TRV as an inducer of gene silencing and the GFP expressing 16c plants to monitor silencing **(Figure 4.1A)**. Recombinant TRVs were generated by introducing a 120 nt fragment from the 35S promoter (TRV-35S) and from the GFP coding region (TRV-GFP) to ensure comparable virus-derived small RNA production **(Figure 4.1B)**. TRV-35S recombinant virus was used to induce transcriptional gene silencing (TGS), while TRV-GFP was generated to trigger post-transcriptional gene silencing (PTGS). Plants inoculated with a TRV empty vector (TRV-WT) were used as viral infection controls. Three-week-old 16c plants were rub inoculated with the viral sap of TRV-35S, TRV-GFP, and TRV-WT, respectively. After rub inoculation, the plants were kept under different temperatures (15℃, 22℃, and 29℃) and different light levels (high light 150 µmol/$m^{-2}s^{-1}$, medium light 75 µmol/$m^{-2}s^{-1}$, and low light 35 µmol/$m^{-2}s^{-1}$) **(Figure 4.2)**. Plants were monitored at regular intervals under UV light. Five plants were used in each treatment group.

4.2.1 Temperature exhibits significant effects on plants growth and viral replications

In accordance with previous reports, we observed that temperature dramatically affected plants growth and development. In general, the growth rate of both infected and uninfected plants was gradually increased with rising temperature. Symptomatically, most severe TRV symptoms were presented at 15℃, whereas mild symptoms at 29℃. To more accurately assess viral RNA accumulation, qRT-PCR was performed using systemic leaves of infected plants kept under different growth conditions at 7 dpi. In agreement with the phenotypes observed, high level of viral RNA was accumulated at 15℃ and less virus at 29℃ **(Figure 4.3)**. Our data is consistent the previous finding that antiviral silencing is temperature dependent (Szittya, 2003). The lower the temperature the higher the virus tire is. Moreover, at 22℃ the amount of virus exhibited a negative correlation with the level of light intensities, more virus was accumulated at low light intensity **(Figure 4.3)**.

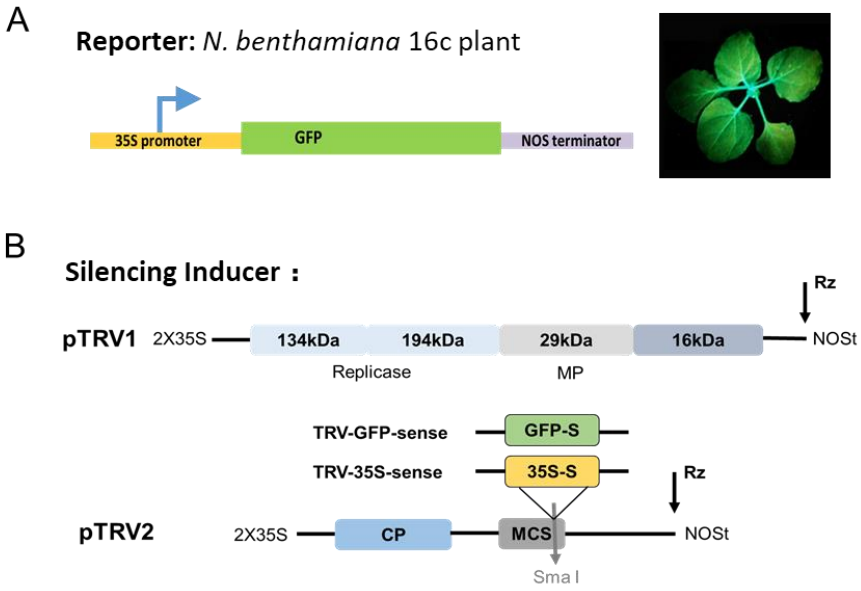

Figure 4.1 Virus-induced gene silencing in *N. benthamiana*. (A) *N. benthamiana* 16c plant harbours the GFP transgene under the control of CaMV 35S promoter. The 16c plants show green fluorescence under UV light. Wild-type plants are red under UV due to the fluorescence of chlorophyll. (B) Construction of the TRV-based VIGS vectors. Schematic presentation of pTRV1 and pTRV2. The unique restriction site SmaI is indicated on pTRV2, which was used to ligate the silencing inducer (a 120 nt fragment either from the GFP coding region (TRV-GFP) or from the 35S promoter (TRV-35S)) into the vectors. The control virus has no insert. pTRV1 is used along with pTRV2 for generating functional viral particles. Rz, self-cleaving ribozyme; MCS, multiple cloning sites; CP, coat protein; MP, movement protein.

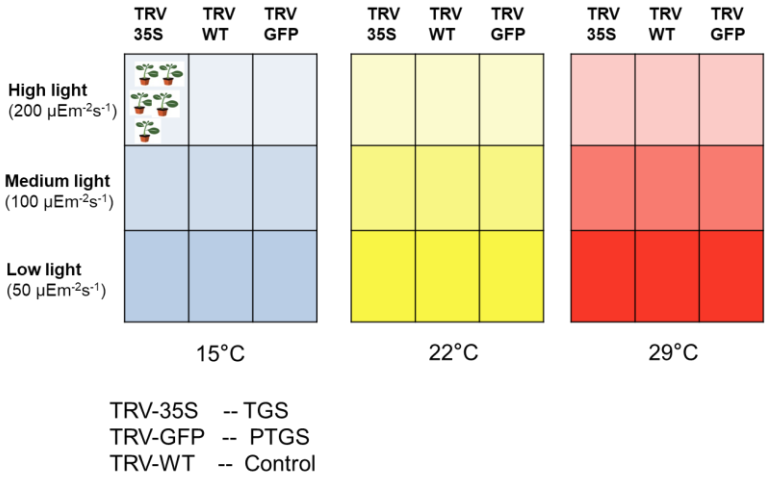

Figure 4.2 Schematic diagram of experimental design to test the effect of light intensity and temperature on VIGS. Three-week old 16c plants were rub inoculated with the infectious sap of TRV-35S, TRV-GFP, and TRV-WT and then the plants were transferred to 15°C, 22°C and 29°C growth cabinets (indicated as blue, yellow and red colours). Light intensity was adjusted to high (200 $\mu Em^{-2}s^{-1}$), medium (100 $\mu Em^{-2}s^{-1}$) and low light (50 $\mu Em^{-2}s^{-1}$) by stagelight filters. Plants were monitored at regular intervals under UV light. Five plants were used in each treatment group.

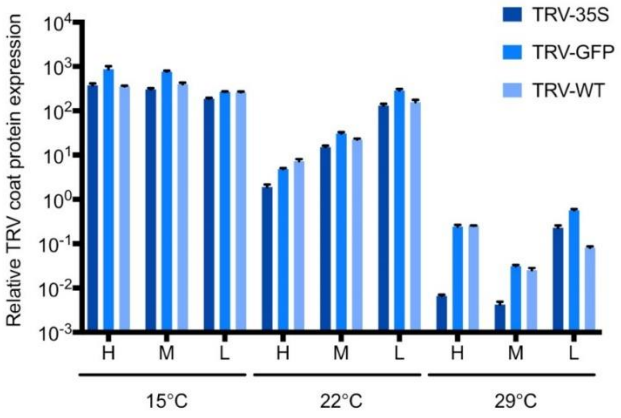

Figure 4.3 Lower temperature accelerates virus infection. qPCR to quantify TRV virus levels in plants shifted to 15/22/29°C under low (L), medium (M) or high light (H) intensities at 7 dpi. EF1α was used as a reference gene. Error bars represent the arithmetic mean of three technical replicates ± SEM.

4.2.2 Both TRV-35S and TRV-GFP could efficiently induce gene silencing at ambient temperature

At ambient plant growth temperature (22°C), both TRV-35S and TRV-GFP infected *N. benthamiana* 16c plants showed GFP silencing, and a loss of GFP fluorescence could be visible in systemic leaves of inoculated plants as early as 7 dpi. The silencing of the reporter gene spread rapidly and consequently, and all infected plants showed strong GFP silencing at 14 dpi **(Figure 4.4)**. To quantify the GFP expression in the infected plants, we used qRT-PCR. GFP expression was normalized to GFP levels of TRV-WT infected plants kept at the same condition, and was set to 1 (**Figure 4.5**; green lines in the panels). Thus, values below 1 indicate suppression of GFP expression. The qRT-PCR results confirmed that GFP expression was significantly reduced to 0 in TRV-35S and TRV-GFP infected plants compared to TRV-WT infected plants at 7 dpi, and the silencing of GFP was maintained at the same level until 35 dpi **(Figure 4.5 middle panel)**. Furthermore, the qRT-PCR data also revealed that the efficiency of TGS and PTGS was similar at 22°C. The different light levels did not affect the initiation, spread and maintenance of GFP silencing at 22°C. The result indicated that TRV-based vectors can effectively introduce both transcriptional gene silencing (TRV-35S) and posttranscriptional gene silencing (TRV-GFP) in *N. benthamiana* 16c plants at ambient temperature (22°C).

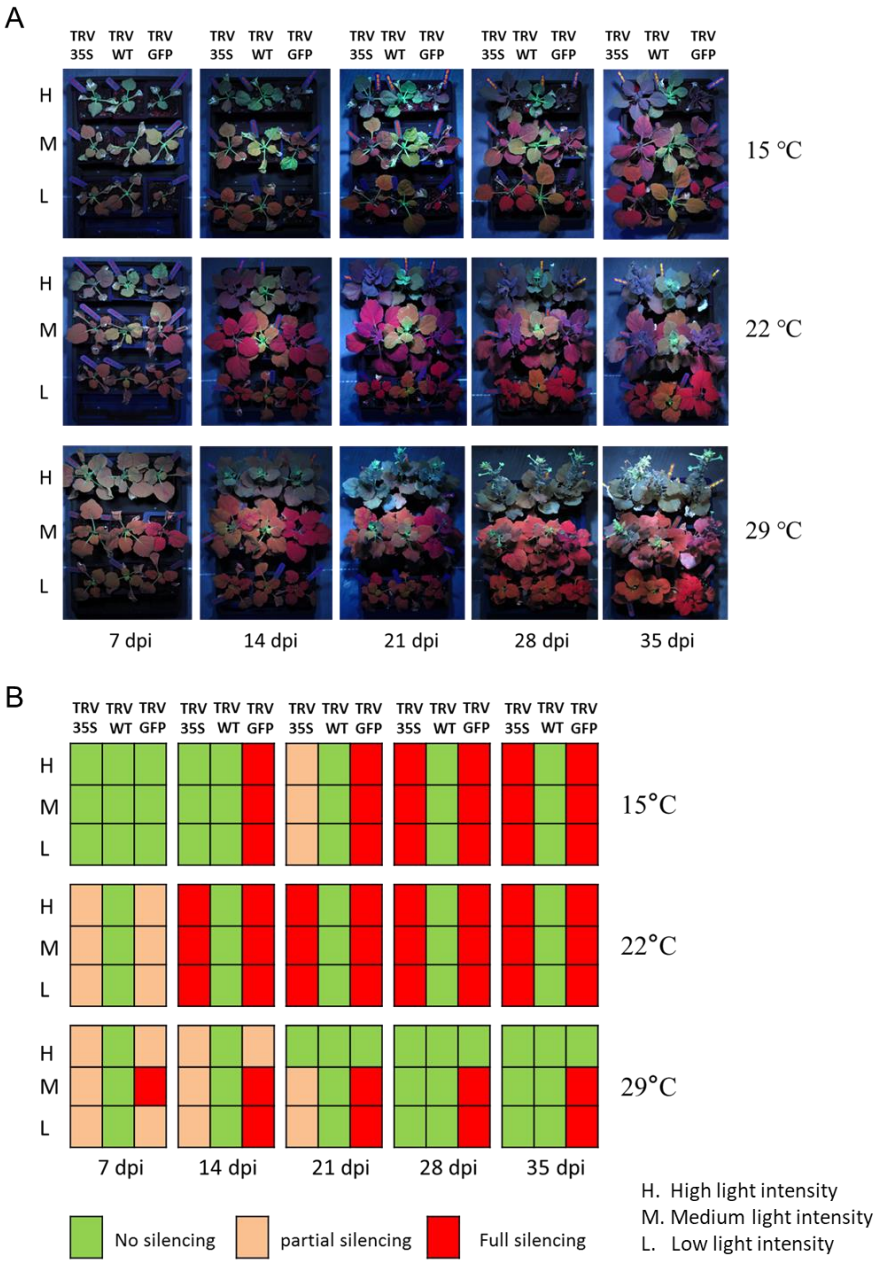

Figure 4.4 Effect of temperature and light intensity on TRV-induced gene silencing in *N. benthamiana* 16c plants. (A) Phenotype of TRV-infected *N. benthamiana* 16c plants kept at the indicated temperature and light intensity. The plants were inoculated with TRV vectors TRV-35S, TRV-WT, and TRV-GFP, which are indicated at the top of each panel. The inoculated plants were photographed under UV light. (B) Schematic presentation of the effect of temperature and light intensity on VIGS. Each cell in the diagram represents the qualitative results of five replicate plants. The silencing status is indicated by different colours (green colour: no silencing; pink colour: partial silencing, the plants developed systemic silencing however they recovered over time; red: full silencing.)

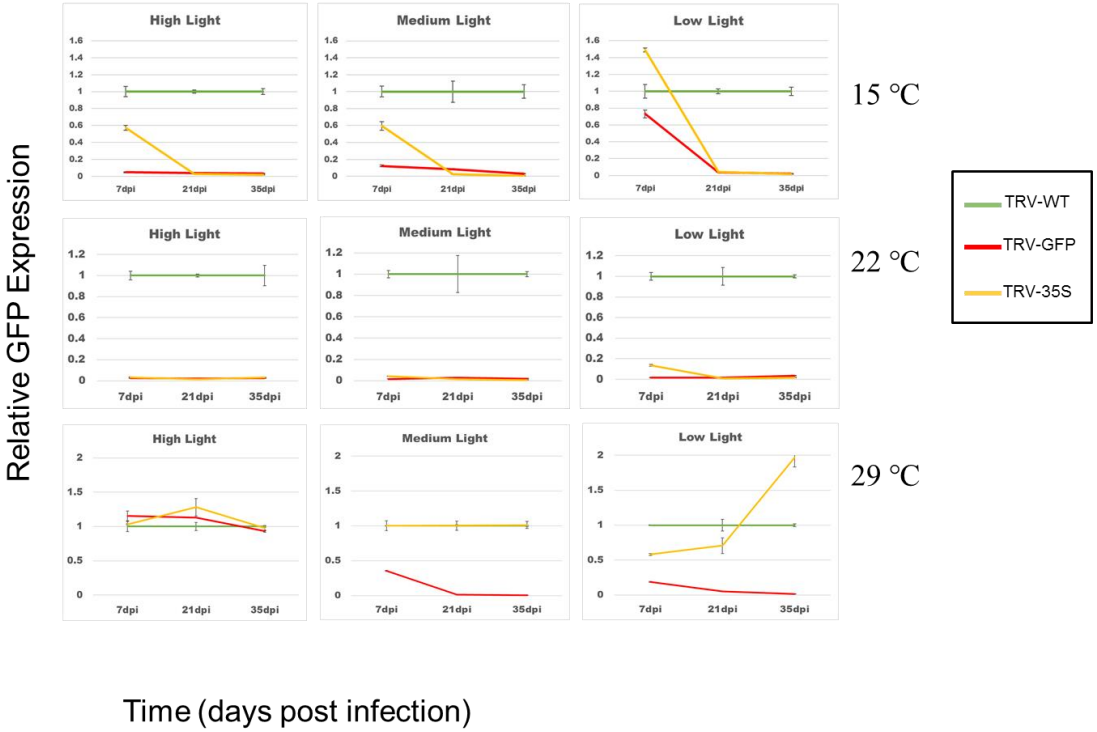

Figure 4.5 qRT-PCR to quantify GFP expression in infected plants shifted to 15/22/29℃ under low, medium or high light intensities. Samples were collected at 7 dpi, 21 dpi and 35 dpi. GFP expression level of TRV-GFP-infected plants (red) and TRV-35S-infected plants (yellow) were normalized to plants inoculated with TRV-WT (green).

4.2.3 The TRV-35S and TRV-GFP-inoculated plants exhibit delayed GFP silencing at low temperature

Compared to the plants kept at 22℃, both the TRV-35S and TRV-GFP infected plants showed delayed GFP silencing at 15℃ **(Figure 4.4)**. The loss of GFP signal could be observed by 14 dpi at 15℃, which was a week later than what we observed at 22℃. In addition, the rate of silencing induction was different between TGS and PTGS at low temperature. The initiation of TGS was slower than PTGS. The PTGS could be clearly visible by 14 dpi, whereas the TGS was very weak at this point **(Figure 4.4)**. Quantification of the GFP expression by qRT-PCR confirmed the phenotypic observation. A full reduction of GFP expression could be detected in TRV-GFP infected plants (PTGS samples) by 7 dpi, whereas TRV-35S infected plants only showed half reduction of GFP mRNAs compared to TRV-WT infected plants at 7 dpi **(Figure 4.5 top panel)**. Interestingly, low light intensity significantly delayed the initiation of both PTGS and TGS at 7dpi, which might be due to the extreme growth-limiting condition (low light and low temperature) affecting plant defence, viral replication and translation. This result is concordant with previous reports that both virus and transgene triggered RNA silencing are less active at low temperature, and the amount of virus- or transgene-derived siRNAs is greatly reduced (Szittya et al, 2003). Due to the insufficient production of siRNA, siRNA-mediated methylation might decrease as well, resulting less efficient TGS and reduced DNA methylation level. Although low temperature (15℃) caused delay in the onset of TGS and PTGS, both TGS and PTGS could be stably maintained. Therefore, low temperature affects RNA silencing mainly in the initiation step but not in maintenance.

4.2.4 High temperature can inhibit ViTGS and ViPTGS in certain condition

At high temperature 29℃, antiviral RNA silencing exhibited a more dynamic response. At early stages of infection (7 dpi), the GFP silencing could be rapidly developed in both TRV-35S and TRV-GFP infected plants. However, TRV-35S induced GFP silencing appeared in some of upper systemic leaves, and could not spread to the whole plants or to the newly emerging leaves **(Figure 4.4A)**. By 28 dpi, GFP fluorescence was fully restored in TRV-35S infected plants. In contrast, TRV-GFP infected plants exhibited stronger and persistent silencing phenotype under medium light and low light, and GFP silencing was stably maintained until 35 dpi **(Figure 4.4)**.

Interestingly, light intensity showed stronger effects on virus-induced gene silencing at 29℃ compared to 15℃ and 22℃. Virus-induced GFP silencing was greatly inhibited under high temperature and high light conditions. No matter whether the plants were inoculated with TRV-35S or TRV-GFP, they could only induce very weak GFP silencing in the first systemic leaves, which did not spread to the whole plants **(Figure 4.4)**.

Consistent with the observed GFP fluorescence in infected plants, qRT-PCR confirmed that the GFP expression was suppressed in TRV-GFP infected plants under medium and low light **(Figure 4.5 bottom panel)**. Furthermore, our data also revealed that the ViTGS was sensitive to high temperature, TRV-35S could only induce silencing in first systemic leaves which did not spread further to the newly emerging leaves.

4.2.5 Inefficient ViTGS cannot get passed to the subsequent generations

It has been shown in previous studies that virus-induced TGS could be heritable to the subsequent generations (Jones *et al.*, 2001, Kanazawa *et al.*, 2011). To determine whether the different growth temperatures affect the inheritance of ViTGS, we analyse the GFP expression in the progeny [named silenced generation 1 (S1) plants] of TRV-35S infected plants [silenced generation 0 (S0) plants] which were grown at 15℃/ 22℃/ 29℃. The progeny of TRV-GFP and TRV-WT infected plants were included as controls. S1 Seedlings were germinated at 22℃. As expected, no GFP silencing could be observed in the progeny of TRV-GFP and TRV-WT infected plants **(Figure 4.6)**. In contrast, the S1 progeny of TRV-35S infected plants that were kept at 22℃ maintained GFP silencing, indicating that TGS was stably inherited to the next generation. This is in line with published reports (Jones *et al.*, 2001, Kanazawa *et al.*, 2011). Interestingly, the progeny of TRV-35S infected plants that were grown at 29℃ did not show any GFP silencing **(Figure 4.6)**. This result suggests that inefficient TGS in the infected plants can greatly reduce or even impair the heritability of ViTGS to the next generation.

To gain insight into the DNA methylation status of the targeted promoter, bisulfite sequencing was used to analyse the level of DNA methylation in infected plants and their progeny. As shown in **Figure 4.7**, high level of DNA methylation was detected in the CaMV 35S promoter (nt -208 to -89) region of TRV-35S infected plants kept at 15℃ and 22℃, and the symmetric DNA methylation patterns (CG and CHG) were greatly maintained in the next generation. In contrast, only a few or no cytosine residues of the promoter were methylated in TRV-35S infected plants kept at 29℃ and in their progeny plants. The bisulfite sequencing results were correlated with the silencing phenotype of the plants, and confirmed that TRV-35S can direct stable and heritable TGS at 15℃ and 22℃, but the virus is inefficient to change the epigenetic status of the target promoter at higher temperature.

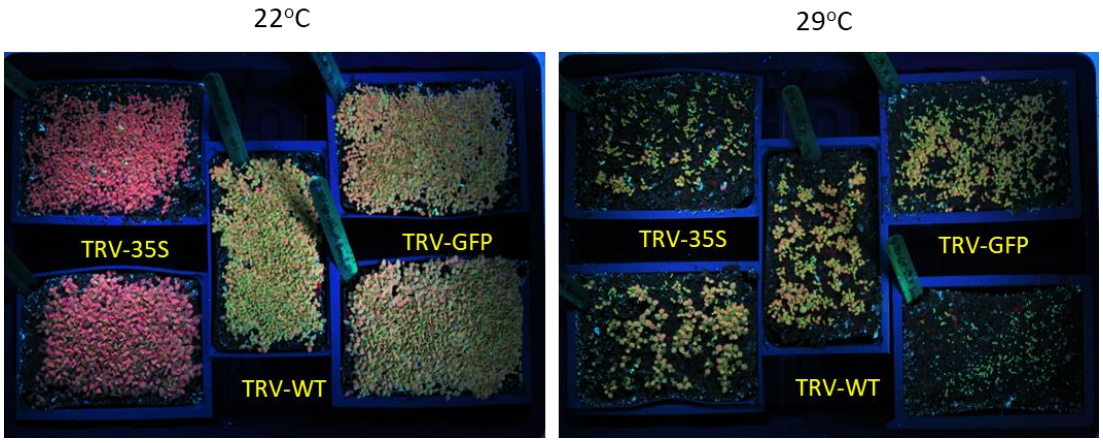

Figure 4.6 Inheritance of virus-induced TGS. S1 Seeds were collected from TRV-35S, TRV-WT and TRV-GFP infected plants (S0) grown at 22°C and 29°C, at medium light intensity. S1 Seedlings were germinated at 22°C and the level of GFP expression was monitored under UV light 10 days after germination.

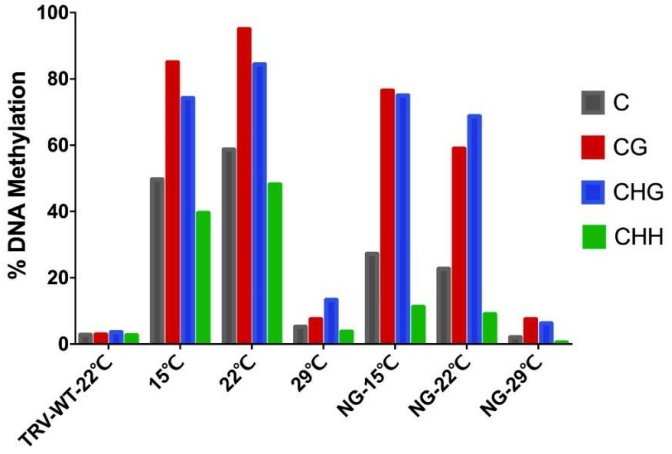

Figure 4.7 Bisulfite sequencing analysis of DNA methylation at 35S promoter (from -208 to -89) region in TRV- infected and their progeny plants. Total plant DNA was extracted from TRV-35S-inoculated *N. benthamiana* 16c plants kept at 15/ 22/29°C at medium light, at 35 dpi. Plant DNA extracted from TRV-WT kept at 22°C was used as negative control. For analysis of DNA methylation in progeny plants, S1 seeds (NG) were collected from the TRV-35S infected plants kept at 15/ 22/29°C at medium light. S1 Seedlings were germinated at 22°C and the DNA used for bisulfite sequencing was extracted from 7-week old plants. The context of methylation is represented by different colours: CG is in red, CHG is in blue, and CHH is in green. The total methylated cytosine is represented by gray bars.

4.2.6 The initiation and maintenance of DNA methylation are not impaired at high temperature

In the above experiment, I demonstrated that high temperature could largely inhibit ViTGS, but not ViPTGS. The inefficient ViTGS at high temperature could be related to reduced siRNA synthesis, siRNA activity or siRNA amplification. To investigate which of these hypothesises is correct, I employed various plant silencing systems.

First, the initiation of TGS under high temperature was assessed through *Agrobacterium*-mediated transient assays. The rationale for using the transient expression system was to enable the direct analysis of the effects of temperature on TGS induction, without needing to consider potentially confounding factors such as viral replication, accumulation and spreading, which would likely affect the rate of silencing induction at different temperatures.

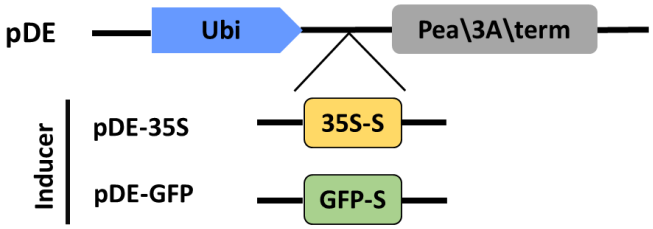

Figure 4.8 Induction of RNA silencing by *Agrobacterium*-mediated transient expression system. Schematic diagram of the constructs used for silencing induction. The vector contains a 120 nt fragment either from the 35S promoter (pDE-35S) or from the GFP coding region (pDE-GFP) to induce TGS or PTGS of GFP in 16c plants, respectively. Ubi, Ubiquitin promoter; Pea\3A\term, terminator.

The 120 nt fragment of silencing inducer from CaMV 35S promoter and GFP coding region used in VIGS experiments (see **Figure 4.1**) were cloned into pDE vector to induce TGS and PTGS, respectively **(Figure 4.8)**. Then, leaves of *N. benthamiana* 16c were infiltrated with cultures of *Agrobacterium* containing the TGS inducer (pDE-35)

or the PTGS inducer (pDE-GFP). Early studies have shown that temperatures around and above 29℃ are nonpermissive by the bacterium as a result of failure in pilus formation (Del Toro *et al.*, 2014). To overcome this, the agro-infiltrated plants were first incubated at 22℃ for two days, allowing the *Agrobacterium*-mediated T-DNA transfer into plant cells, and then shifted to different temperatures 22℃, 25℃, and 29℃. Plants were photographed under UV light every 7 days. Unlike the TRV-VIGS system, in the agropatch assay the efficiency of TGS and PTGS was gradually increased by raising temperature from 22℃ to 29℃, and the earliest GFP silencing was observed at 29℃ by 7 dpi **(Figure 4.9A left panel)**. Then, by 14 dpi, all inoculated patches exhibited completely GFP silencing, which were stably maintained under all different temperatures **(Figure 4.9A middle panel)**. Quantification of the small RNAs by northern blot revealed that 35S- and GFP-derived siRNAs were produced in large quantities in the plants kept at higher temperature (25℃ and 29℃) as early as 7 dpi. The highest level of siRNAs accumulation was observed in the plants grown at 22℃ at 14 dpi **(Figure 4.9B)**. This data confirmed that raising temperature could promote RNA silencing through the increased production of siRNAs.

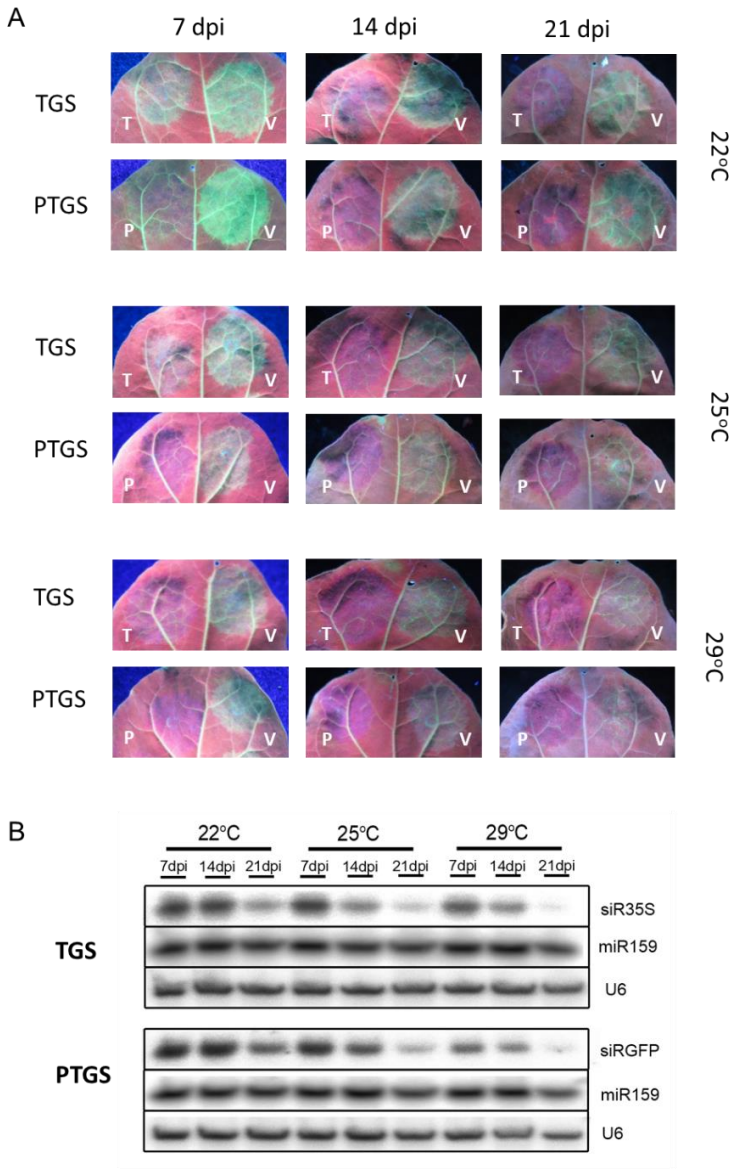

Figure 4.9 Analysis of the efficiency of TGS and PTGS under different temperatures in *Agrobacterium*-mediated transient expression system. (A) Leaves of *N. benthamiana* 16c infiltrated with cultures of *Agrobacterium* containing the TGS inducer (pDE-35) or PTGS inducer (pDE-GFP). Infiltrated plants were first kept at 22°C for two days and then shifted to different temperatures. The inoculated leaves were photographed under UV light. T, TGS inducer; P, PTGS inducer; V, empty vector pDE. (B) Northern blot analysis of small RNA accumulation in infiltrated patches. Leaves samples collected from TGS inducer infiltrated patches were hybridized with 35S promoter-specific probes (upper panel) and samples collected from PTGS inducer infiltrated patches were hybridized with GFP-specific probes (lower panel). miR159 and U6-transcript probe were used as loading controls.

Since the high temperature does not impair the initiation of TGS, the next assumption I wanted to test was whether the maintenance of DNA methylation could be disturbed at the high temperature. To investigate this, I used the seeds of TRV-35S infected plants grown at ambient temperature to ensure high level of transgenerational gene silencing. After germination, the plants were shift to high temperature in order to assess the maintenance of the silencing phenotype (**Figure 4.10)**.

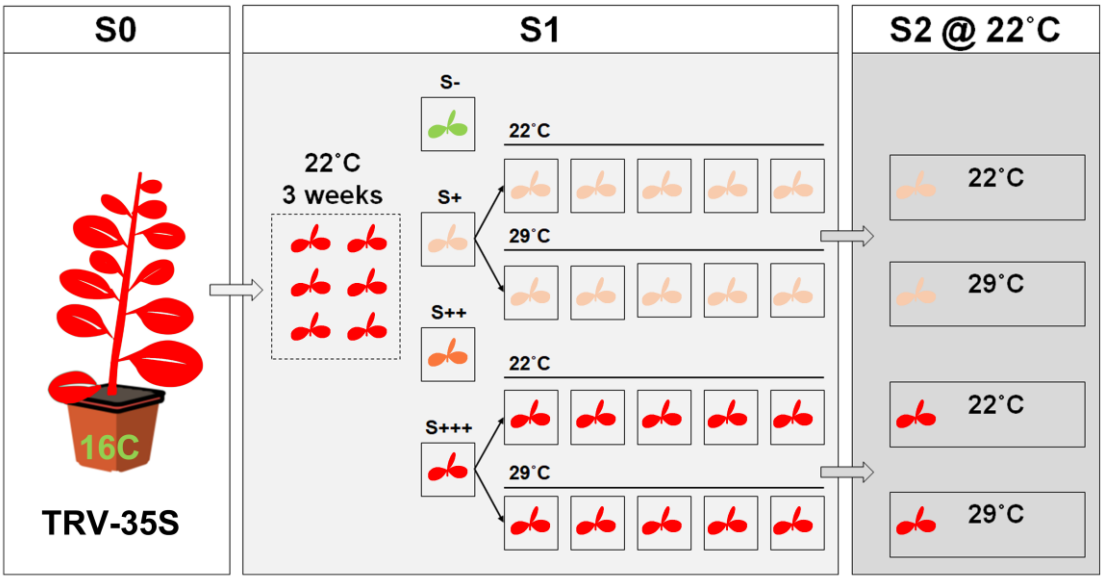

Figure 4.10 Schematic diagram of experimental design to assess the maintenance of DNA methylation at the high temperature. S1 seeds were collected from TRV-35 infected plants (S0) and germinated at 22°C. According to the degree of inherited GFP silencing, three-week-old S1 seedlings were sorted into four groups: no silencing (S-), silencing+ (S+), silencing++ (S++), and silencing+++ (S+++). Plants from S+ and S+++ lines were selected and shifted to 22°C and 29°C, respectively. S2 seeds were collected from S1 plants. S2 Seedlings were germinated at 22°C and the level of GFP expression was monitored under UV light 20 days after germination.

The S1 progeny of the TGS plants usually exhibits variable degree of GFP silencing. To avoid this side effect on assessing the maintenance of TGS, all seeds were firstly germinated at 22℃ for three weeks, and then were sorted into groups based on the degree of inherited GFP silencing. To this end, first, the S1 progeny of TRV-35 infected plants were sorted into four groups according to the degree of inherited GFP silencing: no silencing, silencing+, silencing++, and silencing+++ **(Figure 4.11A)**. No silencing means that plants in this group have similar phenotype to 16c plants. Silencing+ refers to plants showing GFP silencing only in leaves. Silencing ++ means that plants show GFP silencing in leaves and in one pair of petioles. Silencing +++ plants display full GFP silencing both in leaves and in two pairs of petioles. The selected silencing+ and silencing+++ lines were shifted to 22℃ and 29℃, respectively (**Figure 4.10)**. After been shifted to 29℃, the TGS was maintained and GFP silencing was not reversed in S1 plants. Then, S2 seeds were collected from individual S1 plants to assess the TGS in the subsequent generations. All S2 seeds were grown at 22℃. Progeny of TRV-WT infected plants were kept under the same conditions and used as controls. The maintenance of GFP silencing was assessed under UV light at 20 days after germination. This analysis revealed that the S2 generation maintained the same degree of GFP silencing as its previous generations, which suggests that the maintenance of DNA methylation is stable at high temperature **(Figure 4.11B)**.

Taken together, these results suggest that the high temperature does not impair the initiation or maintenance of DNA methylation. Furthermore, our results also indicated that DNA methylation as an epigenetic marker could be stably maintained at high temperature, suggesting that ViTGS can stably and heritably moderate gene expression in crop plant. However, further quantitative analysis on mRNA level and DNA methylation need to be included to confirm the observation. Moreover, since the stable and uniform TGS lines were obtained from the S2 generation. It is worth to challenge these lines at high temperature for several generations to assess the stability of TGS.

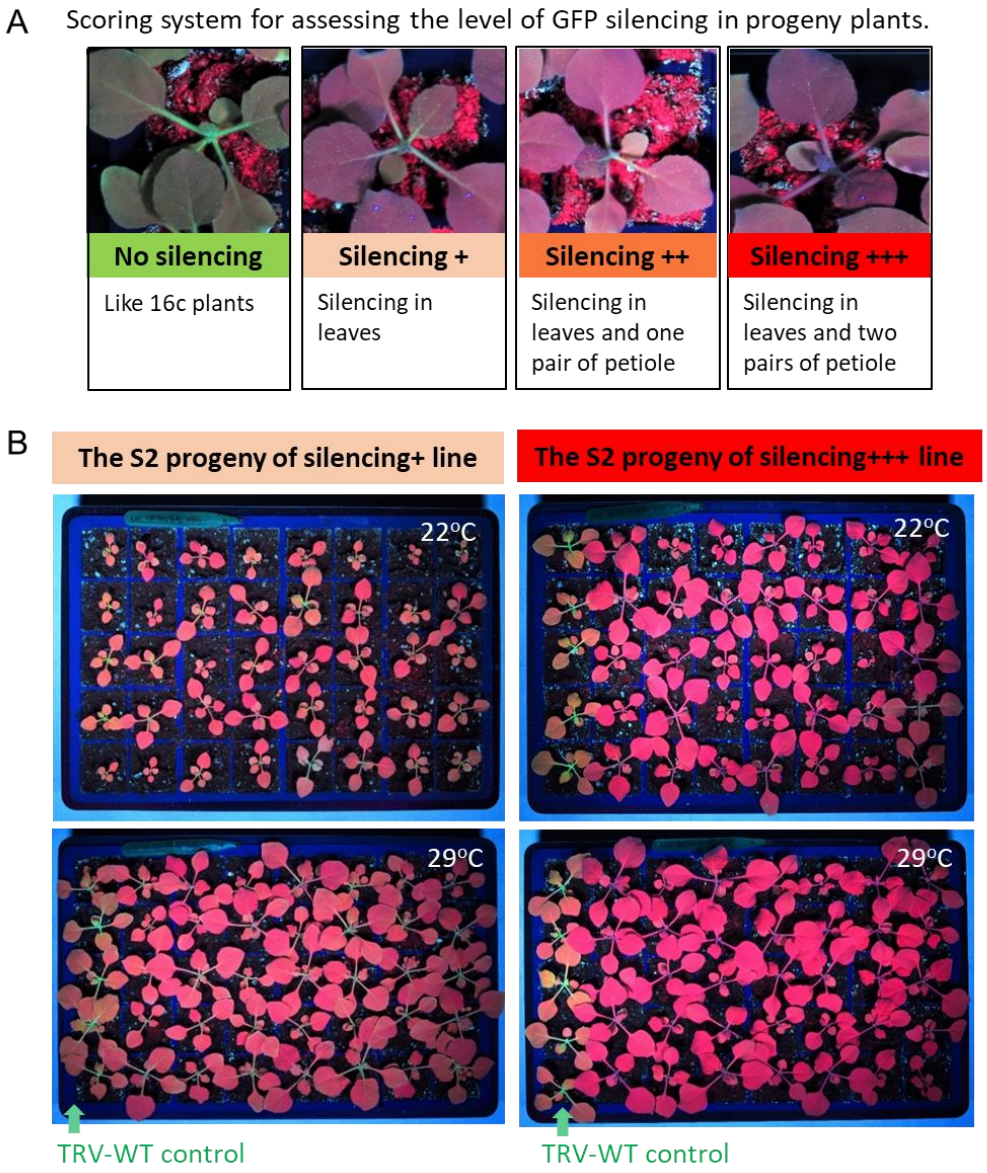

Figure 4.11 The maintenance of DNA methylation under high temperature. (A) Scoring system for assessing the level of GFP silencing in progeny plants. According to the degree of inherited GFP silencing, the S1 progeny of TRV-35S infected plants were sorted into four groups as shown in the figure. (B) Inheritance of virus-induced TGS was not effected by high temperature. The S2 Seeds were collected from silencing+ line (left panel) and silencing+++ line (right panel) grown at 22°C and 29°C, at medium light intensity. S2 Seedlings were germinated at 22°C and the level of GFP expression was monitored under UV light 20 days after germination. Progeny of TRV-WT infected plants were used as GFP fluorescence controls.

4.2.7 Distinguishing primary and secondary small RNA by using specifically designed inducer sequences

Since 29℃ does not impair the initiation and maintenance of DNA methylation, the next hypothesis we tested was that the inefficient TGS at the high temperature might be due to the lack of secondary small RNA production/amplification. It has been well established that PTGS is associated with the production of secondary sRNAs. However, not much is known about secondary sRNAs in ViTGS.

In order to test the above hypothesis, TRV-35S, TRV-35S-2M, TRV-GFP and TRV-GFP-2M recombinant viruses were used in the subsequent experiment **(Figure 4.12A)**. As described in Chapter 3, TRV-35S-2M is the recombinant TRV carrying SNSs every 10 nucleotides in the 120-nt 35S promoter sequence. sRNAs processed from TRV-35S-2M contained at least two mismatches to their target sequence. TRV-GFP-2M was designed with a similar approach targeting a 120-nt segment from the GFP coding region **(Figure 4.12A)**. With the above recombinant TRVs, primary and secondary small RNAs can be well distinguished via high throughput sequencing: sRNAs containing SNSs are primary siRNAs generated from the virus, while sRNAs could perfectly matching to the target sequence are secondary sRNA amplified from the plant **(Figure 4.12B)**.

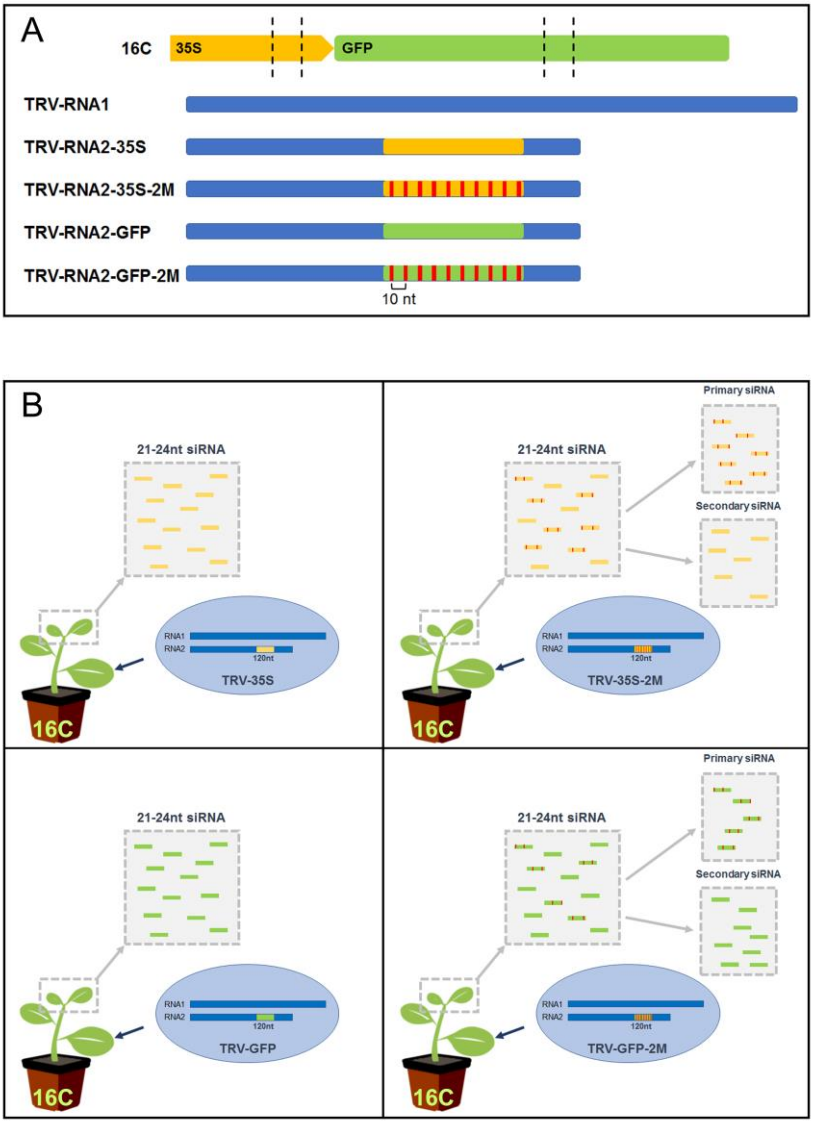

Figure 4.12 Schematic diagram of experimental design to distinguish primary and secondary small RNAs. (A) Schematic diagram of *N. benthamiana* 16c plant harbouring GFP transgene (green) under the control of CaMV 35S promoter (yellow). The target regions are highlighted by dotted lines in the diagram. TRV (blue) was used as VIGS vector. A 120 nt fragment of the CaMV 35S promoter (-208 to -89) and the GFP coding sequence (364 to 483) was cloned into TRV-RNA2 to induce TGS and PTGS, respectively. SNSs were introduced to the 120-nt 35S sequence and the 120-nt GFP sequence at 10 nucleotide intervals to generate TRV-35S-2M and TRV-GFP-2M, respectively. The position of SNSs is indicated in red. TRV-RNA1 was used along with recombinant TRV-RNA2 to generate functional TRV particles. (B) sRNAs contenting SNSs (red) are primary siRNAs generated from the virus, while sRNAs without SNSs are secondary small RNA amplified from the plant.

4.2.8 Increased viral titre enhanced the VIGS at high temperature

In our previous experiment, we found that high temperature had a greater impact on TGS than on PTGS. Thus, 22℃ and 29℃ were examined here. Some changes were also made to the previous experimental design. After infection, the plants were incubated at 22℃ for two days before shifting to different temperatures. The reason for two-day-incubation at 22℃ was to allow virus upload into the phloem. It may reduce the effect of temperature on virus replication and spreading at the early stages of infection.

Indeed, the qRT-PCR analysis of the virus-infected plants indicated that more viruses were detected at 29℃ with a two-day-incubation at 22℃ post inoculation than without incubation **(Figure 4.13A)**. The increased virus level triggered the full GFP silencing in TRV-GFP infected plants at the high temperature even at high light, indicating that the inefficient ViPTGS at high light that we observed previously was likely due to the limited virus loading at the early stages of infection.

In line with the TRV-GFP data, TRV-35S infected plants showed more expanded TGS in the systemic leaves with two-day-incubation at 22℃. At 29 ℃, suppression of GFP expression could be observed in the TRV-35S infected plants by 7 dpi, but the GFP fluorescence was restored in the newly emerging leaves by 21 dpi **(Figure 4.14 and 4.15, left panel)**. In contrast, although the initiation of TGS was slower at 22℃, silencing status was stably maintained throughout the experiment **(Figure 4.14 and 4.15, right panel)**. To accurately measure GFP expression, qRT-PCR was performed using samples collected at 7 dpi and 21 dpi from the infected plants kept at 22℃ and 29℃. In agreement with the silencing phenotype under UV light, the reduction of GFP expression could be detected in TRV-35S infected plants maintained at 22℃ and 29℃ by 7 dpi **(Figure 4.13B)**. At 21 dpi, the GFP expression was completely suppressed in TRV-35S infected plants at 22℃, whereas it was restored at 29℃ **(Figure 4.13B)**.

Plants infected with the recombinant TRV carrying SNSs could also trigger GFP silencing, but the progression of reporter gene silencing was slower than what we observed with the unmodified inducers. Specifically, sRNAs carrying SNSs showed a greater effect on TGS than on PTGS. It normally took 14 days for TRV-35S to induce full GFP silencing at 22℃, whereas TRV-35S-2M needed 21 days to achieve the same phenotype **(Figure 4.15)**. Although TRV-GFP-2M also delayed the onset of PTGS, the GFP silencing could be observed in the whole plant by 14 dpi, which was similar to the TRV-GFP infected plants. Quantification of GFP expression by qRT-PCR revealed no differences between the TRV-WT infected plants and TRV-35S-2M infected plants at 7 dpi, but a more than 2-fold decrease in GFP expression was detected in TRV-35S infected plants **(Figure 4.13B)**. In contrast, the GFP expression was completely repressed in TRV-GFP and TRV-GFP-2M infected plants at 7dpi both at 22℃ and 29℃ **(Figure 4.13B)**. By 21 dpi, the GFP expression in TRV-35S and TRV-35S-2M infected plants reduced to similar level as TRV-GFP and TRV-GFP-2M infected plants at 22℃ **(Figure 4.13B)**.

We expected to see delayed GFP silencing in TRV-35S/GFP-2M infected plants because mismatched sRNAs might reduce targeting efficiency. However, the different rate of TGS and PTGS progression might indicate their differences in silencing signal amplification/ secondary small RNA production.

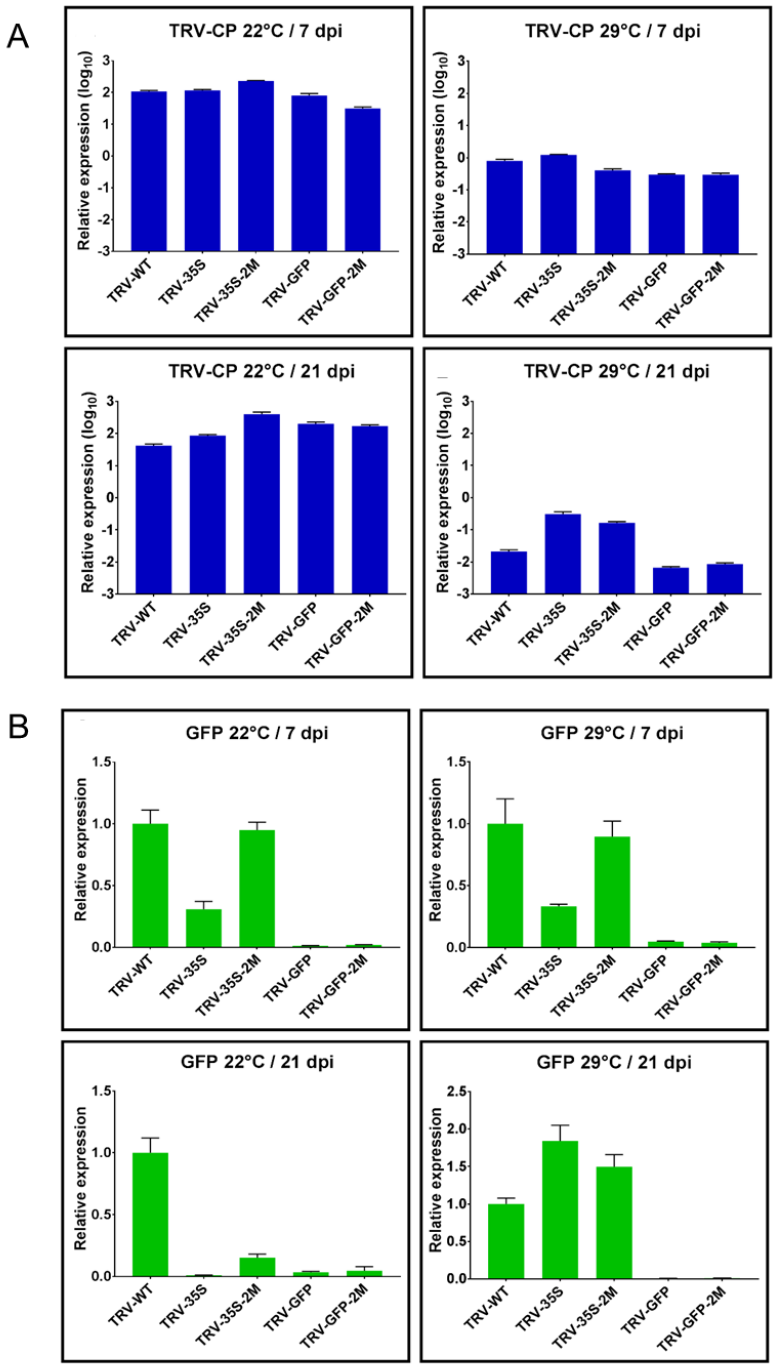

Figure 4.13 Quantification of TRV and GFP expression in TRV-infected plants under different temperatures. qRT-PCR analysis of virus accumulation (A) and GFP expression (B) in TRV-infected plants kept at 22℃ and 29℃. The samples were collected from the systemic tissues of infected plants at 7 dpi and 21 dpi. EF1α was used as a reference gene. Error bars represent the arithmetic mean of three technical replicates ± SEM

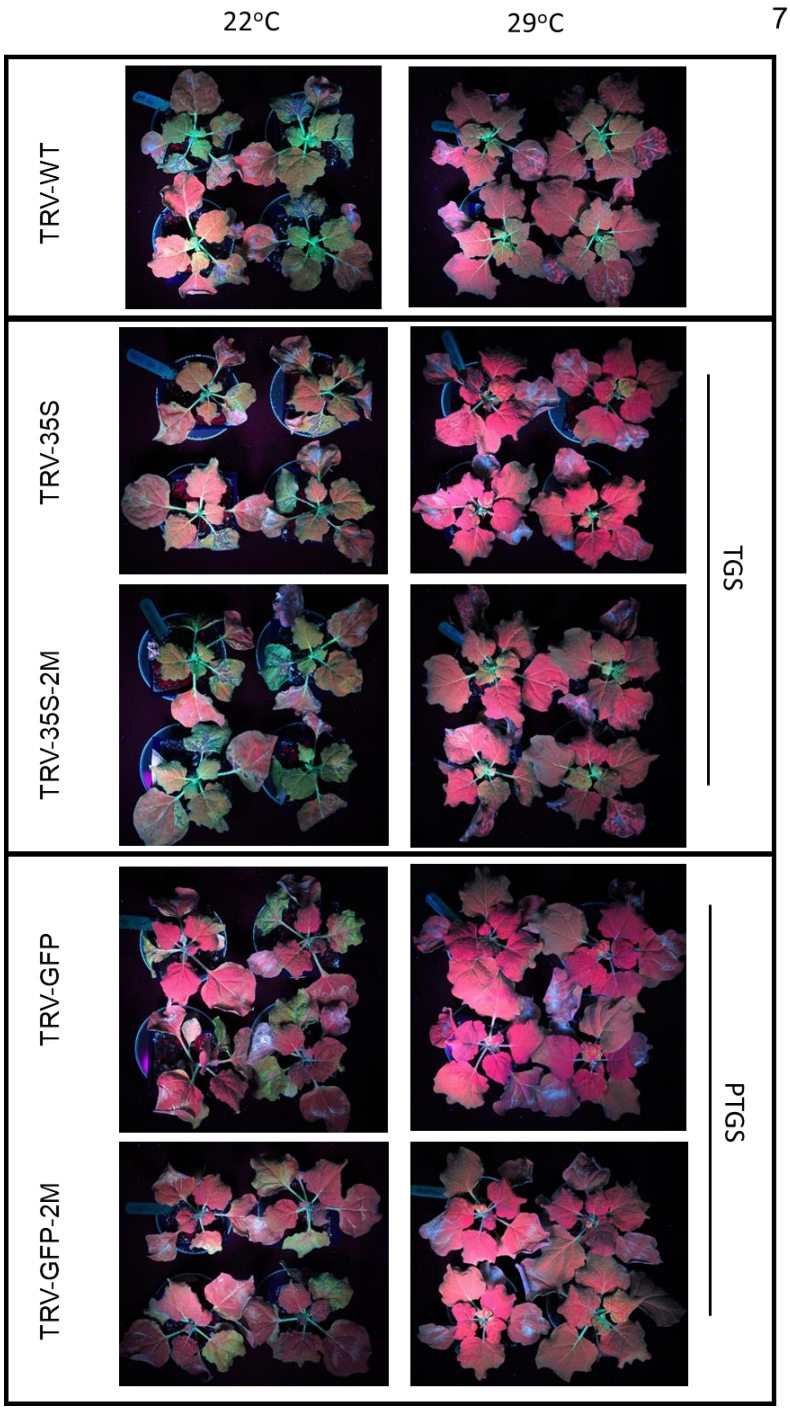

Figure 4.14 Phenotype of recombinant TRV-infected *N. benthamiana* 16c plants at 7 dpi. The plants were inoculated with recombinant TRV viruses as indicated on the left in each panel. After virus infection, plants were incubated at 22°C for 2 days, and then shifted to 22°C and 29°C, respectively. Photographs were taken under UV light at 7 dpi. GFP silencing results in red fluorescence due to the autofluorescence of chlorophyll. The TRV-WT infected *N. benthamiana* 16c plant was used as viral infection control (top).

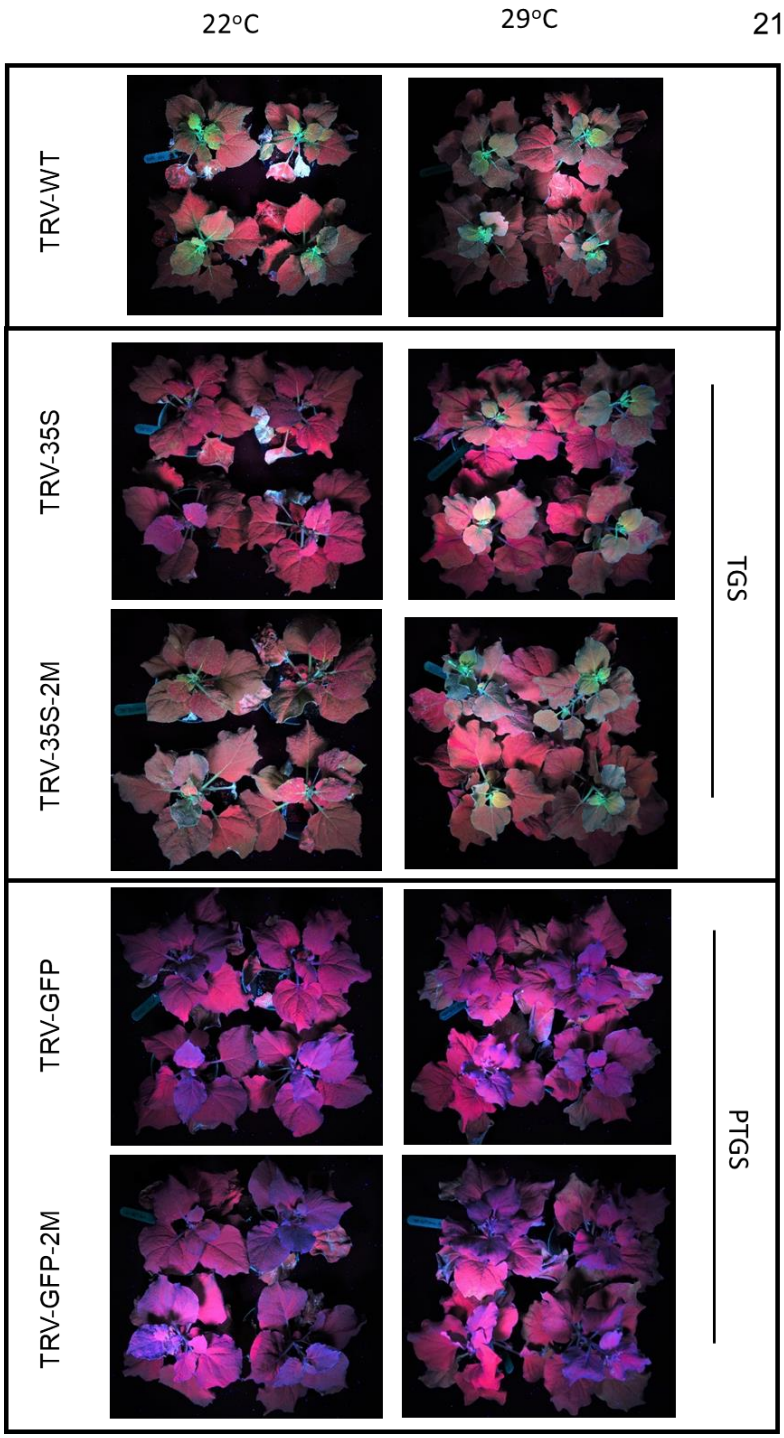

Figure 4.15 Phenotype of recombinant TRV-infected *N. benthamiana* 16c plants at 21 dpi. The plants were inoculated with recombinant TRV viruses as indicated on the left in each panel. After viral infection, plants were incubated at 22°C for 2 days, and then shifted to 22°C and 29°C, respectively. Photographs were taken under UV light at 21 dpi. GFP silencing results in red fluorescence due to the autofluorescence of chlorophyll. The TRV-WT infected *N. benthamiana* 16c plant was used as viral infection control (top).

4.2.9 Inefficient ViTGS at high temperature is associated with the limit production of siRNAs

To investigate whether the different efficiency of ViTGS and ViPTGS was due to differences in secondary sRNA production, small RNA deep sequencing was performed. Small RNA libraries were made from the systemic tissues of infected plants at 7 dpi and 21 dpi maintained under 22℃ and 29℃.

The sRNA reads were size filtered to 21-24 nt. First, sRNA reads were mapped to TRV-RNA2 that carrying the corresponding target sequence. The genome-wide distribution of sRNAs mapped to TRV-RNA2 were similar across all the infected plants kept at 22℃, indicating similar levels of TRV in those infected plants **(Figure 4.16)**. The small RNAs were predominantly 21-22 nt in length and generated from both the sense and antisense viral RNA. The number of small RNA reads, which could perfectly map to TRV-RNA2 was around 520,453 to 746,514 in the infected plants maintained at 22℃ by 7dpi **(Figure 4.16, left panel)**. By contrast, at 29℃ the abundance of TRV-RNA2-derived sRNAs in all size classes was significantly reduced by ~ 5-10 folds at 7 dpi **(Figure 4.17 left panel)**. Specifically, by 21 dpi, only around 1,091 to 20,699 small RNA reads could be mapped to the TRV-RNA2 genome at 29℃ **(Figure 4.17 right panel)**. These data were in agreement with the qRT-PCR results, high level of viral RNAs was detected at 22℃ which could generate large amounts of virus-derived siRNAs, whereas very few viruses were detected at 29℃ resulting low abundance of virus-derived siRNAs.

Strikingly, as shown in **Figure 4.17F**, 7,369 sRNA reads were clustered at the 120-nt GFP locus of TRV-RNA2-GFP in infected plants maintained at 29℃ at 21 dpi, which accounted for 75.36% of the total sRNA reads mapped to the TRV-RNA2-GFP genome. However, only 1.47% of total sRNA reads which mapped to the TRV-RNA2-GFP-2M genome could be mapped to 120-nt GFP-2M locus. It seems that the high level of GFP-derived sRNAs mapped to TRV-RNA2-GFP might be the secondary sRNA generated

from the target GFP mRNA. Interestingly, we could not observe a similar peak at the 35S fragment of TRV-RNA2-35S, and only 1.19% of total sRNA reads could be mapped to the corresponding segment. These data suggested that the different efficiency of ViTGS and ViPTGS at high temperature could be related to differences in secondary sRNA production.

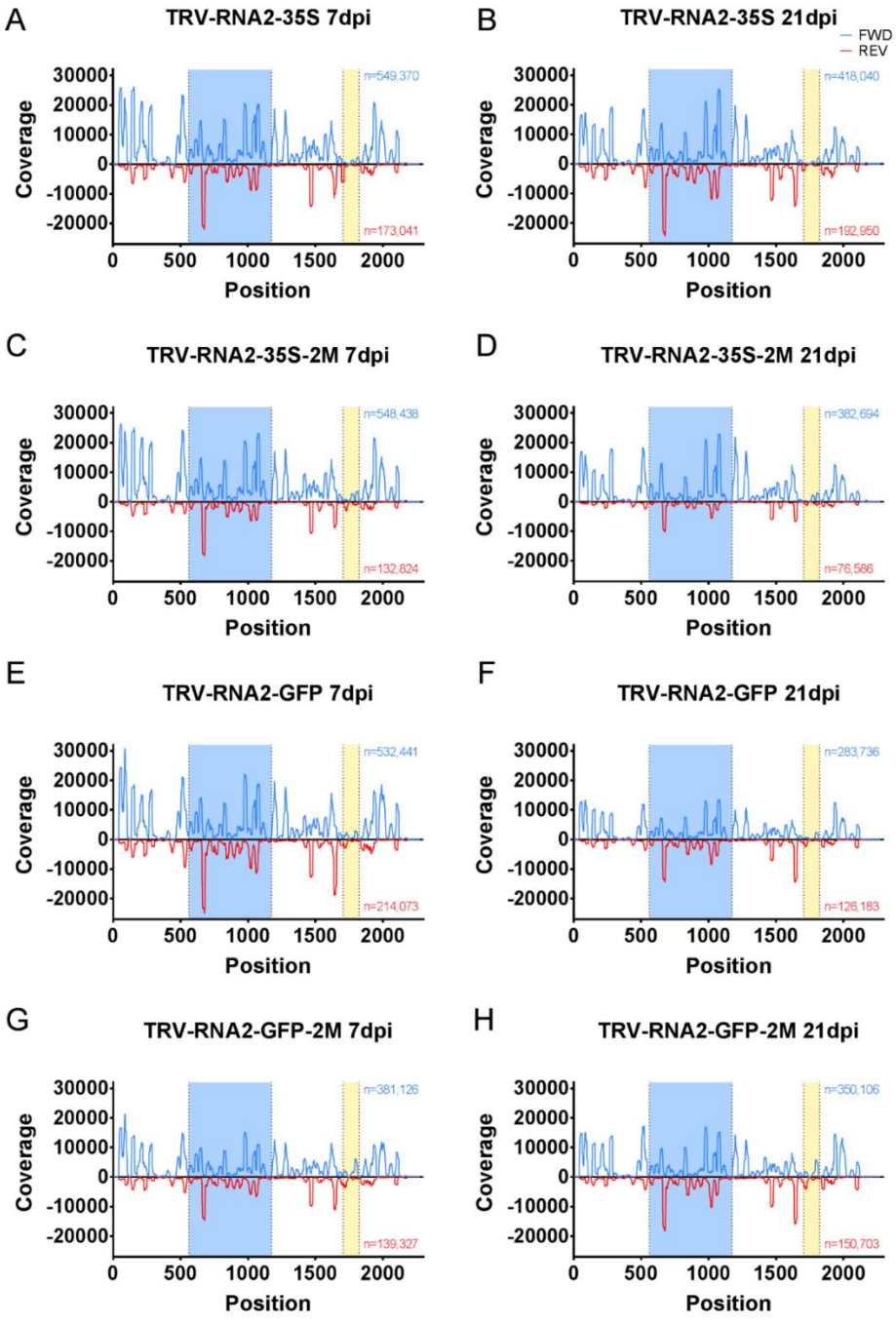

Figure 4.16 Analysis of virus-derived sRNAs in TRV-infected plants maintained at 22°C. Raw sRNA reads were aligned to the corresponding recombinant TRV RNA2 that is indicated above each graph. The positive or negative y axis shows the number of sRNAs on either plus or minus strand as blue or red lines, respectively. The coat protein and the silencing-inducer (35S and GFP-derived sequences are highlighted as blue and yellow boxes, respectively. The total number of sRNAs matching the above selected regions of the viral genome is also indicated in the graph.

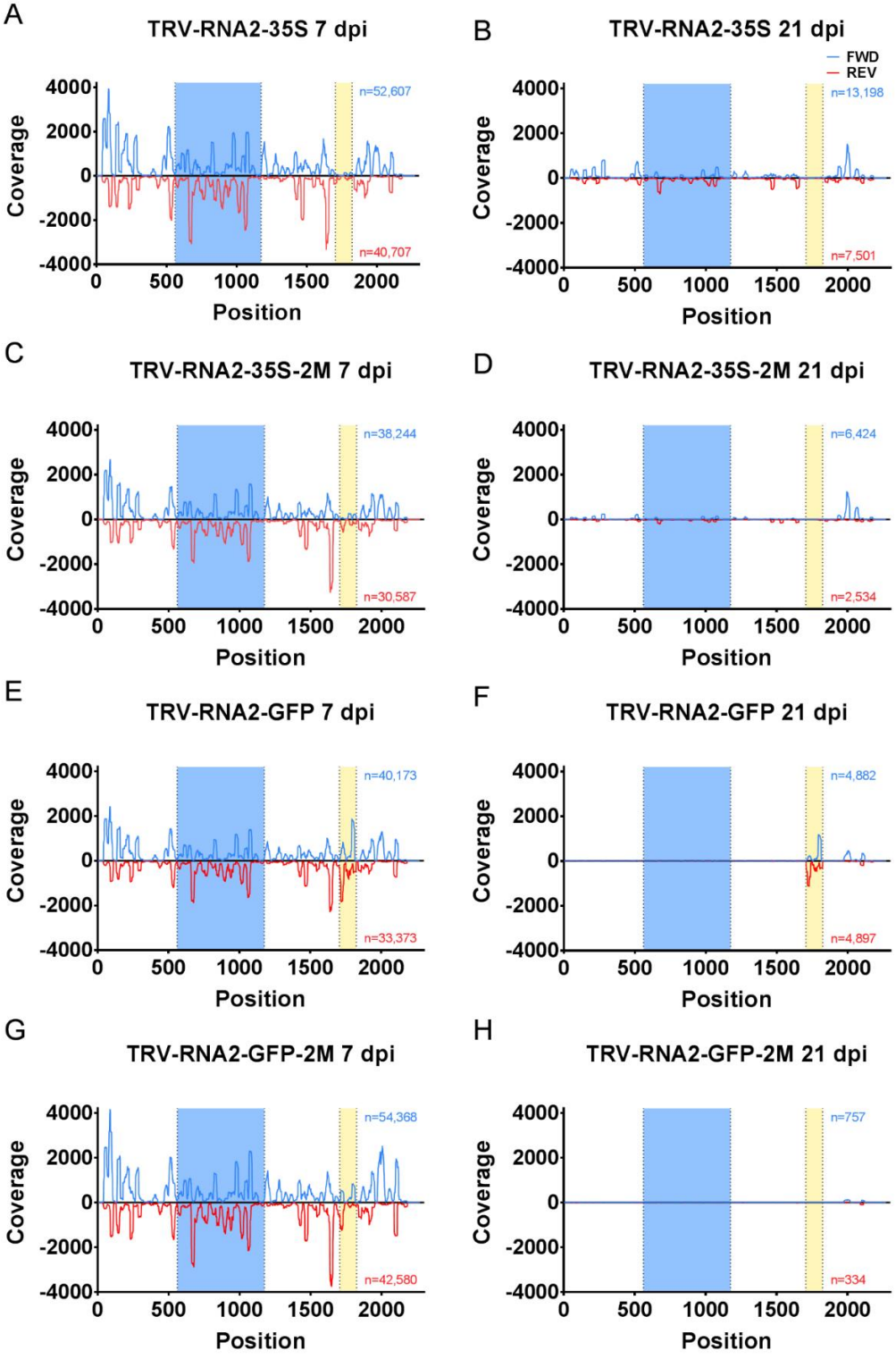

Figure 4.17 Analysis of virus-derived sRNAs in TRV-infected plants maintained at 29°C. Raw sRNA reads were aligned to the corresponding recombinant TRV RNA2 that is indicated above each graph. Labelling is indicated in Figure 4.16.

Then, we used the sRNA data set from TRV-GFP-2M infected plants and dissected the primary and secondary sRNAs by mapping the sRNA reads to GFP carrying the 120-nt mismatched sequence and the original/non-mutated GFP sequence. The sRNAs mapped to the 120-nt mismatched sequence are primary sRNAs produced from the viral genome **(Figure 4.12B)**. Those sRNAs which could perfectly map to the original GFP sequence are secondary sRNAs that are generated from the transgene GFP mRNA **(Figure 4.12B)**. The genome-wide map showed that high abundance of secondary sRNAs were produced from the GFP sequence. Interestingly, the major of sRNAs were mapped to the downstream (3') of the inducer sequence, confirming the previous studies that transitivity of GFP silencing is more dominant from the 5'to 3' direction rather than 3' to 5' **(Figure 4.18)** (Petersen & Albrechtsen, 2005, Vaistij *et al.*, 2013). Moreover, a high level of primary sRNAs could be visible from the 22℃ data sets, while very few primary sRNAs were detected at 29℃ **(Figure 4.18 middle panel)**.

Furthermore, the sRNA reads from TGS data sets were also analysed. In contrast to PTGS, our data revealed that secondary sRNAs were barely produced from the 35S target locus or adjacent regions. In TRV-35S-2M infected plants maintained under 22℃ at 7 dpi, 12,494 primary sRNAs could map to the 35S mismatched target sequence, while only 6 secondary sRNAs were map to the original 35S sequence **(Figure 4.19A)**. Likewise, 1,556 primary sRNAs and 10 secondary sRNAs were detected in TRV-35S-2M infected plants kept at 29℃ by 7dpi **(Figure 4.19B)**. Moreover, by 21 dpi, the number of primary sRNAs was reduced to 96, and none secondary small RNAs could be detected at 29℃. The extremely low number of secondary sRNAs detected from the 35S locus might suggest that they are not *bona fide* secondary sRNAs. It could be the background noise from the locus or the result of sequencing error. Therefore, the data presented here implies that targeting a promoter region with a virus cannot generate secondary sRNAs.

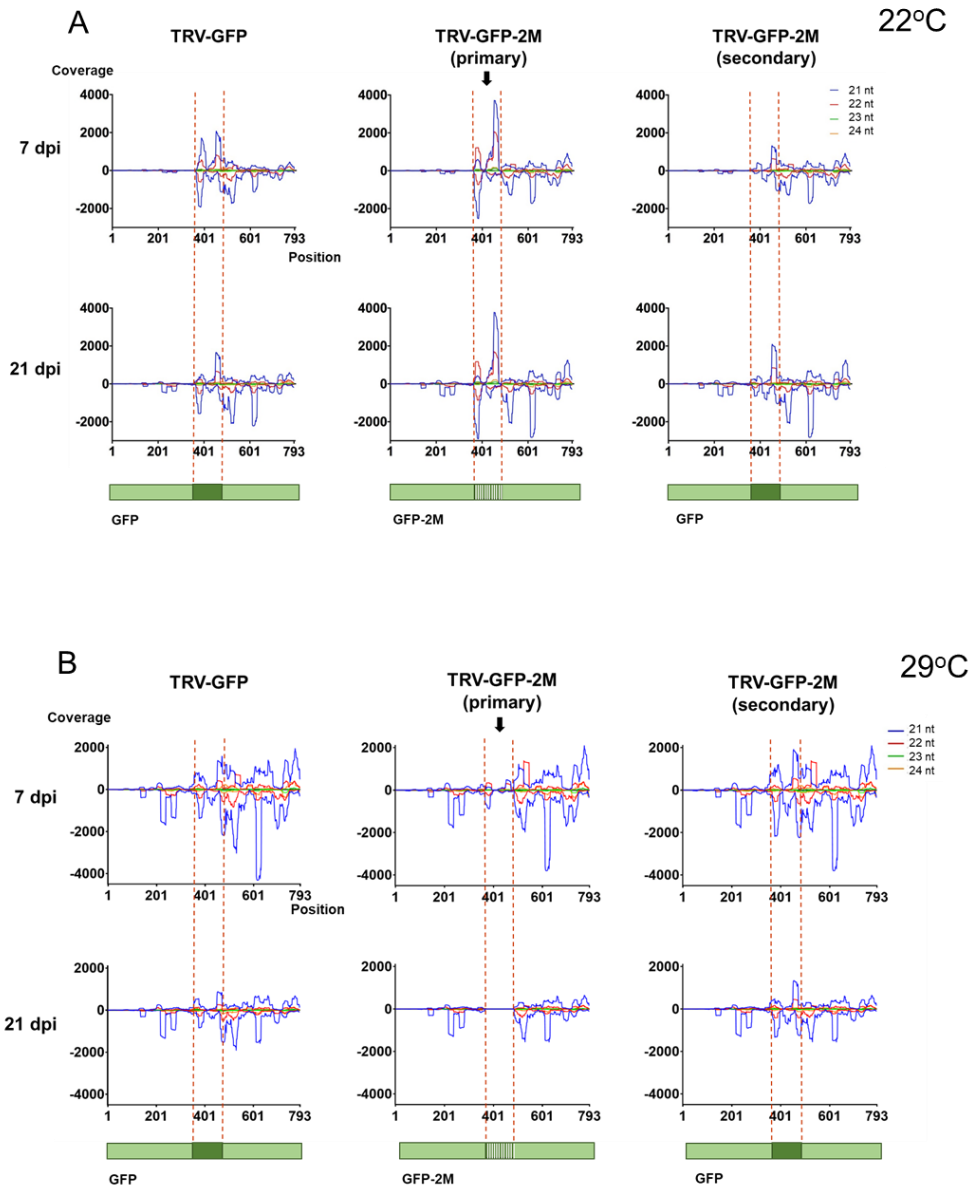

Figure 4.18 Virus-induced PTGS is associated with the accumulation of large amount of secondary sRNAs. sRNA analysis of *N. benthamiana* 16c plants infected with PTGS-inducing viruses TRV-GFP and TRV-GFP-2M maintained at 22°C (A) and 29°C (B). sRNA reads were aligned to the GFP coding sequence and to its variant GFP-2M containing the corresponding SNSs. sRNAs from TRV-GFP-2M infected plants were separated according to SNS content to yield primary (containing SNSs) and secondary sRNA (lacking SNSs). The numbers of sRNAs mapping at each position of the plus strand are shown as positive values, to the minus as negative values, for 21, 22, 23, 24 nt sRNAs separately. The target sequence is highlighted by dotted lines.

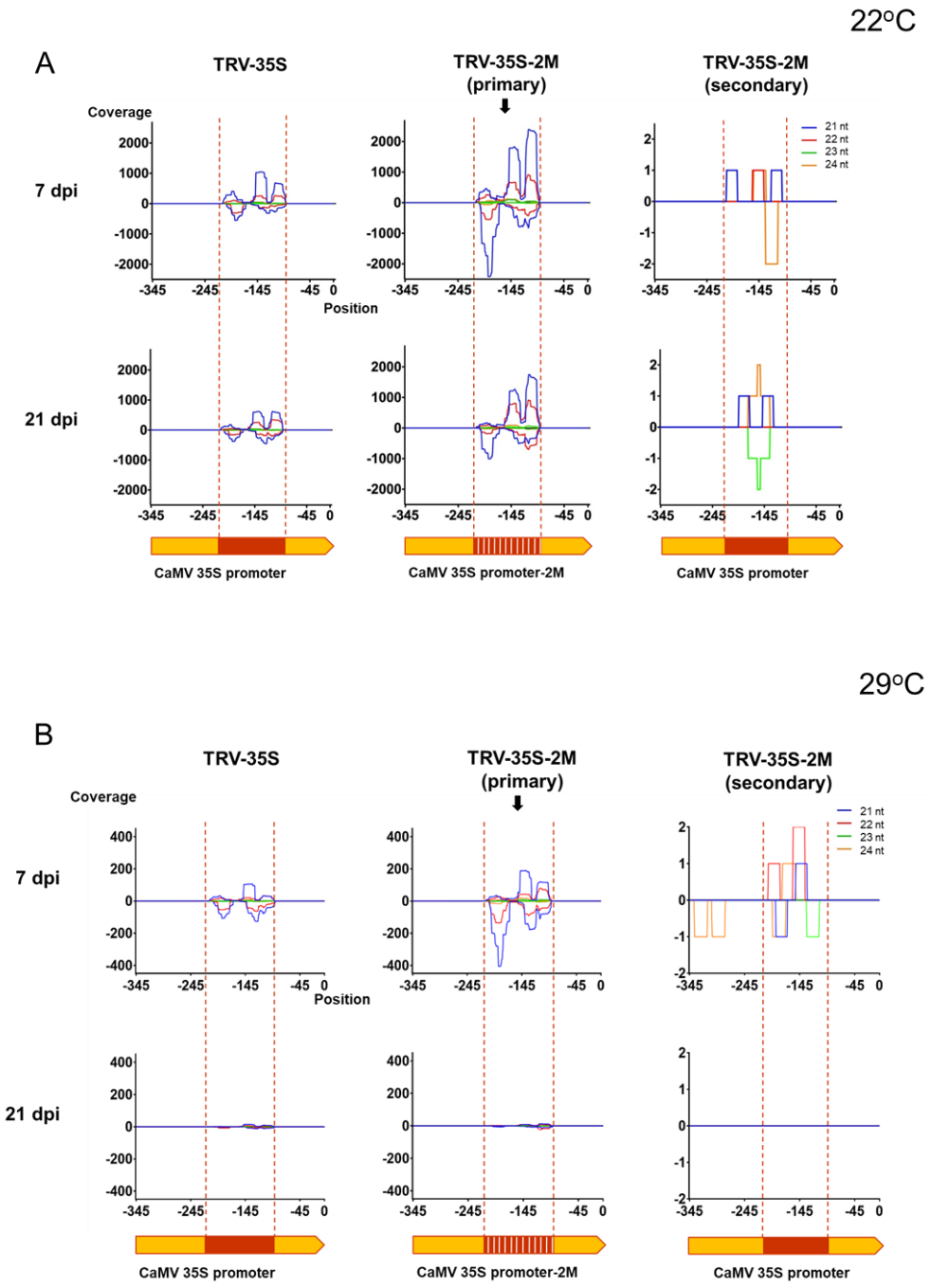

Figure 4.19 Virus-induced TGS is not associated with the production of secondary sRNAs. SRNA analysis of *N. benthamiana* 16c plants infected with TGS-inducing viruses TRV-35S and TRV-35S-2M maintained at 22°C (A) and 29°C (B). sRNA reads were aligned to the 35S promoter sequence and to its variant 35S promoter-2M containing the corresponding SNSs. sRNAs from TRV-35S-2M infected plants were separated into primary and secondary sRNAs according to SNS content. Labelling as in Figure 4.18.

Taken together, these results indicated that the inefficient ViTGS at 29℃ was due to the limit production of primary and secondary sRNAs. Unlike ViPTGS, which is associated with a large number of secondary sRNAs to reinforce their silencing, ViTGS barely produces secondary sRNAs. Since no secondary sRNAs could be generated from the plant genome, virus-derived primary sRNAs became the essential elements to initiate and maintain TGS. When infected plants were maintained at 29℃, viruses were efficiently degraded due to high temperature activation of antiviral RNA silencing. Consequently, it caused the reduction of primary sRNAs. This limited the amount of sRNAs to maintain TGS, therefore ViTGS was inefficient at 29℃.

4.3 Discussion

4.3.1 The effect of temperature on virus-induced gene silencing

It was previously demonstrated that RNA silencing is a temperature-dependent RNA degradation mechanism that operates inefficiently at low temperature likely due to reduced DCL activity and consequently decreased levels of siRNAs (Szittya *et al.*, 2003). Because VIGS operates via sRNAs we hypothesized that VIGS would be inhibited at low temperature. Indeed, unlike at ambient temperature where both TGS and PTGS work very efficiently **(Figure 4.4)**, cold treatment inhibited VIGS-mediated GFP silencing at 7 dpi. However, this was rather a delay than complete suppression of RNA silencing because both TRV-GFP and TRV-35S infected plants showed full GFP silencing by 28 dpi. Intriguingly, there was a difference in the progression of TGS and PTGS at 15℃. Two weeks after infection TRV-GFP infected plants displayed full systemic GFP silencing, while TRV-35S infected plants still exhibited GFP fluorescence. A week later, however, these plants started developing GFP silencing phenotype which were progressed to complete GFP suppression by 28 dpi. Thus, VIGS-induced TGS seems to be a more temperature sensitive process than PTGS. It is likely due to the mechanism of ViTGS, which is heavily depended on the production of virus-derived primary sRNAs. Low temperature reduces the activity of antiviral DCLs, which results in the reduction of virus-derived sRNAs and as consequently delays the initiation of TGS.

At high temperature, RNA silencing operates in an opposite direction. Unlike the previously reported plants grown at 30℃ exhibits reduced transgene S-PTGS due to SGS3 impairment (Zhong *et al.*, 2013), antiviral silencing was efficiently promoted by rising temperature. Early silencing phenotypes could be observed at 7 dpi both in TRV-35S and TRV-GFP infected plants **(Figure 4.14)**. Although S-PTGS overlaps with antiviral silencing in some steps, antiviral silencing turns out to be a more complex and dynamic system. It involves virus replication, host defence, and viral counter-

defence. In the context of results presented herein, it seems more likely that the temperature-sensitive DCLs play critical roles in antiviral silencing. This hypothesis can be further demonstrated by infecting plants deficient for antiviral PTGS. If the virus infected mutants show better recoveries at high temperature, it indicates high temperature can promote antiviral silencing.

It is interesting that there is a significant difference in the maintenance of TGS and PTGS at high temperature. The TRV-35S infected plants resumed GFP expression three weeks after infection, while TRV-GFP plants retained full GFP silencing. The inhibition of TGS at high temperature was caused by limited virus content. Consequently, the number of virus-derived primary sRNAs was reduced, which was not enough for TGS establishment in newly emerging leaves. In contrast, although the amount of virus was also low in the TRV-GFP plants, PTGS could produce large number of secondary sRNAs from the GFP transcript to stably maintain PTGS. This hypothesis is concordant with a recent report using VIGS of an active *FLOWERING WAGENINGEN* epiallele in *Arabidopsis* (Bond & Baulcombe, 2015). This study showed that the viral load in *dcl2/4(FWA^C)* and *dcl2/3/4(FWA^C)* V_0 plants was much higher than Col-0*(FWA^C)* plants, and the greater silencing of *FWA* in *dcl2/4(FWA^C)* V_1 plants than in Col-0*(FWA^C)* V_1 plants. In contrast, the RdDM and *FWA* silencing in the V_1 progeny of infected *dcl2/3/4* plants was not enhanced. To further confirm our hypothesis, it would be interesting to test whether high temperature could affect viral load in *dcl2/4(FWA^C)* V_0 plants and the silencing activity of *FWA* in *dcl2/4(FWA^C)* V_1 plants.

4.3.2 The effect of light intensity on virus-induced gene silencing

In a previous report, high light intensity positively affected RNA silencing initiation and spread (Kotakis *et al.*, 2010). It is inconsistent with our observation. This is likely due to the different experimental systems that were used. The published paper was based on transgene-induced gene silencing, whereas we used viruses to induce gene silencing. The plant-virus interaction is a dynamic process, which is greatly affected by environmental factors. Indeed, temperature has been shown to have a dominant effect on this interaction including my work. Light intensity examined here is likely to be an additive effect on RNA silencing. For instance, when high light is combined with high temperature, it provides an ideal growth condition for plants to outperform virus-infection. On the contrary, under a growth-limiting condition, such as low light and low temperature, the limiting performance of the plant would affect plant defence, viral replication and translation.

Comparing to the natural environment, the experimental design and growth conditions used in our study are rather artificial and simplistic. However, they provide insight into how environmental cues can affect plant-virus interaction under highly controlled conditions. Furthermore, our data can inform us about how to use recombinant viruses for modulating gene expression and the epigenome, which may be harnessed for inducing stable and heritable epigenetic modifications in crop plants.

4.3.3 The effect of secondary small RNA amplification on virus-induced gene silencing

With specially designed silencing inducer sequences, our VIGS system provided a direct method to distinguish primary and secondary siRNAs. In previous studies, they could identify secondary sRNAs only outside the target sequence, because there was no sequence variation between the inducer and the target (Aregger *et al.*, 2012, Härtl *et al.*, 2017). In contrast, our system provided a direct way to find and characterise the secondary sRNAs at the target locus. Mapping sRNAs to the mismatched inducer sequence could identify virus-derived primary sRNAs, whereas secondary sRNAs, which had no SNSs, were generated from the target loci and adjacent regions. Highly abundant secondary sRNAs were detected at the 120-nt GFP target sequence and adjacent regions in TRV-GFP-2M infected plants displaying PTGS **(Figure 4.17)**, indicating that this virus could activate the RDR-dependent production of secondary sRNAs. Interestingly, we found that secondary sRNAs were more abundant than primary sRNAs. This might be due to the transgene system we used, which expressed GFP under the control of a strong promoter (35S promoter), and produced numerous transcripts. Moreover, we observed that secondary sRNAs were spreading to both directions from the target sequences, further confirming the role of RDRs in the amlificication of the silencing signal. It is in accordance with previous studies that show sRNA spreading over a distance of at least 1000 nt from the 5' to 3', and up to 600 nt in the upstream direction in a primer-independent and primer-dependent manner (Petersen & Albrechtsen, 2005, Vaistij *et al.*, 2013).

Intriguingly, unlike PTGS, which generated large number of secondary sRNAs, ViTGS barely produced any secondary sRNAs. Only virus-derived primary sRNAs could be detected at the 120-nt 35S target locus, with no clear indication of sRNA amplification and spreading. Similar result has been observed in a study using a geminivirus Cabbage leaf curl virus (CaLCuV)-induced gene silencing system (Aregger *et al.*, 2012). The authors showed that the transgene GFP mRNA, which was targeted by CaLCuV-derived primary sRNAs generating massive amounts of secondary sRNAs.

In contrast, targeting the 35S promoter region by CaLCuV-derived primary sRNAs cause GFP silencing without secondary sRNA production. From these experiments, we conclude that virus-derived primary sRNAs are the only determinants in the establishment of RdDM. Deep sequencing of sRNAs revealed that the most abundant sRNAs in TRV-infected plants are the 21/22-nt size classes generated by DCL4 and DCL2. Thus, it is likely that 21-22 nt virus-derived sRNAs are the direct mediators of RdDM, This is in agreement with a previous study which suggested that DNA methylation in VIGS is initiated by virus-derived 21/22-nt sRNAs and reinforced or maintained by 24-nt sRNAs (Bond & Baulcombe, 2015).

VIGS is one of the most widely used plant functional genomics tools. Most of the VIGS vectors are used to induce PTGS through mRNA degradation or translation inhibition. ViPTGS is associated with the production of large amount of secondary sRNAs. They facilitate rapid gene silencing of the target genes. However, the phenotype of ViPTGS does not get passed on to the next generation. In the contrast, ViTGS is mediated by RdDM, which is heritable to the next generation. Similar to other methods, ViPTGS and ViTGS also have some limitations. For example, the efficiency of VIGS can be influenced by environmental factors. Results presented herein clearly show that environmental factors could significantly affect VIGS and plant-virus interactions. Our data further demonstrate that the inefficient ViTGS at high temperature is due to the limited production of secondary sRNAs. This study deepens our knowledge about the use of VIGS vectors as potential tools for epigenetic modification in crop plants.

Chapter 5: Assessing the effects of viral suppressors of RNA silencing on TGS and plant epigenome

5.1 Introduction

Plant viruses encode viral suppressors of RNA silencing (VSRs), as the most common strategy, to protect their genome against antiviral RNA silencing. VSRs of each virus genus and family are extraordinary diverse in structure and function, implying their diverse mechanistic activities. Indeed, VSRs were shown to block all steps of RNA silencing such as dicing, effector assembly, targeting, amplification, and transcriptional regulation of endogenous factors (Incarbone & Dunoyer, 2013).

The virus and host interactions at the PTGS level has been well documented, while the viral suppression at a TGS level is poorly understood. It was known that VSRs encoded by some DNA viruses could interfere with DNA methylation by mainly disrupting the methyl cycle, minimizing the methylation of their viral genome by the host defence (Buchmann *et al.*, 2009, Yang *et al.*, 2011). On the other hand, whether RNA viruses encoded VSRs could suppress TGS or not, has not been fully demonstrated. In previous study, it was shown that both VSRs HcPro and 2b can reverse PTGS of nitrite reductase gene (Nii), but failed to reverse TGS of 35S-GUS transgenes in the same plant (Marathe *et al.*, 2000). It is suggested that VSRs could affect transgene-induced PTGS mediated by 21-22-nt siRNAs, but not transgene-induced TGS mediated by 24-nt siRNAs. More recently, studies have been shown that HcPro can decrease the DNA methylation of endogenous gene promoters, which activated SA pathway and induced defence-related genes in virus-infected plants (Yang *et al.*, 2016). Additionally, the VSR protein 2b of RNA virus CMV was suggested to interfere with the RdDM pathway through binding of 24-nt siRNA in the nucleus, resulting in the inhibition of AGO4 activities (Duan *et al.*, 2012, Hamera *et al.*, 2012).

VSRs are recognised as pathogenicity factors that cause disease or developmental

abnormalities. One notable reason for disease symptom is that the antiviral and endogenous silencing pathways share common elements, and VSRs could interfere with these pathways. It was shown that VSRs from multiple viruses could inhibit miRNA activities and caused severe developmental defects in transgenic *Arabidopsis* overexpressing VSRs (Chapman *et al.*, 2004). Alternatively, another hypothesis is that VSRs, as pathogenicity factors, may have impact on DNA methylation of host genome and could alter gene expression epigenetically. Specifically, recent study reported that the CMV silencing suppressor 2b protein could cause reduction of DNA methylation in a genome-wide scale and reactivate some TEs in the 2b-transgenic plants (Zhao *et al.*, 2016). However, very little is known about how plant viruses can alter the epigenome in virus infected plants, how stable these epigenetic changes are over generations and how they affect gene expression and pathogen defence.

In this chapter, I firstly assessed the capability of RNA silencing suppressors interfering with PTGS and TGS through *Agrobacterium*-mediated transient expression system. Four well-studied silencing suppressors were selected from RNA viruses, including the *Cucumber mosaic virus* (CMV) 2b, *Tomato bushy stunt virus* (TBSV) P19, *Beet yellows virus* (BYV) P21, and *Turnip mosaic virus* (TuMV) P1/HC-Pro. Then, I developed recombinant viral vectors to assess the activity of silencing suppressor in virus-induced PTGS and TGS. Moreover, I also generated transgenic *Arabidopsis* overexpressing VSRs and compared with virus-infected *Arabidopsis*, to further investigate how the VSRs interfere with transcriptional gene silencing and alter plant epigenome.

5.2 Results

5.2.1 Induction and suppression of RNA silencing by Agrobacterium-mediated transient expression system

To determine if VSRs would interfere with TGS, different VSRs and TGS/PTGS inducers were analysed using *Agrobacterium*-mediated transient assays in *N. benthamiana* leaves. Transgenic *N. benthamiana* (line 16c) expressing GFP under the control of CaMV 35S promoter were used in this infiltration assay **(Figure 5.1A)**. Two sets of constructs were used in the subsequent experiments. One set of constructs are silencing inducers, containing a 120-bp fragment of silencing inducer either from the CaMV 35S promoter (pDE-35S) or GFP coding region (pDE-GFP) to trigger GFP silencing in the leaves of *N. benthamiana* 16c **(Figure 5.1B)**. Another set of constructs are silencing suppressors that harbouring different VSRs with an influenza hemagglutinin (HA) epitope tag added to the C terminus. The CMV 2b, TBSV P19, BYV P21, and TuMV P1/HC-Pro silencing suppressors were analysed in this assay **(Figure 5.1B)**. These four silencing suppressors derive from different virus families, and represent evolutionarily and structurally unrelated proteins. Leaves of *N. benthamiana* plants were co-infiltrated with silencing inducer and silencing suppressor constructs, and then GFP fluorescence was monitored under UV light. An empty vector construct was used as a negative control.

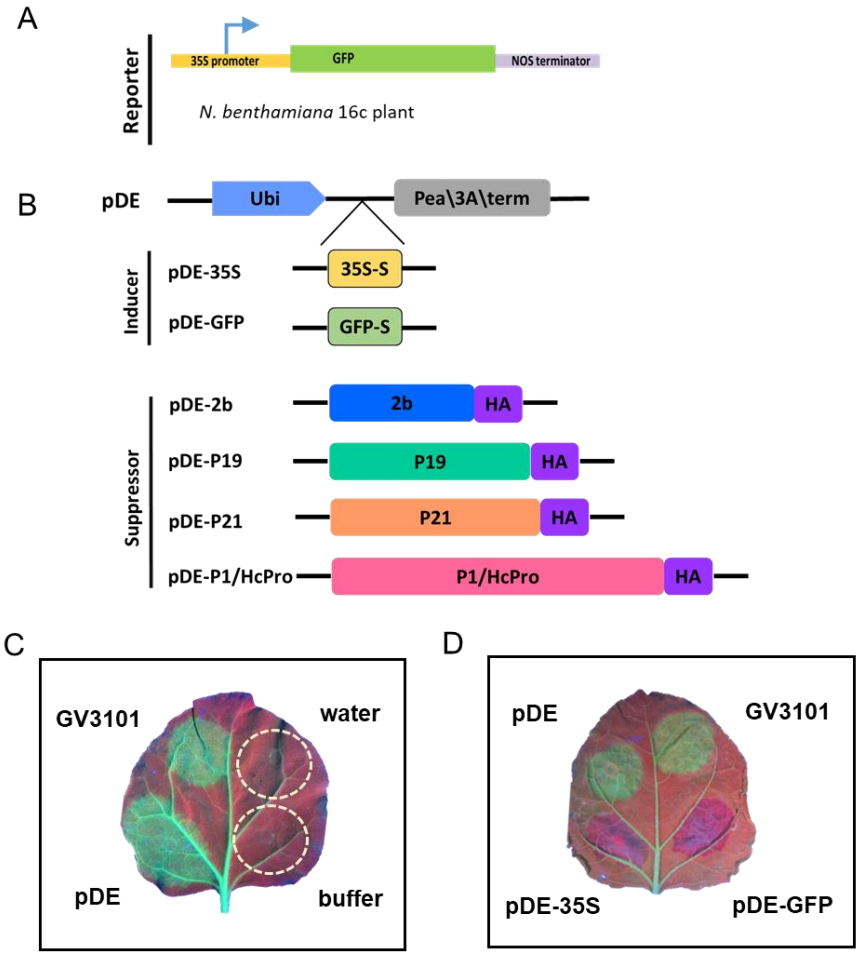

Figure 5.1 Induction and suppression of RNA silencing in *Agrobacterium*-mediated transient expression system. (A) *N. benthamiana* 16c plant was used as silencing reporter. The 16c plant harbors the GFP transgene under the control of CaMV 35S promoter and shows green fluorescence under UV light. (B) Constructs used for silencing inducer and silencing suppressor. Silencing inducer contained a 120-bp fragment either from the 35S promoter (pDE-35S) or from the GFP coding region (pDE-GFP) to induce TGS or PTGS of GFP in 16c plants, respectively. Each silencing suppressor construct contained the gene for one of the viral suppressors with HA epitope-tagged. Ubi, Ubiquitin promoter; Pea\3A\term, terminator. (C) Leaves of *N. benthamiana* 16c infiltrated with water, infiltration buffer, *Agrobacterium* strains GV3103, and empty vector (pDE), respectively. The leaf was photographed at 5 dpi under UV illumination. (D) Leaves of *N. benthamiana* 16c infiltrated with empty vector (pDE) or silencing inducers (pDE-35S, pDE-GFP). *Agrobacterium* strains GV3103 was used as infiltration control. The leaf was photographed at 21 dpi under UV illumination.

First, the ability of two silencing inducers (pDE-35S and pDE-GFP) was assessed. As shown in **Figure 5.1C**, transgenic *N. benthamiana* 16c exhibited green fluorescence under the UV light. GFP was highly expressed through the vein. The whole leaf appeared light red fluorescence due to chlorophyll autofluorescence which was masking GFP fluorescence to some extent. Tissue infiltrated with the empty vector (pDE) or *Agrobacterium tumefaciens* strain GV3101 exhibited brighter green fluorescence, which was side effects of *Agrobacterium* infection (**Figure 5.1C**). Tissue infiltrated with silencing inducer (pDE-35S or pDE-GFP) showed loss of green fluorescence by 21 dpi (**Figure 5.1D**). Intriguingly, PTGS inducer (pDE-GFP) could trigger GFP silencing more rapidly than that of TGS inducer, which is related to the different mechanism between each RNA silencing pathways. This result also demonstrated that the ubiquitin promoter is sufficient to drive high level expression of the silencing inducer and a 120-bp fragment of target region could efficiently trigger the silencing of GFP gene either transcriptionally or post-transcriptionally in *Agrobacterium*-mediated transient expression systems. In addition, we concluded that empty vector did not trigger silencing until three weeks (**Figure 5.1D**). Next, the silencing inducers and suppressors were co-infiltrated into 16c leaves to determine the activities of the different silencing suppressors on TGS and PTGS. In co-infiltration experiments, two agrobacterium cultures were mixed in equal parts prior to all injections and inoculated into the bottom left part of each leaf (**Figure 5.2A**). As controls, the same silencing inducer was infiltrated into the top left part of same leaf, followed by empty vector infiltrated into top right, and the corresponding viral suppressor to the bottom right corner (**Figure 5.2A**).

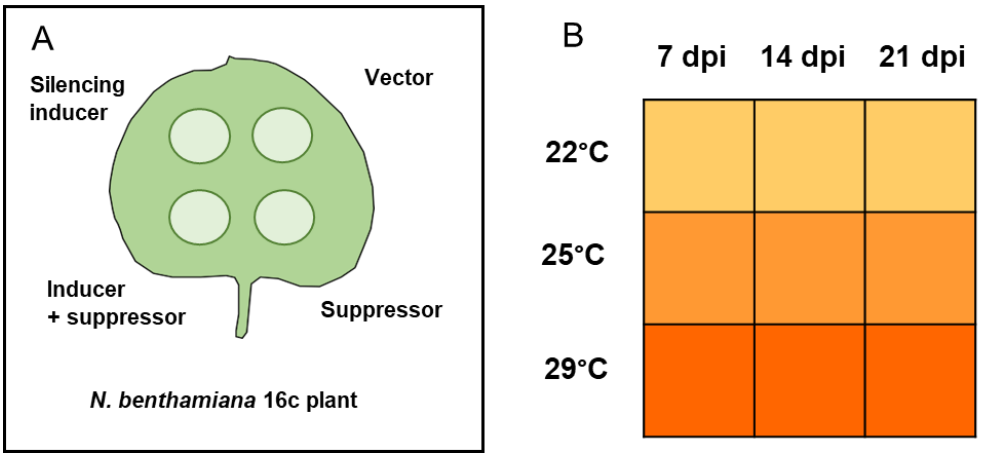

Figure 5.2 Schematic of experimental design to test the effect of temperature on RNA silencing and activities of silencing suppressors in the agropatch assay. (A) Two agrobacterium cultures of silencing inducer and silencing suppressor were equally mixed prior to all injections and inoculated into the bottom left of leaves of *N. benthamiana* 16c plants. As controls, the same silencing inducer was infiltrated into the top left part of same leaf, followed by empty vector infiltrated into top right, and corresponding viral suppressor was infiltrated into the bottom right corner. (B) *N. benthamiana* 16c infiltrated with *Agrobacterium* were kept at the 22℃ for two days. Then, plants were shifted to 22℃, 25℃ and 29℃. Plants were monitored at regular intervals under UV light. Three leaves were infiltrated from one plants and six plants were used in each treatment group.

5.2.2 Raising temperature promote RNA silencing, but does not affect activities of silencing suppressors

To assess how temperature affects RNA silencing and the activities of silencing suppressors, three different temperature (22℃, 25℃, and 29℃) were included in the agropatch assay (**Figure 5.2B**). The agro-infiltrated plants were first kept at 22℃ for two days, allowing the agrobacterium-mediated T-DNA transfer into plant cells, and then shifted to different temperatures 22℃, 25℃, and 29℃ (Del Toro *et al.*, 2014). Plants were photographed under UV light every 7 days. In the temperature gradient and time course assay, we founded that activities of RNA silencing increased as the temperature was raised over a range of 22℃ to 29℃, which is in accordance with previous studies (Szittya, 2003, Chellappan *et al.*, 2005) (**Figure 5.3, 5.4, 5.5, and 5.6**). Moreover, rising temperature didn't affect the capabilities of silencing suppressors, each silencing suppressors maintained their suppression abilities under different temperatures (**Figure 5.3, 5.4, 5.5, and 5.6**). However, differences were found that four VSRs exhibiting variable strength in suppression of RNA silencing, which will be described and discussed in the subsequent paragraph.

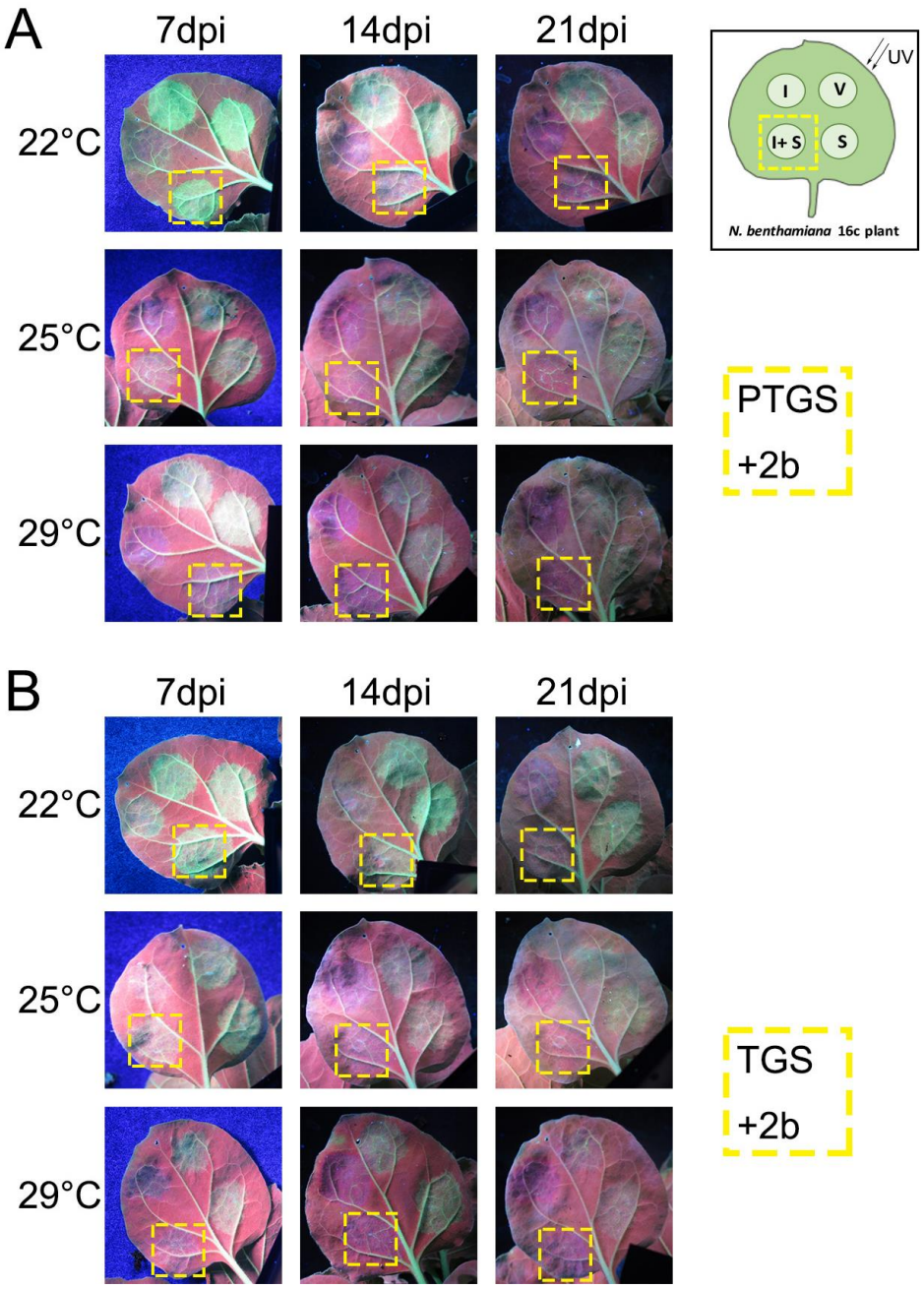

Figure 5.3 Time course UV imaging of *N. benthamiana* 16c leaves co-infiltrated with silencing inducers and silencing suppressor 2b. (A) PTGS inducer pDE-GFP was co-infiltrated with silencing suppressor pDE-2b into left bottom part of each *N. benthamiana* 16c leaves (highlighted in yellow dash box). (B) TGS inducer pDE-35S was co-infiltrated with silencing suppressor pDE-2b into left bottom part of each *N. benthamiana* 16c leaves (highlighted in yellow dash box). The leaf was photographed at 7/14/21 dpi under UV illumination. I, silencing inducer (pDE-GFP or pDE-35S); S, silencing suppressor (pDE-2b); V, empty vector (pDE).

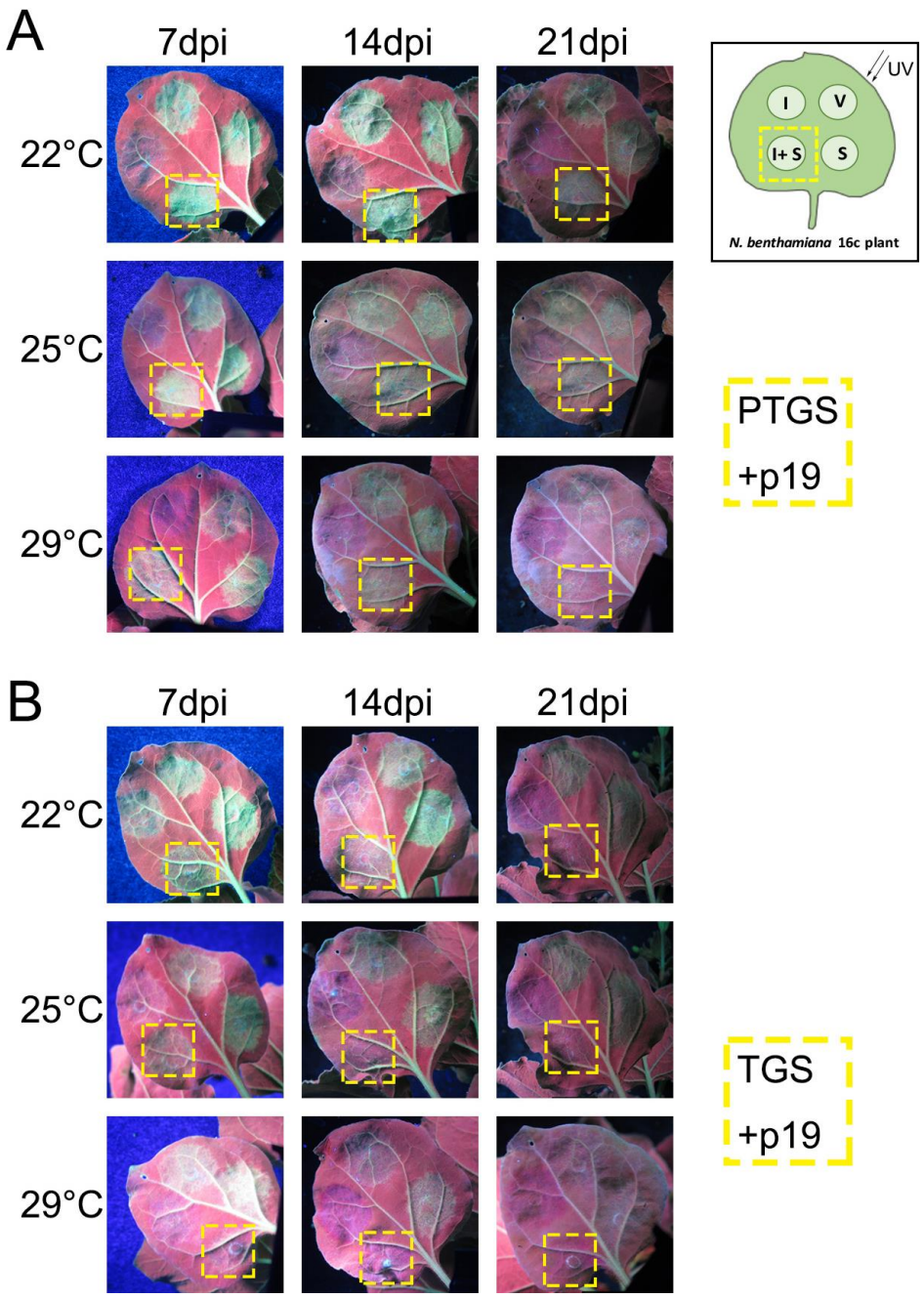

Figure 5.4 Time course UV imaging of *N. benthamiana* 16c leaves co-infiltrated with silencing inducers and silencing suppressor P19. (A) PTGS inducer pDE-GFP was co-infiltrated with silencing suppressor pDE-P19 into left bottom part of each *N. benthamiana* 16c leaves (highlighted in yellow dash box). (B) TGS inducer pDE-35S was co-infiltrated with silencing suppressor pDE-P19 into left bottom part of each *N. benthamiana* 16c leaves (highlighted in yellow dash box). The leaf was photographed at 7/14/21 dpi under UV illumination. I, silencing inducer (pDE-GFP or pDE-35S); S, silencing suppressor (pDE-P19); V, empty vector (pDE).

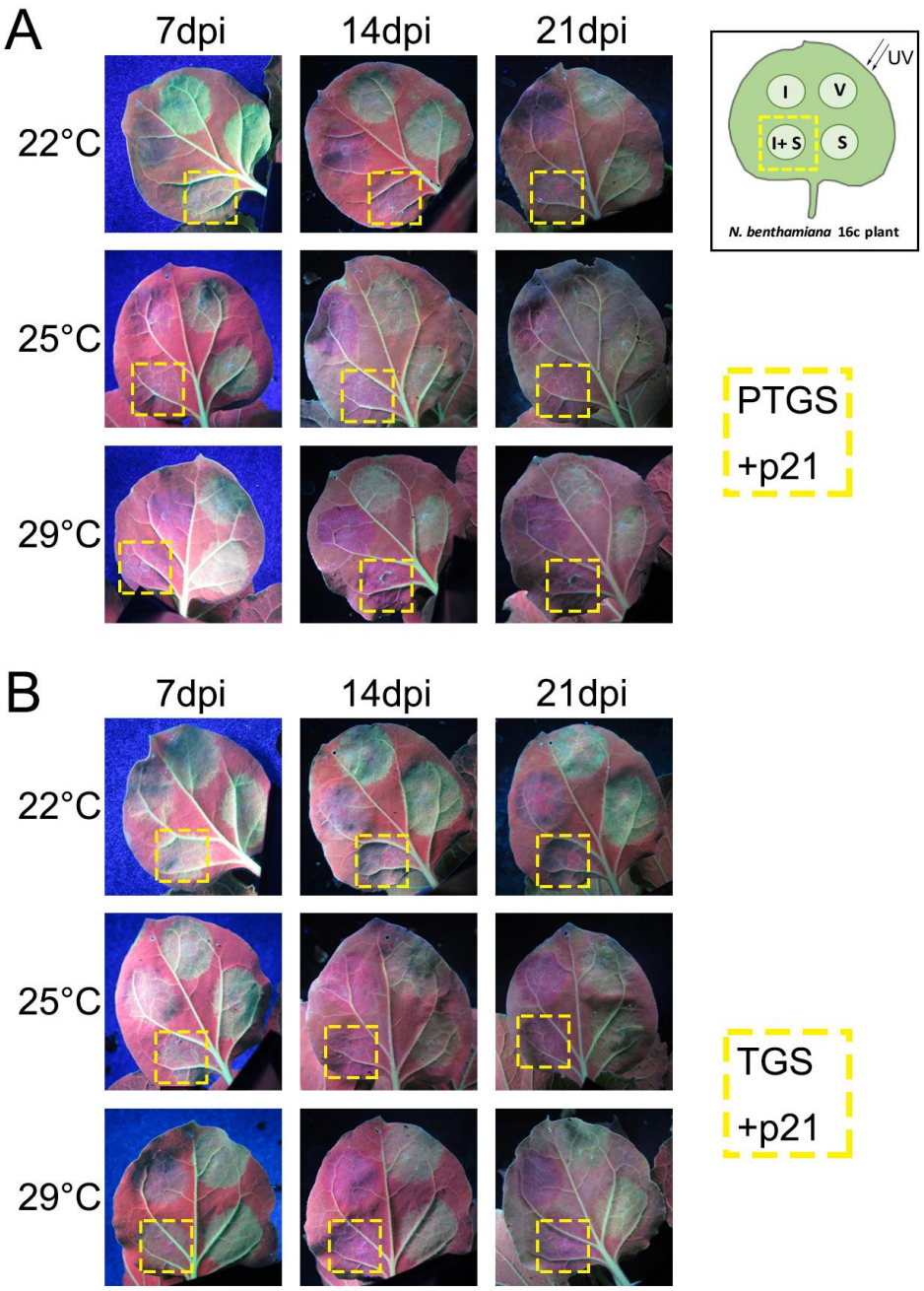

Figure 5.5 Time course UV imaging of *N. benthamiana* 16c leaves co-infiltrated with silencing inducers and silencing suppressor P21. (A) PTGS inducer pDE-GFP was co-infiltrated with silencing suppressor pDE-P21 into left bottom part of each *N. benthamiana* 16c leaves (highlighted in yellow dash box). (B) TGS inducer pDE-35S was co-infiltrated with silencing suppressor pDE-P21 into left bottom part of each *N. benthamiana* 16c leaves (highlighted in yellow dash box). The leaf was photographed at 7/14/21 dpi under UV illumination. I, silencing inducer (pDE-GFP or pDE-35S); S, silencing suppressor (pDE-P21); V, empty vector (pDE).

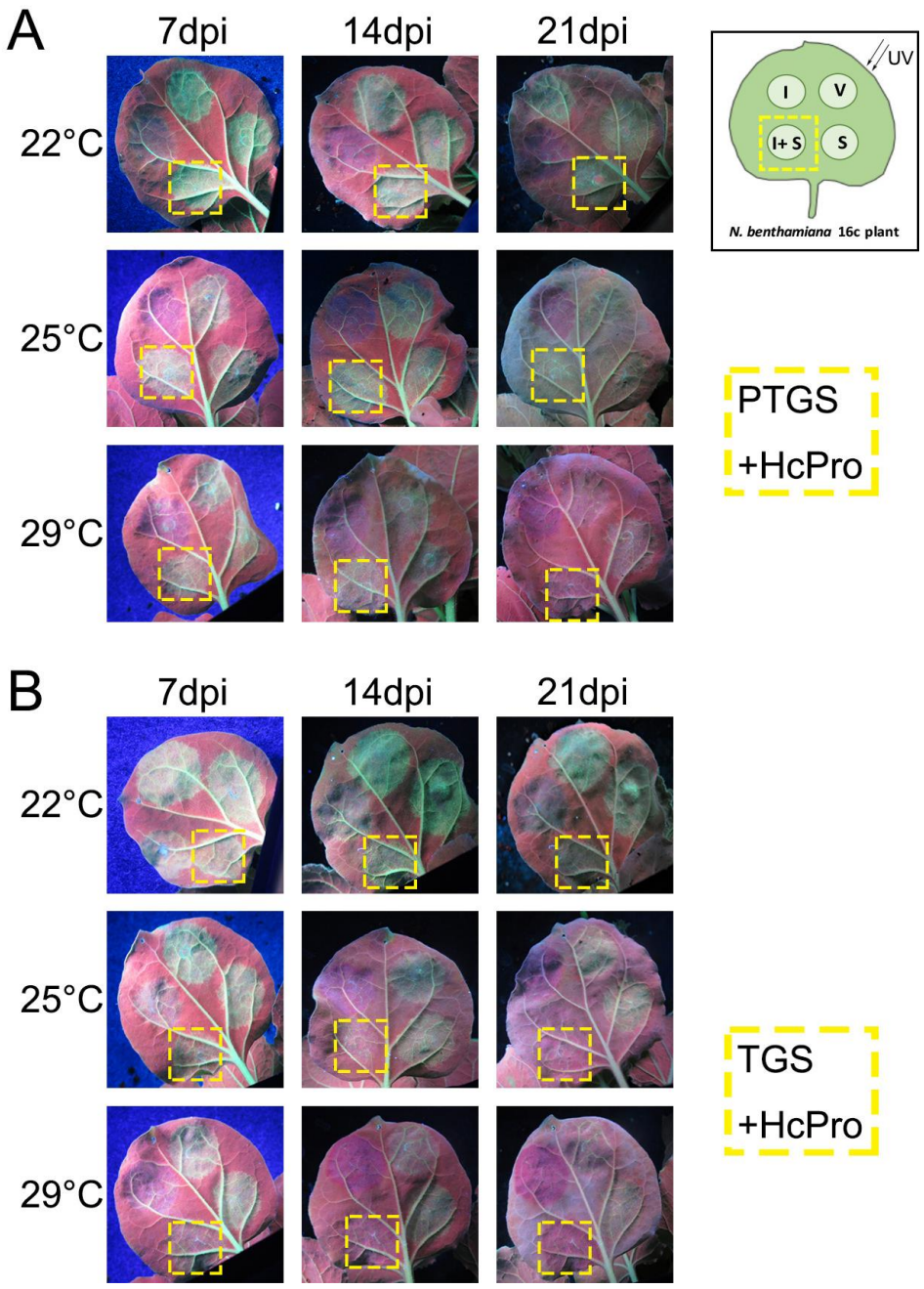

Figure 5.6 Time course UV imaging of *N. benthamiana* 16c leaves co-infiltrated with silencing inducers and silencing suppressor HcPro. (A) PTGS inducer pDE-GFP was co-infiltrated with silencing suppressor pDE-HcPro into left bottom part of each *N. benthamiana* 16c leaves (highlighted in yellow dash box). (B) TGS inducer pDE-35S was co-infiltrated with silencing suppressor pDE-HcPro into left bottom part of each *N. benthamiana* 16c leaves (highlighted in yellow dash box). The leaf was photographed at 7/14/21 dpi under UV illumination. I, silencing inducer (pDE-GFP or pDE-35S); S, silencing suppressor (pDE-HcPro); V, empty vector (pDE).

5.2.3 Ubiquitin promoter driven viral suppressors of RNA silencing can efficiently inhibit PTGS

It has been demonstrated that VSRs could inhibit PTGS through interfering with sRNA guided silencing pathways. However, in those experiments, the VSRs were expressed under a very strong viral promoter. Thus, the activity of ubiquitin promoter-driven VSRs interfering with PTGS were firstly assessed by *Agrobacterium*-mediated transient expression system. Based on to the GFP expression level under the UV light, the silencing suppressors showed variable strength in suppression of PTGS. At 22℃, GFP fluorescence was retained in patches co-infiltrated with pDE-P19 and pDE-GFP for three weeks (**Figure 5.4A**). Similar results could also be observed in pDE-HcPro and pDE-GFP co-infiltrated patches (**Figure 5.6A**). These results confirmed that both P19 and HcPro are strong silencing suppressors in repression of PTGS. Comparing to P19 and HcPro, silencing suppressor 2b could only inhibit GFP silencing at the early stages, but losing its suppression activity later on (**Figure 5.3A**). P21 is the mildest suppressor among the four suppressors tested, no obvious inhibition of GFP silencing could be observed under UV light (**Figure 5.5A**). Similar results were observed in the infiltrated plants kept at 25℃ and 29℃, suggesting that rising temperature didn't affect the activities or functions of VSRs.

Northern blot was used to detect the accumulation of small RNAs in the infiltrated tissues kept at 22℃ (**Figure 5.7A**). sRNAs extracted from the *Agrobacterium*-infiltrated leaves at 14 dpi were analysed by blot hybridization with a radiolabelled probe specific for the GFP target sequence. As expected, large amount of the GFP-specific small RNAs were detected in the pDE-GFP infiltrated patch. In contrast to the silencing inducer (pDE-GFP) infiltrated patches, the accumulation of sRNAs was significantly reduced in the co-infiltrated patches, confirming efficient suppression of PTGS by all for VSRs **(Figure 5.7B)**.

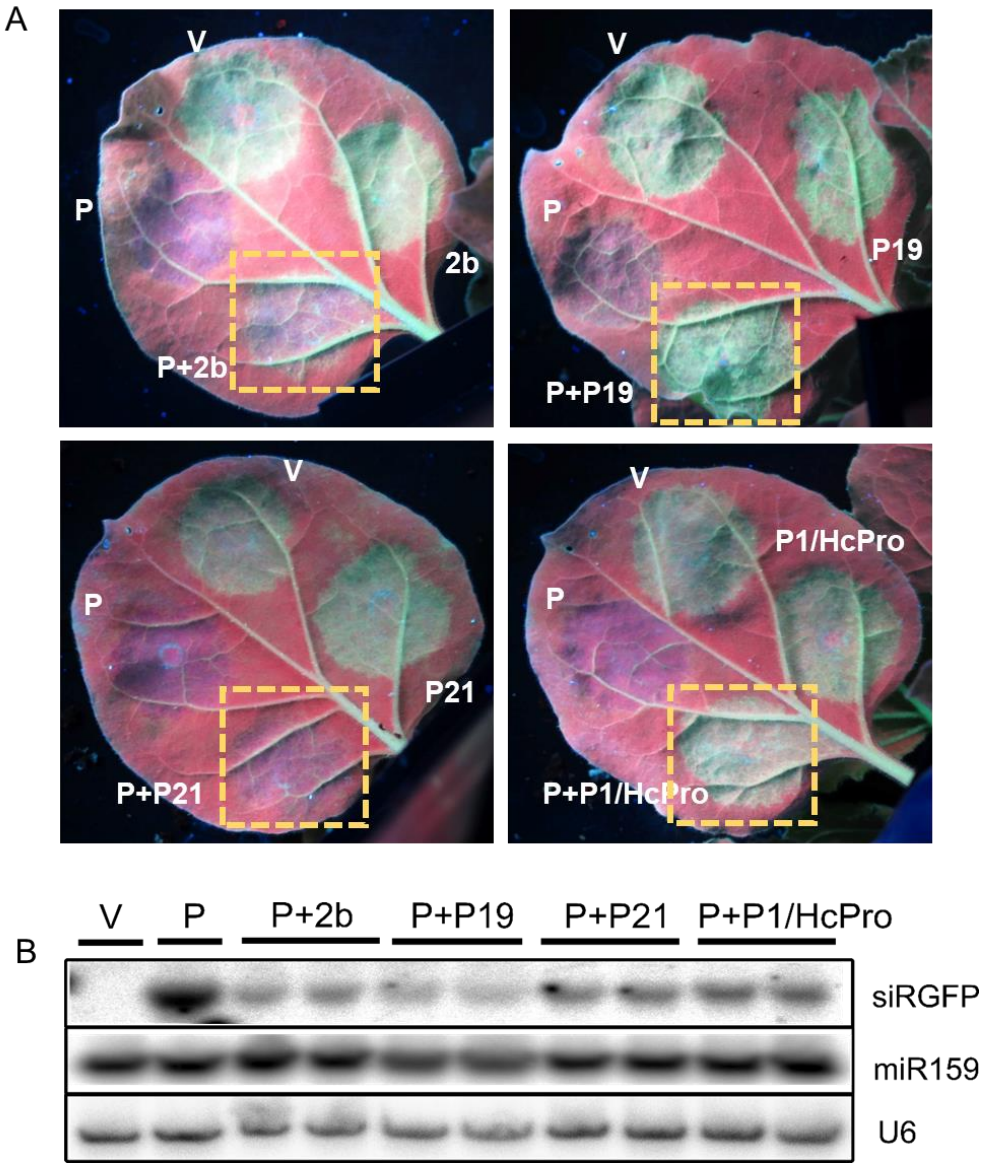

Figure 5.7 Activity of silencing suppressors interfere with PTGS. (A) PTGS inducer pDE-GFP (P) was co-Agroinfiltrated with silencing suppressors P1/HcPro, P21, P19, or 2b on left bottom of *N. benthamiana* 16c leaf. pDE-GFP (P) and empty vector (V) were used as positive and negative controls, respectively. The leaf was photographed at 14 dpi under UV illumination. (B) GFP-specific siRNA accumulation in co-Agro-infiltrated tissues. Blot hybridization was performed using duplicate low molecular weight RNA samples prepared from leaf tissues that were infiltrated with the *Agrobacterium* strains shown in (A). miRNA159 and U6 were used as loading controls.

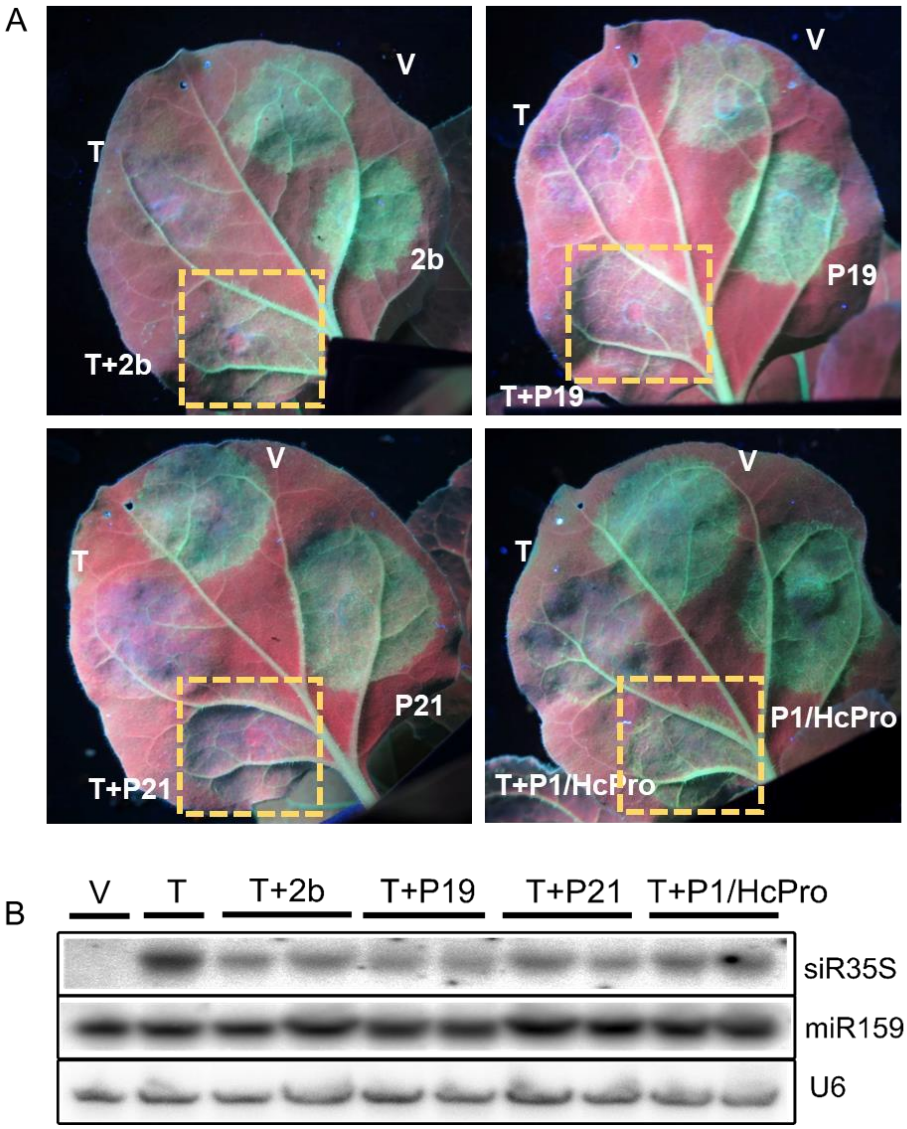

Figure 5.8 Activity of silencing suppressors interfere with TGS. (A) TGS inducer pDE-35S (T) was co-Agro-infiltrated with silencing suppressors P1/HcPro, P21, P19, or 2b on left bottom of *N. benthamiana* 16c leaf. pDE-35S (T) and empty vector (V) were used as positive and negative controls, respectively. The leaf was photographed at 14 dpi under UV illumination. (B) 35S siRNA accumulation in co-Agroinfiltrated tissues. Blot hybridization was performed using duplicate low molecular weight RNA samples prepared from leaf tissues that were infiltrated with the *Agrobacterium* strains shown in (A). miRNA 159 and U6 were used as loading controls.

5.2.4 Viral RNA silencing suppressors can inhibit the initiation of TGS

The ability of silencing suppressors interfering with TGS was further assessed with same procedure. The intensity of GFP fluorescence in the co-infiltrated tissue suggested the silencing suppressors were less active in suppression of TGS than that of PTGS. Only P1/HcPro showed moderate suppression of TGS **(Figure 5.6B and Figure 5.8A)**. Both 2b and P19 proteins displayed mild repression of TGS at early stages of inoculation (**Figure 5.3B and 5.4B**). Similar to that of PTGS, P21 didn't exhibit visible inhibition of GFP silencing (**Figure 5.5**). Northern blot confirmed the reduction of 35S specific sRNA in co-infiltrated tissue, but the amount of reduction were less than that of PTGS **(Figure 5.8B)**. These data suggest that all four silencing suppressors could inhibit TGS by interfere with sRNAs. VSRs show lower activity in repression of TGS in comparing to PTGS. This is probably due to the timing of silencing suppressor expression. It might take more time for TGS to be set, which were not overlapping with the most active period of suppressor proteins. Alternatively, it might take more time to see the effect of TGS due to the high stability of GFP.

To overcome this problem, I performed two-round infiltration assays. The leaves were first infiltrated with suppressor proteins, and then three days later silencing inducer was applied on the same patch. However, silencing could not be observed on any of the double-infiltrated patches, no matter the first-round infiltration was performed with suppressor protein or vector control. This might be due to the plant immunity responses to agrobacterium infections or the established anti-silencing response from the first round agro-infiltration preventing the induction of RNA silencing in the second round of agro-infiltration.

Taken together, our data suggested that all four silencing suppressors could inhibit both PTGS and TGS. However, due to the limitation of the *Agrobacterium*-mediated transient expression system, assessing the inhibition of TGS under the UV light was ambiguous. The results presented in this section are generally preliminary data that

assessing the effect of VSRs is on TGS. To obtain more accurate and quantitative results, qRT-PCR can be used to detect the accumulation of GFP mRNA, and bisulfite sequencing can also be performed to determine the status of DNA methylation at 35S target sequence.

5.2.5 Construction of TBSV-based silencing vectors and assessing their ability to induce gene silencing in N. benthamiana 16c

In *Agrobacterium*-mediated transient assays, P19 and HcPro exhibited strong repression of RNA silencing. To assess the ability of these strong VSRs interfering with ViPTGS and ViTGS in natural virus-plant system, RNA viruses containing corresponding silencing suppressors were selected to further analysis. Similar silencing inducer sequences (a 120-bp fragment of 35S promoter or GFP coding region) were cloned into viral vectors, inoculated *N. benthamiana* 16c plants, and assessed the capacity of each RNA virus for inducing PTGS and TGS of GFP gene, respectively.

First, TBSV was used to assess the effect of the silencing suppressor protein P19 on VIGS in plant-virus systems. P19 encoded by TBSV and its related tombusviruses is one of the structurally best-studied and most widely used suppressors, making TBSV a very good model virus for studying RNA silencing and silencing suppressor activity.

The original TBSV vector was engineered by integrating an XhoI restriction site 13-nt downstream of the stop codon of the coat protein (CP, P41) coding region (Pignatta *et al.*, 2007). In order to provide a functional P41 protein, we restored the missing 13 nt from the 3' end of CP by adding the remaining nucleotides to the 5' end of the silencing inducing inserts **(Figure 5.9A)**. Although the coat protein of TBSV is not required for infection of *N. benthamiana* plants (Scholthof, 1993), it is essential for efficient systemic spread in most hosts (Qiu *et al.*, 2002). Thus, a fully functional coat protein could help the systemic invasion of TBSV *in planta*. The silencing target sequence in sense and antisense orientation was cloned into TBSV vectors, respectively **(Figure 5.9A)**. To investigate the effect of P19 on TGS and PTGS, we cloned the inducer sequences into the silencing suppressor mutant version of TBSV (delete P19), too**.**

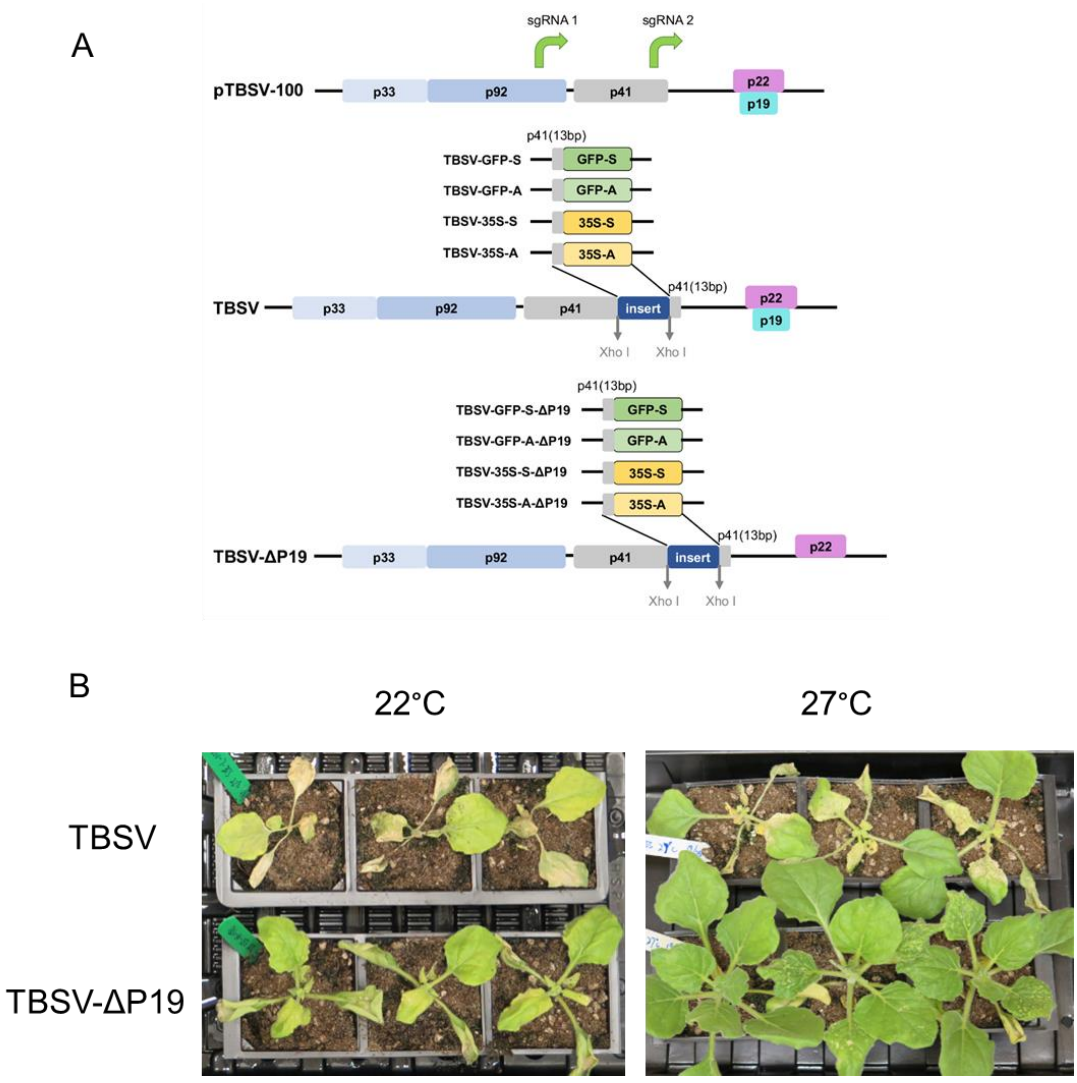

Figure 5.9 TBSV-based virus-induced gene silencing. (A). Schematic diagram of TBSV-VIGS vectors. TBSV wild type (pTBSV-100) genome map showing sgRNA1 and 2 transcription initiation sites (indicated by bent arrows). TBSV vector genome map showing XhoI restriction site with inactive P19 (middle panel). TBSV-△p19 vector genome map showing XhoI restriction site with inactive P19 (bottom panel). Extra 13 nt of 3' end of p41 coat protein was added before the inserting target fragments (120-bp sense/antisense GFP sequence or 120-bp sense/antisense 35S sequence). The insertion was ligated into the vectors using the XhoI restriction site. (B). TBSVs-infected *N. benthamiana* 16c plants kept at 22℃ and 27℃. The photographs were taken photographed at 10 dpi under normal light.

TBSV is an aggressive virus, which can induce severe viral symptoms and lethality in *N. benthamiana* plants. It is demonstrated by the fact that our TBSV inoculated plants that we kept at standard temperature (22℃) died within 2 weeks of infection **(Figure 5.9B)**. It has been shown in previously report that the Cymbidium ringspot virus (CymRSV)-infected *N. benthamiana* plants can only survive at and above 27℃. CymRSV and TBSV are in the same *Tombusvirus* genus and they share similar genome structures and silencing suppressor strategies. Therefore, we decided to move the TBSV-infected plants to higher temperature (27℃) in subsequent experiments.

At 27℃, the recombinant TBSV with active P19 caused a severe leaf curling and stunting phenotype in the infected plants, whereas the *N. benthamiana* 16c plants inoculated with inactive P19 TBSV developed mild leaf curling symptoms **(Figure 5.9B)**. Most likely, this is because the silencing suppression activity of P19 could interfere with the endogenous RNA silencing pathways. With active P19, TBSV delayed the onset of GFP silencing. GFP silencing phenotype could only be observed in TBSV-GFP and TBSV-35S inoculated plants at 20 dpi **(Figure 5.10B)**. With inactive P19, both TBSV-GFP-△P19 and TBSV-35S-△P19 inoculated plants showed GFP silencing earlier in the systemic leaves (10 dpi) **(Figure 5.10A)**. Intriguingly, Virus-induced PTGS was more rapid and persistent than TGS, regardless of the present of silencing suppressor P19 **(Figure 5.10B)**. TBSV carrying different orientations of the target sequence didn't show much difference in inducing PTGS and TGS **(Figure 5.10B)**.

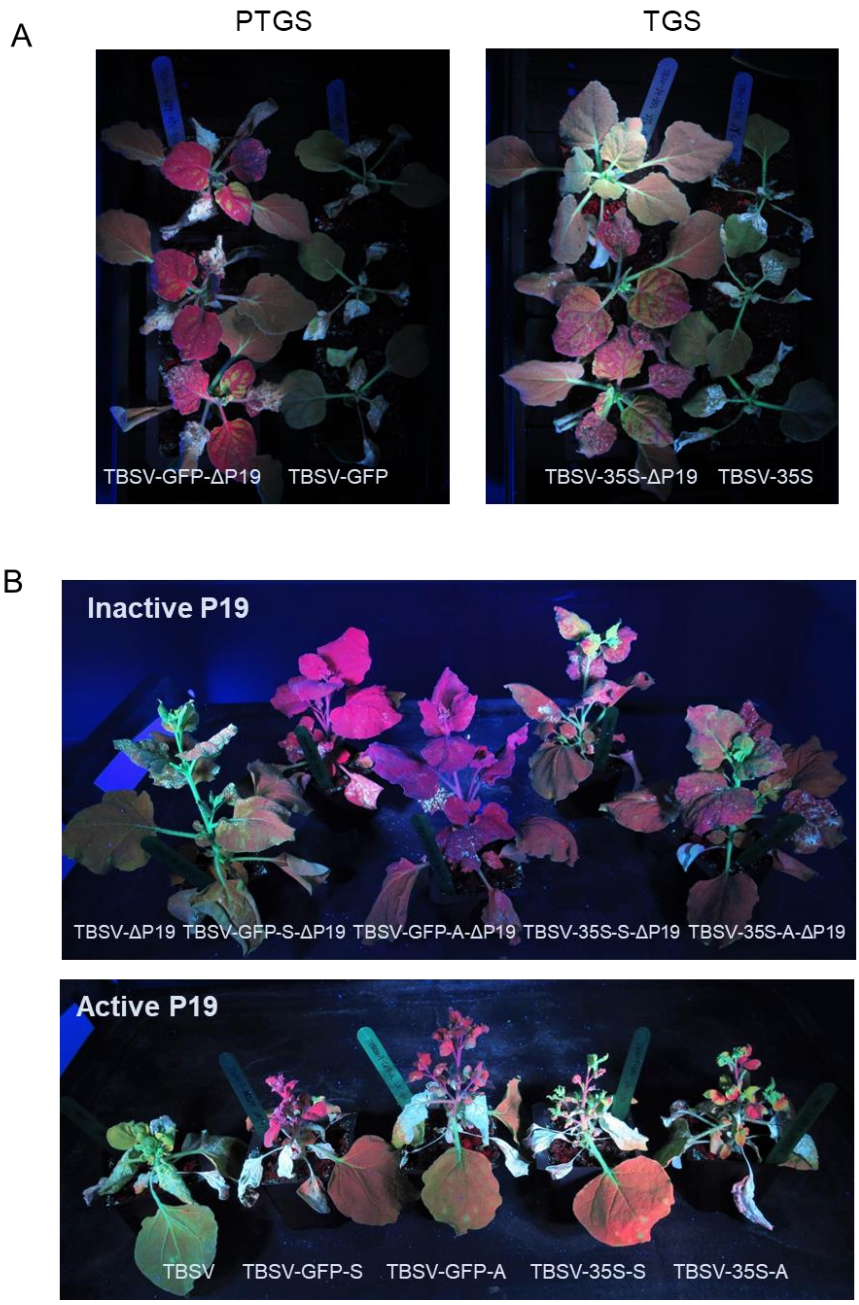

Figure 5.10 TBSV-induced GFP silencing in *N. benthamiana* 16c plants. Specific silencing vectors are indicated on each photograph. TBSVs-infected *N. benthamiana* 16c plants kept at 27°C. (A). the plants were photographed under UV illumination at 10 dpi. (B). the plants were photographed under UV illumination at 20 dpi.

5.2.6 Construction of TuMV based silencing vectors and their ability to induce gene silencing in N. benthamiana 16c

Next, we used TuMV as a model virus to examine effect of HcPro on gene silencing in host-virus interaction. TuMV belongs to the *Potyvirus* genus, and its genome consists of a positive-sense single-stranded RNA molecule of about 9830 nt in length. The genome encodes a single open reading frame (ORF), flanked by two untranslated regions (UTR). The ORF is translated into a single polyprotein, which is co- and post-translationally processed by three virus-encoded proteases (Walsh & Jenner, 2002).

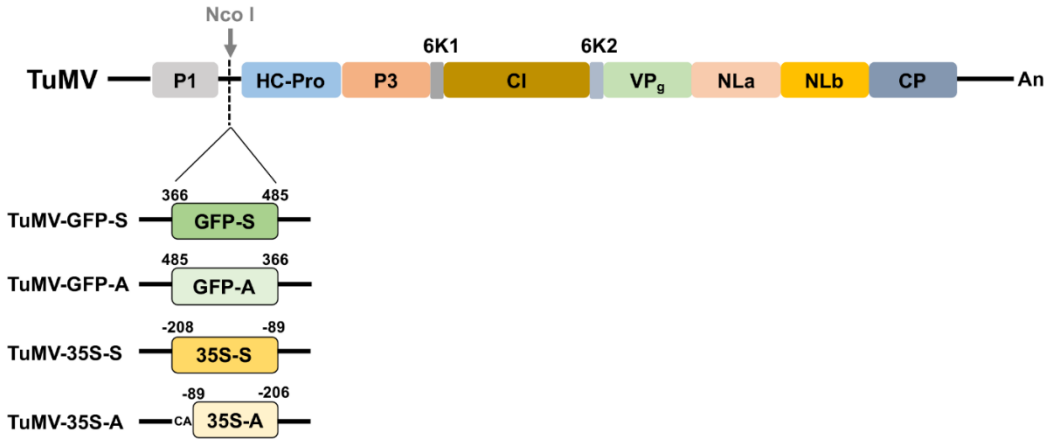

Figure 5.11 TuMV-based virus-induced gene silencing. Schematic of the TuMV genome. The target gene fragment (120-nt sense/antisense GFP sequence, 120-nt sense 35S sequence, and 118-nt antisense 35S sequence with additional CA added in 5' site) was inserted through NcoI restriction sites between P1 and Hc-Pro.

To induce TGS, the CaMV 35S promoter (nt -208 to -89) was cloned into the TuMV vector through NcoI restriction site to create TuMV-35S-S **(Figure 5.11)**. As the TuMV ORF is translated into a single polyprotein, the open reading frame should be preserved. However, the antisense sequence of 35S promoter (nt -208 to -89) could introduce a stop codon in TuMV vector. Therefore, to keep the corresponding ORF, a new antisense sequence of 35S promoter was designed by adding two nucleotides (CA) at the 5' of antisense sequence of 35S promoter (nt -206 to -89) and was then used to

generate the TuMV-35S-A construct. For inducing PTGS of GFP gene in *N. benthamiana* 16c plants, an equally sized coding sequence (nt 366 to 485) of the GFP gene was cloned in sense and antisense orientations into the TuMV vector to obtain TuMV-GFP-S and TuMV-GFP-A, respectively **(Figure 5.11)**.

The TuMV-inoculated plants developed typical viral symptoms showing severe leaf curling and stunting at 22℃ **(Figure 5.12A)**. Interestingly, the TuMV carrying different orientations of inserts developed variable viral symptom. Plants infected with TuMV-35S-A show more severe symptom than that of TuMV-35S-S. Intriguingly, TuMV with 120-bp GFP inserts showing completely opposite results. The infection of TuMV carrying sense GFP sequence caused lethality in *N. benthamiana* plants, while TuMV-GFP-A infected plants exhibited a good recovery from viral infection **(Figure 5.13)**. Furthermore, only TuMV-GFP-A infected plants showed strong GFP silencing **(Figure 5.12A)**.

Similar to TBSV, TuMV encodes a strong silencing suppressor protein, which inhibits the host plants antiviral silencing pathway and causes strong viral infection symptom in infected plants. In TBSV experiment, the elevated temperature was used to promote RNA silencing and rescue infected plants. Therefore, TuMV infected plants were shifted to 25℃ after inoculation. At higher temperature, infected plants showed moderate viral symptoms. Although virus symptoms were developed more rapidly in locally infected tissues, they were also associated with faster recovery. Moreover, strong GFP silencing phenotype could be observed in TuMV-GFP-S and TuMV-GFP-A infected plants, indicating the RNA silencing was indeed accelerated at higher temperature **(Figure 5.12B)**. However, in accordance with 22℃, neither TuMV-35S-S nor TuMV-35S-A could trigger TGS of GFP in infected plants. This data suggests that the strong silencing suppressor HcPro encoded by TuMV may interfere with RdDM.

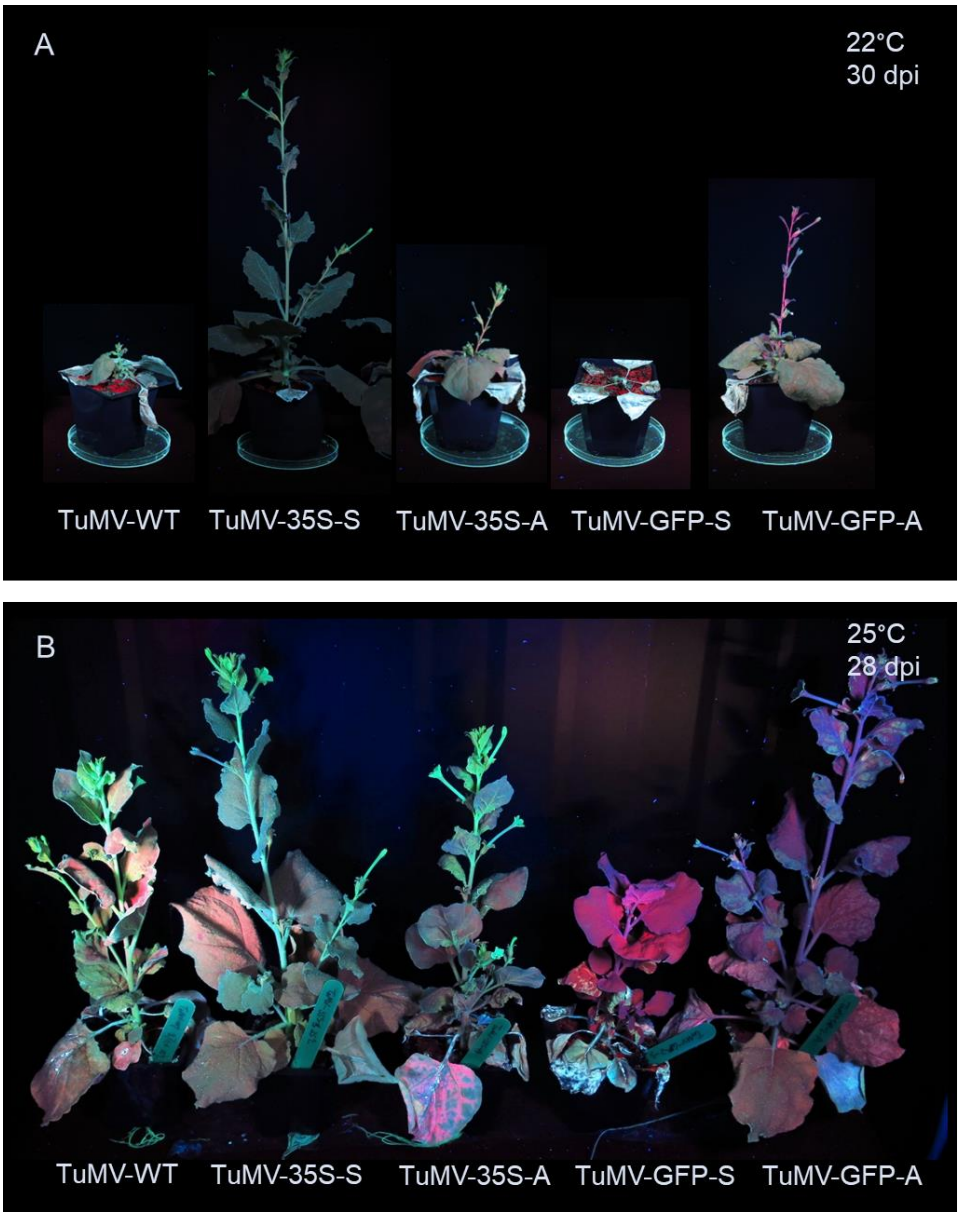

Figure 5.12 TuMV-induced GFP silencing in *N. benthamiana* 16c plants. The 16c plants inoculated with recombinant TuMVs kept at 22℃ (A) and at 25℃ (B). The plants were photographed under UV illumination. Specific silencing vectors are indicated on each photograph.

Figure 5.13 the TuMV vector containing 120-nt sense GFP sequence triggered plant death at 22℃. The 16c plants infected with TuMV-GFP-S (upper panel) and TuMV-GFP-A (bottom panel) kept at 22℃. The plants were photographed at 20 dpi under normal light.

From TuMV-VIGS experiment at 22℃ and 25℃, we observed significant difference viral symptom caused by TuMV carrying different orientations of target sequence. Especially, the TuMV vector containing sense GFP sequence triggered plant death at 22℃ **(Figure 5.13)**. In order to test whether it was due to the orientation of insert or the sequence specificity, another two target regions from GFP coding sequence were chosen. Two sets of primers were designed to amplify GFP sequences from the 5' end of the ORF and 3' end of the ORF **(Figure 5.14)**. Each of the two regions was inserted into the TuMV through NcoI site as previously described. Intriguingly, TuMV vector carrying inserts from different target regions also induced variable viral symptoms. Inserts from central region of the GFP coding sequence developed the most severe symptoms, while inserts from 5'ORF only showed mild symptoms **(Figure 5.14)**. All of antisense inserts from three regions induced strong GFP silencing and showed better recoveries from viral infection than those of sense inserts **(Figure 5.14)**.

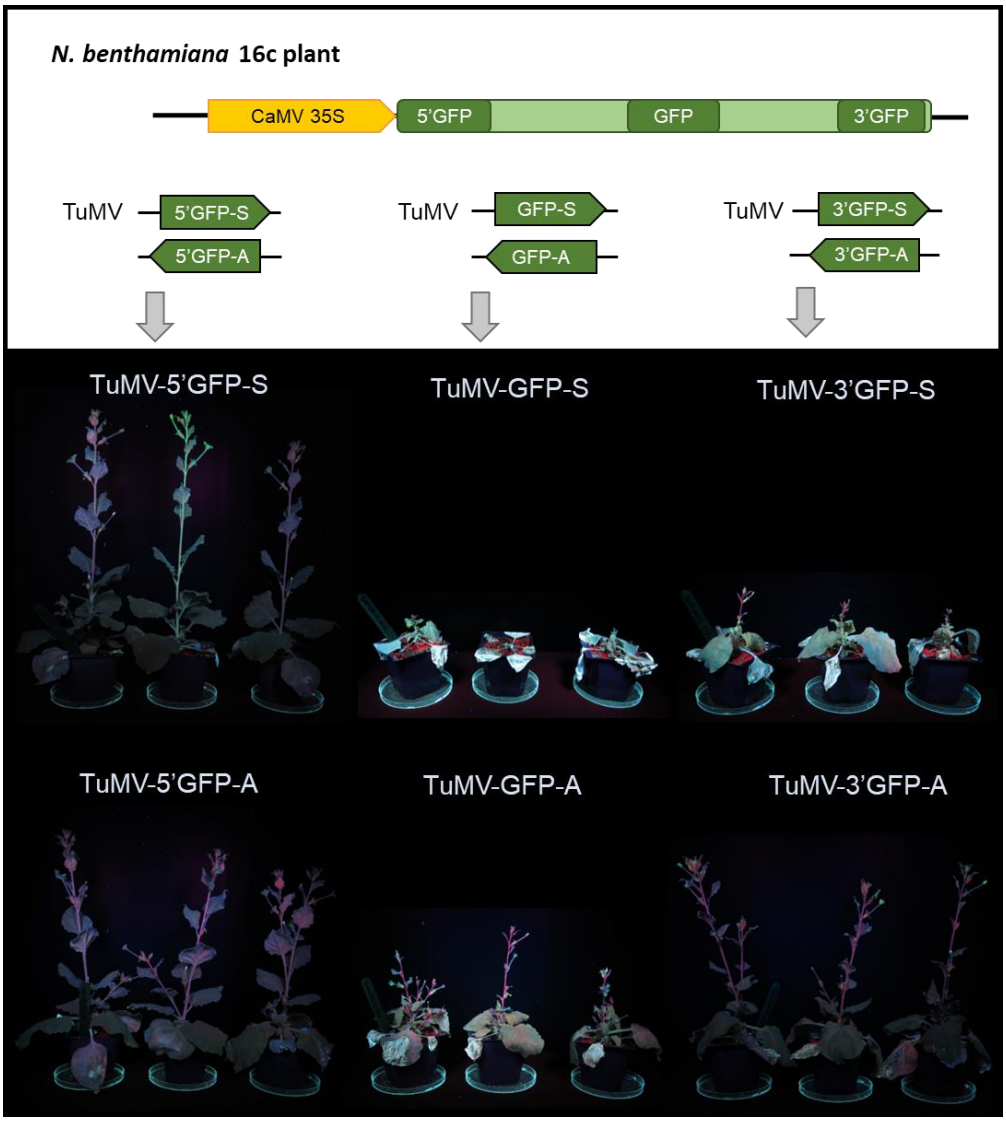

Figure 5.14 TuMV vector carrying GFP sequence from different target regions induced variable viral symptoms. Three 120-nt GFP sequences were chosen from different region of GFP coding sequence. Each target sequence was PCR amplified and inserted into the TuMV vector with sense (S) or antisense (A) orientation. The 16c plants infected with recombinant TuMVs were kept at 22°C. The plants were photographed under UV illumination at 30 dpi. Specific silencing vectors are indicated on each photograph.

The above results indicate that extra care should be taken if TuMV was used as a VIGS vector. It might be due to unique viral structure and replication strategy of TuMV. TuMV is firstly expressed as single polyprotein precursors, and subsequent proteolysis yields mature viral gene products. Although the inserts were cloned in frame, the translated peptide from the foreign sequences might results in unanticipated phenotypes. Additionally, the NcoI restriction site sits between the P1 and the HcPro protein **(Figure 5.11)**. P1 and HcPro act as viral suppressors of RNA silencing and are critical for viral symptom development. The inserted sequence might affect the formation or activity of P1/HcPro protein and cause the variable viral symptoms.

In this section, we used two plant RNA viruses carrying strong silencing suppressors to assess their capacities for PTGS and TGS inductions in natural virus-plant system. With strong VSRs expression, both TBSV and TuMV delayed the onset of silencing, but they were still able to induce PTGS of GFP. Specifically, PTGS induction was more efficient and persistent than TGS in both TBSV and TuMV systems. This is probably due to the distinct mechanism between PTGS and TGS. The mechanism of PTGS is associated with the amplification of secondary sRNAs, while TGS barely produces any secondary sRNAs. Therefore, virus-derived primary sRNAs are essential for initiation and maintenance of TGS. Strong VSRs encoded by these two viruses could actively bind virus-derived siRNAs. Decreased abundance of active sRNAs is very likely to hinder silencing, especially for TGS. Our results were in accordance with the previous observation that VSRs 2b and P19 could inhibit Apple latent spherical virus (ALSV)-mediated TGS of the GFP gene in 16c plants (Kon & Yoshikawa, 2014).

We also tested the effect of the orientation of inserts on RNA silencing induction in these two viruses. Previously, it has been shown that antisense inserts in bean pod mottle virus (BPMV) and turnip yellow mosaic virus (TYMV) vectors could induce more efficient PDS silencing than sense inserts (Pflieger *et al.*, 2008, Zhang *et al.*, 2010). Similar results were observed in TuMV vectors, the antisense 120-bp GFP

inserts were more effective to induce GFP silencing in 16c plants. However, the orientation of inserts didn't show any difference symptoms/phenotypic in TBSV-vector-induced silencing system. It is probably due to different virus replication strategies and the way how they produce secondary siRNAs.

5.3 Discussion

5.3.1 Altered results of the ability of VSRs between transient expression and natural virus-plant systems

In this chapter, I assessed the ability of viral suppressors of RNA silencing in interfering gene silencing both in transient expression system and virus-plant system. Consistent with previous studies, both P19 and HcPro showed strong suppression of gene silencing (Chapman *et al.*, 2004, Lakatos *et al.*, 2006, Burgyán & Havelda, 2011).

Interestingly, depending on which assaying systems was used, there was a difference in suppressing TGS and PTGS. In agroinfiltration, VSRs are more efficient in suppression of PTGS, whereas it is opposite in virus-plant system. The data obtained from agroinfiltration is in line with the previous works that plant viral suppressors of PTGS do not reverse transgene-induced TGS (Marathe *et al.*, 2000, Mette *et al.*, 2001). As argobacterium-mediated transient expression is a transgene-based system, it is possible that VSRs could affect transgene-induced PTGS mediated by 21-22-nt siRNAs, but not transgene-induced TGS mediated by 24-nt siRNAs. Furthermore, the agroinfiltration assay is one of the most commonly used systems for studying RNA silencing, but it is probably an oversimplified method for assessing the ability of VSRs. Actually, VSRs are not only restricted a single function in antiviral defence. They are often multifunctional proteins which play other essential roles in the virus life cycle. Therefore, an analysis of VSRs in their natural virus backgrounds is more informative.

In natural virus-plant system, VSRs exhibited more impact on TGS during plant-virus interaction. It is probably because that ViTGS is initiated by virus-derived 21-22-nt sRNAs and maintained by 24-nt sRNAs. VSRs might affect both ViTGS and ViPTGS by interfering the virus-derived 21-22-nt sRNAs. ViPTGS could counter the VSR suppression by amplifying large amount of secondary sRNAs. However, due to the limited amplification of sRNAs from ViTGS, when strong VSRs bind most of 21-22-

nt sRNAs, there are less sRNAs can be used for TGS. Consistently, most well-known ViTGS vectors carry a relatively moderate or weak silencing suppressor, such as 16K from TRV, 2b from CMV, and P25 from PVX (Jones *et al.*, 1999, 2001, Kanazawa *et al.*, 2011).

5.3.2 Actions of VSRs in natural virus-plant system

To assess the ability of P19 and HcPro interfering with ViPTGS and ViTGS in natural virus-plant system, TBSV and TuMV-based silencing vectors were used to assess their abilities of inducing RNA silencing. Both TBSV and TuMV can mediate PTGS, but the latter could not induce TGS. A possible explanation for this is that the sRNAs driven from the 120-nt 35S inducer locus only accounts for a small portion of the total sRNAs generated from the 10-kb TuMV genome. Strong silencing suppressor HcPro encoded by TuMV could efficiently bind 21 nt, 22 nt, and 24 nt sRNAs to sequester them away from antiviral RISCs (Lakatos *et al.*, 2006). The reduced accumulation of sRNAs greatly inhibited the ViTGS. Comparing to the TuMV genome, the TBSV genome is only half size of it. It is possible that the relative more number of sRNAs were generated from the 120-nt 35S inducer locus in TBSV genome. Although P19 is a strong silencing suppressor, it could not sequester all of sRNAs. Those non-sequestered sRNAs resulted in incomplete GFP silencing phenotype in TBSV-35S-infected plants.

Alternatively, it could be due to the different actions of HcPro and P19 in suppression of RNA silencing. It is known that VSRs interfere different steps of RNA silencing. In recent publication, HcPro encoded by *tobacco vein banding mosaic virus* (TVBMV) was shown to reduce the level of cytosine methylation in promoter regions of endogenous genes ACD6 and NPR1, which activated the SA pathway and induced defence-related gene expressions (L. Yang *et al.*, 2016). The result suggests that HcPro affects accumulation of vsiRNAs and interfere with RdDM. However, the tombusviral P19 protein prefer to sequester 21 nt siRNAs rather than 24 nt siRNAs, therefore P19 might be less effective in interfering with RdDM.

Therefore, future experiments can increase the size of the inducer sequence to further test whether TuMV vector containing a longer inducer sequence can trigger TGS. Alternatively, a mutated TuMV vector carrying an abrogate HcPro or replacing HcPro

by P19 could be used to test whether HcPro is responsible for the inhibition of ViTGS.

5.3.3 VSRs and RNA virus interfering with plant epigenome

VSRs have been recognised as the pathogenicity factors that are responsible for viral symptoms (Voinnet, 2005). In early studies, it was shown that VSR-transgenic lines displayed developmental defects and growth reduction, similarly to virus infected plants. Some VSRs could inhibit miRNA activities and interfere with endogenous silencing pathways (Kasschau *et al.*, 2003, Chapman *et al.*, 2004). Recently, several papers reported that VSRs could interact with RdDM and alter DNA methylation status of transposable elements (Duan *et al.*, 2012, Ivanov *et al.*, 2016, L. Yang *et al.*, 2016). In addition, it was also found that expressing VSRs 2b encoded by CMV could cause genome-wide reduction of CHH and CHG methylation in 2b-transgenic *Arabidopsis* plants (Zhao *et al.*, 2016).

To further understand the interaction between viral infection and the plant epigenome, the global methylation pattern need to be investigated at whole genome level. By comparing the differential methylation regions (DMRs) among VSR transgenic plants, virus-infected plants, and their progeny, it might be possible to identify genes or certain loci associated with viral-induced hypo- and hyper- methylation. The results will help us to understand virus-induced epigenetic modification in infected plant and can be further applied to future crop breeding.

Chapter 6: Conclusions and future outlook

6.1 The importance of virus-plant interaction research in the context of ensuring global food security

Food security is one of the most significant challenges of the 21st century. In the past 40 years, improvements in pest and disease management have doubled world food production, however, pathogens still claim 10-16% of the global harvest (Strange & Scott, 2005, Chakraborty & Newton, 2011). It is generally accepted that viruses are the most damaging molecular parasites after hyphal pathogens (fungi and oomycetes) (Hull, 2014). There are more than 700 known plant viruses, most of which have very wide host ranges and cause devastating diseases. To overcome viral infections, plants evolved an RNA-based adaptive immune system referred to as RNA silencing (Voinnet, 2001). sRNAs are the central molecules of RNA silencing, which play a fundamental role in gene regulation in eukaryotes. Interestingly, sRNAs are able to target and methylate homologous DNA sequences in the nucleus to induce TGS of target genes. Thus, this mechanism opens up new research aspects to investigate how plant viruses interact with the host epigenome and affect gene expression.

This thesis endeavoured to gain a deeper understanding of virus-induced epigenetic modifications in the infected plants and in their progeny, focussing both on the intracellular molecular mechanism and the external environmental influence. Our findings contribute to better understanding of the role of epigenetics in plant-microbe interactions and generate new knowledge about how to efficiently harness pathogens to modify the epigenome for plant breeding.

6.2 Exploring the molecular mechanism between virus and plant interaction

sRNAs act as molecular postcodes and guide AGO proteins to target nucleic acids. In plants, sRNA-mediated RdDM is involved in genome stability through transposon silencing, mobile signalling for epigenetic gene control and hybrid vigour. TGS has been widely assumed to occur via 24 nt sRNAs with complete homology to the target sequence. Results presented in chapter 3 demonstrate that initiation of RdDM does not require 100% sequence complementarity between the sRNAs and their nuclear target sequences. It was shown that virus-derived sRNAs carrying one or two mismatches to their target sequence (35S promoter) were sufficient to trigger strong TGS of GFP reporter gene through RdDM in transgenic *N. benthamiana* 16c plants. Interestingly, the mismatched sRNA-induced TGS was heritable to the next generation. Furthermore, our data also revealed that symmetric cytosine methylation (CG and CHG) was frequently inherited regardless of the number of mismatches in the sRNA inducer of TGS.

These results demonstrate unexpected flexibility in sRNA-induced transgenerational epigenetic gene modifications, which bring up new aspects to investigate the intimate interaction between invading molecules (transposons and viruses) and the epigenome. In addition, it warrants more careful design and application of novel dsRNA sprays in plant protection to avoid "off-target" effects (Koch *et al.*, 2016, Mitter *et al.*, 2017). Processing of exogenously applied antifungal or antiviral dsRNA *in planta* might result in sRNAs with partial complementarity to promoter sequences, which could induce heritable RdDM and consequently influence the expression of genes controlling agronomic traits. Further work is required to identify the specific nucleases and chromatin modifying complexes associated with virus-induced RdDM and to test whether the targeting rule for sRNA-mediated RdDM differs between endogenous genes and transposons.

6.3 Harnessing virus as a powerful tool for functional genomics and crop improvement

It has been previously demonstrated that RNA silencing is a temperature-dependent RNA degradation mechanism that operates inefficiently at low temperature (Szittya *et al.*, 2003). The rising temperature promotes antiviral silencing, which is frequently associated with attenuated symptoms and with low virus content. VIGS is based on the plant antiviral silencing mechanism, which can also be affected by the external environmental stimuli. However, there was little information available on this topic. Thus, we investigated the effect of environmental factors on the initiation and stability of ViTGS.

Consistent with previous observations, VIGS is a temperature-dependent mechanism. Unlike at ambient temperature where VIGS worked very efficiently, cold treatment inhibited VIGS and delayed the progression of RNA silencing. In contrast, high temperature could efficiently trigger VIGS and rapidly induced silencing phenotypes at the early stage of virus infection. However, there was a significant difference in the maintenance of ViPTGS and ViTGS at high temperature. The former exhibited stronger and persistent silencing phenotype, whereas the latter was greatly inhibited at high temperature. Using RNA-seq, we found that inefficient ViTGS at high temperature was due to the limited production of primary and secondary sRNAs. Unlike ViPTGS, which is associated with a large number of secondary sRNAs to reinforce silencing, ViTGS barely produces secondary sRNAs and this limited spreading of virus-induced DNA methylation to neighbouring cells and consequently prevented epigenetic inheritance of the TGS phenotype.This study provides insight into how environmental cues can affect plant-virus interaction. Furthermore, our data can inform us about how to use VIGS vectors for modulating gene expression and the epigenome, which may be harnessed for inducing stable and heritable epigenetic modifications in crop plants.

Nicotiana benthamiana is an ideal model plant to study RNA silencing and plant-virus interaction, because it a natural *rdr1* mutant which is hypersusceptible to plant viruses (Yang *et al.*, 2004). The line 16c of *N. benthamiana* expressing GFP under constitutive 35S promoter is one of major resource for visualising the mobility and actions of small RNAs, which has been widely used in plant RNA silencing study community. Hence, GFP reporter system in 16c was selected to assess the ViTGS and ViPTGS in this thesis.

However, it has long been known that transgenes do not behave as endogenous genes and transgene responses vary from one transgene locus to another. Moreover, in a previous study, RdDM of target promoter sequences was easily induced in seven endogenous rice genes, but TGS was not observed expect for one gene (Okano *et al.*, 2008). On the other hand, expression of 35S::GFP was strongly suppressed by RdDM-mediated TGS in transgenic rice (Okano *et al.*, 2008).

RdDM-mediated TGS is a promising new plant breeding techniques approach, and TGS induction toward endogenous genes has been reported in Arabidopsis, potato, petunia, tomato, tobacco and rice (Heilersig *et al.*, 2006, Kanazawa *et al.*, 2011, Kon & Yoshikawa, 2014, Bond & Baulcombe, 2015, Kasai *et al.*, 2016, Wakasa *et al.*, 2018). So, it is worth to further investigate whether the results obtained using *N.benthamiana* line 16c can apply to VIGS of endogenous gene. Applying RdDM-mediated TGS in endogenous gene could be useful tool for crop plant improvement.

6.4 The effect of viruses and their pathogenicity factors on the plant epigenome

As a counter defence strategy, plant viruses encode VSRs to protect their genome against antiviral RNA silencing. VSRs are recognised as pathogenicity factors that cause disease or developmental abnormalities. One notable reason for disease symptom is that the antiviral and endogenous silencing pathways share common elements, and VSRs could interfere with these pathways. Indeed, it was shown that

VSRs from multiple viruses could inhibit miRNA activities and cause severe developmental defects in transgenic *Arabidopsis* expressing VSRs (Chapman et al. 2004). However, very little is known about how plant viruses and their VSRs can alter the epigenome and consequently plant gene expression in the infected plants and their progeny.

In chapter 5, I first assessed the ability of VSRs in interfering gene silencing both in transient expression system and in virus-plant system. Using *Agrobacterium*-mediated transient expression, I demonstrated that the VSRs 2b, P19, P21, and HcPro could inhibit both PTGS and TGS by interfering with siRNAs. Furthermore, the ability of VSRs P19 and HcPro to interfere with ViPTGS and ViTGS was assessed in their natural virus background. Our data revealed that RNA viruses carrying strong VSRs could suppress DNA methylation and TGS of target gene in virus infected plants. This is in agreement with previous publications that VSRs may interfere with RdDM via affecting the accumulation of siRNAs (Duan *et al.*, 2012, Yang *et al.*, 2016). In order to gain further insight into virus-induced epigenetic changes in host plants, examining of the DNA methylation status at whole genome level rather than at specific loci has been proposed. Hence, I generated transgenic *Arabidopsis* overexpressing VSRs. These plants showed distinct developmental defects, which suggested that VSRs might alter the plant epigenome and affected gene expression. Further work is required including high throughput sequencing to determine the DNA methylation status at genome-wide scale in those VSRs transgenic plants, virus-infected plants, and their progeny. By comparing the DMRs among those plants, it might be possible to identify genes associated with virus infection and pathogen defence. The findings are expected to reveal fundamental insights into pathogen-induced changes of the epigenome at single nucleotide resolution, the stability of these epigenetic modifications over generations in response to virus infection and its effect on pathogen defence. It may also help us to develop novel strategies in order to breed virus-resistant plants.

6.5 Concluding remarks

This thesis has focussed on exploring the molecular mechanisms of pathogen-induced epigenetic changes in virus-infected plants, and deepened our knowledge about how to harness plant viruses to induce epigenetic modification in crop plants. These insights help us to understand the impact of virus infection on the epigenome of the host plants, and may be used to develop new strategies for crop protection. This will be an important step towards for reducing the crop losses to pathogenic disease.

References

Allen, E., Xie, Z., Gustafson, A. M. and Carrington, J. C. (2005) microRNA-Directed Phasing during Trans-Acting siRNA Biogenesis in Plants, *Cell*, **121**(2), 207–221.

Amarzguioui, M. (2003) Tolerance for mutations and chemical modifications in a siRNA, *Nucleic Acids Research*, **31**(2), 589–595.

Aravin, A. A., Hannon, G. J. and Brennecke, J. (2007) The Piwi-piRNA Pathway Provides an Adaptive Defense in the Transposon Arms Race, *Science*, **318**(5851), 761–764.

Aregger, M., Borah, B. K., Seguin, J., Rajeswaran, R., Gubaeva, E. G., Zvereva, A. S., *et al.* (2012) Primary and Secondary siRNAs in Geminivirus-induced Gene Silencing, *PLoS Pathogens*, **8**(9), e1002941.

Arribas-Hernández, L., Marchais, A., Poulsen, C., Haase, B., Hauptmann, J., Benes, V., *et al.* (2016) The Slicer Activity of ARGONAUTE1 is Required Specifically for the Phasing, Not Production, of Trans-Acting Short Interfering RNAs in Arabidopsis, *The Plant Cell*, **28**(7), tpc.00121.2016.

Axtell, M. J. (2013) Classification and Comparison of Small RNAs from Plants, *Annual Review of Plant Biology*, **64**(1), 137–159.

Azevedo, J., Garcia, D., Pontier, D., Ohnesorge, S., Yu, A., Garcia, S., *et al.* (2010) Argonaute quenching and global changes in Dicer homeostasis caused by a pathogen-encoded GW repeat protein, *Genes & Development*, **24**(9), 904–915.

Bartel, D. P. (2009) MicroRNAs: Target Recognition and Regulatory Functions, *Cell*, 215–233.

Baulcombe, D. (2004) RNA silencing in plants., *Nature*, **431**(7006), 356–63.

Baulcombe, D. C. and Dean, C. (2014) Epigenetic Regulation in Plant Responses to the Environment, *Cold Spring Harbor Perspectives in Biology*, **6**(9), a019471–a019471.

Bernstein, E., Caudy, A. A., Hammond, S. M. and Hannon, G. J. (2001) Role for a bidentate ribonuclease in the initiation step of RNA interference., *Nature*, **409**(6818), 363–6.

Blevins, T., Rajeswaran, R., Shivaprasad, P. V., Beknazariants, D., Si-Ammour, A., Park, H.-S., *et al.* (2006) Four plant Dicers mediate viral small RNA biogenesis and DNA virus induced silencing., *Nucleic acids research*, **34**(21), 6233–46.

Bond, D. M. and Baulcombe, D. C. (2015) Epigenetic transitions leading to heritable, RNA-mediated de novo silencing in *Arabidopsis thaliana*, *Proceedings of the National Academy of Sciences*, **112**(3), 917–922.

Borges, F. and Martienssen, R. A. (2015) The expanding world of small RNAs in plants, *Nature Reviews Molecular Cell Biology*, **16**(12), 727–741.

Borsani, O., Zhu, J., Verslues, P. E., Sunkar, R. and Zhu, J. K. (2005) Endogenous siRNAs derived from a pair of natural cis-antisense transcripts regulate salt tolerance in Arabidopsis, *Cell*, **123**(7), 1279–1291.

Brodersen, P., Sakvarelidze-Achard, L., Bruun-Rasmussen, M., Dunoyer, P., Yamamoto, Y. Y., Sieburth, L., *et al.* (2008) Widespread translational inhibition by plant miRNAs and siRNAs, *Science*, **320**(5880), 1185–1190.

Brodersen, P. and Voinnet, O. (2009) Revisiting the principles of microRNA target recognition and mode of action, *Nature Reviews Molecular Cell Biology*, **10**(2), 141–148.

Buchmann, R. C., Asad, S., Wolf, J. N., Mohannath, G. and Bisaro, D. M. (2009) Geminivirus AL2 and L2 Proteins Suppress Transcriptional Gene Silencing and Cause Genome-Wide Reductions in Cytosine Methylation, *Journal of Virology*, **83**(10), 5005–5013.

Burch-Smith, T. M., Anderson, J. C., Martin, G. B. and Dinesh-Kumar, S. P. (2004) Applications and advantages of virus-induced gene silencing for gene function studies in plants, *The Plant Journal*, **39**(5), 734–746.

Burgyán, J. and Havelda, Z. (2011) Viral suppressors of RNA silencing, *Trends in Plant Science*, **16**(5), 265–272.

Carthew, R. W. and Sontheimer, E. J. (2009) Origins and Mechanisms of miRNAs and siRNAs, *Cell*, **136**(4), 642–655.

Chakraborty, S. and Newton, A. C. (2011) Climate change, plant diseases and food security: An overview, *Plant Pathology*, 2–14.

Chan, S. W.-L. (2004) RNA Silencing Genes Control de Novo DNA Methylation, *Science*, **303**(5662), 1336–1336.

Chapman, E. J., Prokhnevsky, A. I., Gopinath, K., Dolja, V. V. and Carrington, J. C. (2004) Viral RNA silencing suppressors inhibit the microRNA pathway at an intermediate step, *Genes and Development*, **18**(10), 1179–1186.

Chellappan, P., Vanitharani, R., Ogbe, F. and Fauquet, C. M. (2005) Effect of temperature on geminivirus-induced RNA silencing in plants, *Plant Physiology*, **138**(4), 1828–1841.

Chellappan, P., Xia, J., Zhou, X., Gao, S., Zhang, X., Coutino, G., *et al.* (2010) siRNAs from miRNA sites mediate DNA methylation of target genes, *Nucleic Acids Research*, **38**(20), 6883–6894.

Chen, H.-M., Chen, L.-T., Patel, K., Li, Y.-H., Baulcombe, D. C. and Wu, S.-H. (2010) 22-nucleotide RNAs trigger secondary siRNA biogenesis in plants, *Proceedings of the National Academy of Sciences*, **107**(34), 15269–15274.

Chen, H.-M., Li, Y.-H. and Wu, S.-H. (2007) Bioinformatic prediction and experimental validation of a microRNA-directed tandem trans-acting siRNA cascade in Arabidopsis, *Proceedings of the National Academy of Sciences*, **104**(9), 3318–3323.

Chen, W., Zhang, X., Fan, Y., Li, B., Ryabov, E., Shi, N., *et al.* (2018) A Genetic Network for Systemic RNA Silencing in Plants, *Plant Physiology*, **176**(4), 2700–2719.

Cheo, P. C. (1971) Effect in different plant species of continuous light and dark treatment on tobacco mosaic virus replicating capacity, *Virology*, **46**(2), 256–265.

Creasey, K. M., Zhai, J., Borges, F., Van Ex, F., Regulski, M., Meyers, B. C., *et al.* (2014) MiRNAs trigger widespread epigenetically activated siRNAs from transposons in Arabidopsis, *Nature*, **508**(7496), 411–415.

Cuerda-Gil, D. and Slotkin, R. K. (2016) Non-canonical RNA-directed DNA methylation, *Nature Plants*, **2**(11), 16163.

Cuperus, J. T., Carbonell, A., Fahlgren, N., Garcia-Ruiz, H., Burke, R. T., Takeda, A., *et al.* (2010) Unique functionality of 22-nt miRNAs in triggering RDR6-dependent siRNA biogenesis from target transcripts in Arabidopsis, *Nature Structural and Molecular Biology*, **17**(8), 997–1003.

Deleris, A., Gallago-Bartolome, J., Bao, J., Kasschau, K. D., Carrington, J. C. and Voinnet,

O. (2006) Hierarchical action and inhibition of plant dicer-like proteins in antiviral defense, *Science*, **313**(5783), 68–71.

Diéguez, M. J., Vaucheret, H., Paszkowski, J. and Mittelsten Scheid, O. (1998) Cytosine methylation at CG and CNG sites is not a prerequisite for the initiation of transcriptional gene silencing in plants, but it is required for its maintenance, *Molecular and General Genetics*.

Duan, C.-G., Fang, Y.-Y., Zhou, B.-J., Zhao, J.-H., Hou, W.-N., Zhu, H., *et al.* (2012) Suppression of Arabidopsis ARGONAUTE1-Mediated Slicing, Transgene-Induced RNA Silencing, and DNA Methylation by Distinct Domains of the Cucumber mosaic virus 2b Protein, *The Plant Cell*, **24**(1), 259–274.

Dunoyer, P., Melnyk, C., Molnar, A. and Keith Slotkin, R. (2013) Plant mobile small RNAs, *Cold Spring Harbor Perspectives in Biology*, **5**(7), 3–6.

Dunoyer, P., Himber, C. and Voinnet, O. (2005) DICER-LIKE 4 is required for RNA interference and produces the 21-nucleotide small interfering RNA component of the plant cell-to-cell silencing signal, *Nature Genetics*, **37**(12), 1356–1360.

Fei, Q., Xia, R. and Meyers, B. C. (2013) Phased, Secondary, Small Interfering RNAs in Posttranscriptional Regulatory Networks, *The Plant Cell*, **25**(7), 2400–2415.

Fultz, D., Choudury, S. G. and Slotkin, R. K. (2015) Silencing of active transposable elements in plants, *Current Opinion in Plant Biology*, **27**, 67–76.

Fusaro, A. F., Matthew, L., Smith, N. A., Curtin, S. J., Dedic-Hagan, J., Ellacott, G. A., *et al.* (2006) RNA interference-inducing hairpin RNAs in plants act through the viral defence pathway, *EMBO Reports*, **7**(11), 1168–1175.

Garcia-Ruiz, H., Takeda, A., Chapman, E. J., Sullivan, C. M., Fahlgren, N., Brempelis, K. J., *et al.* (2010) Arabidopsis RNA-Dependent RNA Polymerases and Dicer-Like Proteins in Antiviral Defense and Small Interfering RNA Biogenesis during Turnip Mosaic Virus Infection, *The Plant Cell*, **22**(2), 481–496.

Garcia-Ruiz, H., Carbonell, A., Hoyer, J. S., Fahlgren, N., Gilbert, K. B., Takeda, A., *et al.* (2015) Roles and Programming of Arabidopsis ARGONAUTE Proteins during Turnip Mosaic Virus Infection, *PLoS Pathogens*, **11**(3), 1–27.

Gerik, J. S. (1990) Etiology of Tomato Plant Decline in the California Desert, *Phytopathology*, 1352.

Giner, A., Lakatos, L., García-Chapa, M., López-Moya, J. J. and Burgyán, J. (2010) Viral protein inhibits RISC activity by argonaute binding through conserved WG/GW motifs, *PLoS Pathogens*, **6**(7), 1–13.

Glick, E., Zrachya, A., Levy, Y., Mett, A., Gidoni, D., Belausov, E., *et al.* (2008) Interaction with host SGS3 is required for suppression of RNA silencing by tomato yellow leaf curl virus V2 protein, *Proceedings of the National Academy of Sciences*, **105**(1), 157–161.

Goto, K., Kobori, T., Kosaka, Y., Natsuaki, T. and Masuta, C. (2007) Characterization of silencing suppressor 2b of cucumber mosaic virus based on examination of its small RNA-binding abilities, *Plant and Cell Physiology*, **48**(7), 1050–1060.

Haas, G., Azevedo, J., Moissiard, G., Geldreich, A., Himber, C., Bureau, M., *et al.* (2008) Nuclear import of CaMV P6 is required for infection and suppression of the RNA silencing factor DRB4, *The EMBO Journal*, **27**(15), 2102–2112.

Hajeri, S., Killiny, N., El-Mohtar, C., Dawson, W. O. and Gowda, S. (2014) Citrus tristeza virus-based RNAi in citrus plants induces gene silencing in Diaphorina citri, a phloem-sap sucking insect vector of citrus greening disease (Huanglongbing), *Journal of Biotechnology*, **176**(1), 42–49.

Hamera, S., Song, X., Su, L., Chen, X. and Fang, R. (2012) Cucumber mosaic virus suppressor 2b binds to AGO4-related small RNAs and impairs AGO4 activities, *The Plant Journal*, **69**(1), 104–115.

Hamilton, A. J. and Baulcombe, D. C. (1999) A species of small antisense RNA in posttranscriptional gene silencing in plants, *Science*, **286**(5441), 950–952.

Härtl, K., Kalinowski, G., Hoffmann, T., Preuss, A. and Schwab, W. (2017) RNAi-mediated endogene silencing in strawberry fruit: detection of primary and secondary siRNAs by deep sequencing, *Plant Biotechnology Journal*, **15**(5), 658–668.

Havecker, E. R., Wallbridge, L. M., Hardcastle, T. J., Bush, M. S., Kelly, K. A., Dunn, R. M., *et al.* (2010) The Arabidopsis RNA-Directed DNA Methylation Argonautes

Functionally Diverge Based on Their Expression and Interaction with Target Loci, *The Plant Cell*, **22**(2), 321–334.

Heilersig, B. H. J. B., Loonen, A. E. H. M., Janssen, E. M., Wolters, A. M. A. and Visser, R. G. F. (2006) Efficiency of transcriptional gene silencing of GBSSI in potato depends on the promoter region that is used in an inverted repeat, *Molecular Genetics and Genomics*.

Helms, K. (1965) Role of temperature and light in lesion development of tobacco mosaic virus.

Herr, A. J., Molnar, A., Jones, A. and Baulcombe, D. C. (2006) Defective RNA processing enhances RNA silencing and influences flowering of Arabidopsis, *Proceedings of the National Academy of Sciences*, **103**(41), 14994–15001.

Hetzl, J., Foerster, A. M., Raidl, G. and Scheid, O. M. (2007) CyMATE: a new tool for methylation analysis of plant genomic DNA after bisulphite sequencing, *The Plant Journal*, **51**(3), 526–536.

Howell, M. D., Fahlgren, N., Chapman, E. J., Cumbie, J. S., Sullivan, C. M., Givan, S. A., *et al.* (2007) Genome-wide analysis of the RNA-DEPENDENT RNA POLYMERASE6/DICER-LIKE4 pathway in Arabidopsis reveals dependency on miRNA- and tasiRNA-directed targeting., *The Plant Cell*, **19**(3), 926–42.

Hull, R. (2014) *Plant Virology*. Fifth.

Incarbone, M. and Dunoyer, P. (2013) RNA silencing and its suppression: Novel insights from in planta analyses, *Trends in Plant Science*, **18**(7), 382–392.

Ivanov, K. I., Eskelin, K., Bašić, M., De, S., Lõhmus, A., Varjosalo, M., *et al.* (2016) Molecular insights into the function of the viral RNA silencing suppressor HCPro, *The Plant Journal*, **85**(1), 30–45.

Johnson, J. (1922) The relation of air temperature to the mosaic disease of potatoes and other plants, *Phytopathology*, **12**, 438–440.

Johnson, L. M., Du, J., Hale, C. J., Bischof, S., Feng, S., Chodavarapu, R. K., *et al.* (2014) SRA- and SET-domain-containing proteins link RNA polymerase V occupancy to DNA methylation, *Nature*, **507**(7490), 124–128.

Jones, L., Hamilton, A. J., Voinnet, O., Thomas, C. L., Maule, A. J. and Baulcombe, D. C. (1999) RNA–DNA Interactions and DNA Methylation in Post-Transcriptional Gene Silencing, *The Plant Cell*, **11**(12), 2291–2301.

Jones, L., Ratcliff, F. and Baulcombe, D. C. (2001) RNA-directed transcriptional gene silencing in plants can be inherited independently of the RNA trigger and requires Met1 for maintenance, *Current Biology*, **11**(10), 747–757.

Jouannet, V., Moreno, A. B., Elmayan, T., Vaucheret, H., Crespi, M. D. and Maizel, A. (2012) Cytoplasmic Arabidopsis AGO7 accumulates in membrane-associated siRNA bodies and is required for ta-siRNA biogenesis., *The EMBO journal*, **31**(7), 1704–13.

Kanazawa, A., Inaba, J. I., Shimura, H., Otagaki, S., Tsukahara, S., Matsuzawa, A., *et al.* (2011) Virus-mediated efficient induction of epigenetic modifications of endogenous genes with phenotypic changes in plants, *Plant Journal*, **65**(1), 156–168.

Kasai, A., Bai, S., Hojo, H. and Harada, T. (2016) Epigenome editing of potato by grafting using transgenic tobacco as siRNA donor, *PLoS ONE*.

Kasschau, K. D., Xie, Z., Allen, E., Llave, C., Chapman, E. J., Krizan, K. A., *et al.* (2003) P1/HC-Pro, a viral suppressor of RNA silencing, interferes with Arabidopsis development and miRNA function, *Developmental Cell*.

Khraiwesh, B., Arif, M. A., Seumel, G. I., Ossowski, S., Weigel, D., Reski, R., *et al.* (2010) Transcriptional Control of Gene Expression by MicroRNAs, *Cell*, **140**(1), 111–122.

Koch, A., Biedenkopf, D., Furch, A., Weber, L., Rossbach, O., Abdellatef, E., *et al.* (2016) An RNAi-Based Control of Fusarium graminearum Infections Through Spraying of Long dsRNAs Involves a Plant Passage and Is Controlled by the Fungal Silencing Machinery., *PLoS pathogens*, **12**(10), e1005901.

Kon, T. and Yoshikawa, N. (2014) Induction and maintenance of DNA methylation in plant promoter sequences by apple latent spherical virus-induced transcriptional gene silencing, **5**(November), 1–11.

Kotakis, C., Vrettos, N., Kotsis, D., Tsagris, M., Kotzabasis, K. and Kalantidis, K. (2010) Light intensity affects RNA silencing of a transgene in Nicotiana benthamiana plants., *BMC plant biology*, **10**(1), 220.

Lahmy, S., Pontier, D., Bies-Etheve, N., Laudié, M., Feng, S., Jobet, E., *et al.* (2016) Evidence for ARGONAUTE4–DNA interactions in RNA-directed DNA methylation in plants, *Genes and Development*.

Lakatos, L., Csorba, T., Pantaleo, V., Chapman, E. J., Carrington, J. C., Liu, Y.-P., *et al.* (2006) Small RNA binding is a common strategy to suppress RNA silencing by several viral suppressors., *The EMBO journal*, **25**(12), 2768–80.

Law, J. A. and Jacobsen, S. E. (2010) Establishing, maintaining and modifying DNA methylation patterns in plants and animals, *Nature Reviews Genetics*, **11**(3), 204–220.

Liu, N., Xie, K., Jia, Q., Zhao, J., Chen, T., Li, H., *et al.* (2016) *Foxtail Mosaic Virus* - Induced Gene Silencing in Monocot Plants, *Plant Physiology*, **171**(3), 1801–1807.

Lu, J., Zhang, C., Baulcombe, D. C. and Chen, Z. J. (2012) Maternal siRNAs as regulators of parental genome imbalance and gene expression in endosperm of Arabidopsis seeds, *Proceedings of the National Academy of Sciences*, **109**(14), 5529–5534.

MacFarlane, S. A. (1999) Molecular biology of the tobraviruses, *Journal of General Virology*, **80**(11), 2799–2807.

Mallory, A. C., Reinhart, B. J., Jones-Rhoades, M. W., Tang, G., Zamore, P. D., Barton, M. K., *et al.* (2004) MicroRNA control of PHABULOSA in leaf development: importance of pairing to the microRNA 5′ region, *The EMBO Journal*, **23**(16), 3356–3364.

Mallory, A. C. and Vaucheret, H. (2009) ARGONAUTE 1 homeostasis invokes the coordinate action of the microRNA and siRNA pathways., *EMBO Reports*, **10**(5), 521–6.

Manavella, P. A., Koenig, D. and Weigel, D. (2012) Plant secondary siRNA production determined by microRNA-duplex structure, *Proceedings of the National Academy of Sciences*, **109**(7), 2461–2466.

Manfre, a, Glenn, M., Nuñez, a, Moreau, R. a and Dardick, C. (2011) Light quantity and photosystem function mediate host susceptibility to Turnip mosaic virus via a salicylic acid-independent mechanism., *Molecular plant-microbe interactions : MPMI*, **24**(3), 315–327.

Marathe, R., Smith, T. H., Anandalakshmi, R., Bowman, L. H., Fagard, M., Mourrain, P., *et*

al. (2000) Plant viral suppressors of post-transcriptional silencing do not suppress transcriptional silencing, *Plant Journal*.

Marí-Ordóñez, A., Marchais, A., Etcheverry, M., Martin, A., Colot, V. and Voinnet, O. (2013) Reconstructing de novo silencing of an active plant retrotransposon, *Nature Genetics*, **45**(9), 1029–1039.

Matzke, M. a and Mosher, R. a (2014) RNA-directed DNA methylation: an epigenetic pathway of increasing complexity., *Nature reviews. Genetics*, **15**(6), 394–408.

McCue, A. D., Panda, K., Nuthikattu, S., Choudury, S. G., Thomas, E. N. and Slotkin, R. K. (2015) ARGONAUTE 6 bridges transposable element mRNA-derived siRNAs to the establishment of DNA methylation, *The EMBO Journal*, **34**(1), 20–35.

McHale, M., Eamens, A. L., Finnegan, E. J. and Waterhouse, P. M. (2013) A 22-nt artificial microRNA mediates widespread RNA silencing in Arabidopsis, *The Plant Journal*, **76**(3), 519–529.

Melnyk, C. W., Molnar, A., Bassett, A. and Baulcombe, D. C. (2011) Mobile 24 nt small RNAs direct transcriptional gene silencing in the root meristems of Arabidopsis thaliana, *Current Biology*, **21**(19), 1678–1683.

Merai, Z., Kerenyi, Z., Molnar, A., Barta, E., Valoczi, A., Bisztray, G., *et al.* (2005) Aureusvirus P14 Is an Efficient RNA Silencing Suppressor That Binds Double-Stranded RNAs without Size Specificity, *Journal of Virology*, **79**(11), 7217–7226.

Merai, Z., Kerenyi, Z., Kertesz, S., Magna, M., Lakatos, L. and Silhavy, D. (2006) Double-Stranded RNA Binding May Be a General Plant RNA Viral Strategy To Suppress RNA Silencing, *Journal of Virology*, **80**(12), 5747–5756.

Mette, M. F., Matzke, A. J. M. and Matzke, M. A. (2001) Resistance of RNA-mediated TGS to HC-Pro, a viral suppressor of PTGS, suggests alternative pathways for dsRNA processing, *Current Biology*.

Mitter, N., Worrall, E. A., Robinson, K. E., Li, P., Jain, R. G., Taochy, C., *et al.* (2017) Clay nanosheets for topical delivery of RNAi for sustained protection against plant viruses, *Nature Plants*, **3**(2), 16207.

Mlotshwa, S., Pruss, G. J., Peragine, A., Endres, M. W., Li, J., Chen, X., *et al.* (2008) Dicer-

like2 plays a primary role in transitive silencing of transgenes in Arabidopsis, *PLoS ONE*, **3**(3).

Molnar, A., Csorba, T., Lakatos, L., Varallyay, E., Lacomme, C. and Burgyan, J. (2005) Plant Virus-Derived Small Interfering RNAs Originate Predominantly from Highly Structured Single-Stranded Viral RNAs, *Journal of Virology*, **79**(12), 7812–7818.

Molnar, A., Melnyk, C. W., Bassett, A., Hardcastle, T. J., Dunn, R. and Baulcombe, D. C. (2010) Small silencing RNAs in plants are mobile and direct epigenetic modification in recipient cells, *Science*, **328**(5980), 872–875.

Molnar, A., Melnyk, C. and Baulcombe, D. C. (2011) Silencing signals in plants: a long journey for small RNAs, *Genome Biology*, **12**(1), 215.

Montgomery, T. A., Howell, M. D., Cuperus, J. T., Li, D., Hansen, J. E., Alexander, A. L., *et al.* (2008) Specificity of ARGONAUTE7-miR390 Interaction and Dual Functionality in TAS3 Trans-Acting siRNA Formation, *Cell*, **133**(1), 128–141.

Nuthikattu, S., McCue, A. D., Panda, K., Fultz, D., DeFraia, C., Thomas, E. N., *et al.* (2013) The Initiation of Epigenetic Silencing of Active Transposable Elements Is Triggered by RDR6 and 21-22 Nucleotide Small Interfering RNAs, *Plant Physiology*, **162**(1), 116–131.

Okano, Y., Senshu, H., Hashimoto, M., Neriya, Y., Netsu, O., Minato, N., *et al.* (2014) In Planta Recognition of a Double-Stranded RNA Synthesis Protein Complex by a Potexviral RNA Silencing Suppressor, *The Plant Cell*, **26**(5), 2168–2183.

Okano, Y., Miki, D. and Shimamoto, K. (2008) Small interfering RNA (siRNA) targeting of endogenous promoters induces DNA methylation, but not necessarily gene silencing, in rice, *Plant Journal*.

Otagaki, S., Kawai, M., Masuta, C. and Kanazawa, A. (2011) Size and positional effects of promoter RNA segments on virus-induced RNA-directed DNA methylation and transcriptional gene silencing, *Epigenetics*, **6**(6), 681–691.

Parent, J.-S., Bouteiller, N., Elmayan, T. and Vaucheret, H. (2015) Respective contributions of Arabidopsis DCL2 and DCL4 to RNA silencing, *The Plant Journal*, **81**(2), 223–232.

Pedersen, I. and David, M. (2008) MicroRNAs in the immune response, *Cytokine*, 391–394.

Peragine, A., Yoshikawa, M., Wu, G., Albrecht, H. L. and Poethig, R. S. (2004) SGS3 and SGS2/SDE1/RDR6 are required for juvenile development and the production of trans-acting siRNAs in Arabidopsis, *Genes and Development*, **18**(19), 2368–2379.

Petersen, B. O. and Albrechtsen, M. (2005) Evidence implying only unprimed RdRP activity during transitive gene silencing in plants, *Plant Molecular Biology*, **58**(4), 575–583.

Pflieger, S., Blanchet, S., Camborde, L., Drugeon, G., Rousseau, A., Noizet, M., *et al.* (2008) Efficient virus-induced gene silencing in Arabidopsis using a 'one-step'TYMV-derived vector, *The Plant Journal*, **56**(4), 678–690.

Pignatta, D., Kumar, P., Turina, M., Dandekar, A. and Falk, B. W. (2007) Quantitative Analysis of Efficient Endogenous Gene Silencing in Nicotiana benthamiana Plants Using Tomato bushy stunt virus Vectors That Retain the Capsid Protein Gene, *Molecular Plant-Microbe Interactions*, **20**(6), 609–618.

Pontier, D., Picart, C., Roudier, F., Garcia, D., Lahmy, S., Azevedo, J., *et al.* (2012) NERD, a Plant-Specific GW Protein, Defines an Additional RNAi-Dependent Chromatin-Based Pathway in Arabidopsis, *Molecular Cell*, **48**(1), 121–132.

Pooggin, M. M. (2013) How can plant DNA viruses evade siRNA-directed DNA methylation and silencing?, *International Journal of Molecular Sciences*, 15233–15259.

Pumplin, N. and Voinnet, O. (2013) RNA silencing suppression by plant pathogens: Defence, counter-defence and counter-counter-defence, *Nature Reviews Microbiology*, **11**(11), 745–760.

Pyott, D. E. and Molnar, A. (2015) Going mobile: Non-cell-autonomous small RNAs shape the genetic landscape of plants, *Plant Biotechnology Journal*, **13**(3), 306–318.

Qiu, W., Park, J.-W. and Scholthof, H. B. (2002) Tombusvirus P19-mediated suppression of virus-induced gene silencing is controlled by genetic and dosage features that influence pathogenicity., *Molecular plant-microbe interactions : MPMI*, **15**(3), 269–280.

Raja, P., Wolf, J. N. and Bisaro, D. M. (2010) RNA silencing directed against geminiviruses: Post-transcriptional and epigenetic components, *Biochimica et Biophysica Acta (BBA) - Gene Regulatory Mechanisms*, **1799**(3–4), 337–351.

Reinhart, B. J., Weinstein, E. G., Rhoades, M. W., Bartel, B. and Bartel, D. P. (2002) MicroRNAs in plants, *Genes and Development*, **16**(13), 1616–1626.

Ruiz, M. T., Voinnet, O. and Baulcombe, D. C. (1998) Initiation and Maintenance of Virus-Induced Gene Silencing, *The Plant Cell*, **10**(6), 937.

Scholthof, H. B. (1993) The Capsid Protein Gene of Tomato Bushy Stunt Virus Is Dispensable for Systemic Movement and Can Be Replaced for Localized Expression of Foreign Genes, *Molecular Plant-Microbe Interactions*, 309.

Schott, G., Mari-Ordonez, A., Himber, C., Alioua, A., Voinnet, O. and Dunoyer, P. (2012) Differential effects of viral silencing suppressors on siRNA and miRNA loading support the existence of two distinct cellular pools of ARGONAUTE1, *The EMBO Journal*, **31**(11), 2553–2565.

Senthil-Kumar, M., Rame Gowda, H. V., Hema, R., Mysore, K. S. and Udayakumar, M. (2008) Virus-induced gene silencing and its application in characterizing genes involved in water-deficit-stress tolerance, *Journal of Plant Physiology*, **165**(13), 1404–1421.

Senthil-Kumar, M. and Mysore, K. S. (2011) New dimensions for VIGS in plant functional genomics, *Trends in Plant Science*, **16**(12), 656–665.

Senthil-Kumar, M. and Mysore, K. S. (2014) Tobacco rattle virus-based virus-induced gene silencing in Nicotiana benthamiana., *Nature protocols*, **9**(7), 1549–62.

Shivaprasad, P. V., Dunn, R. M., Santos, B. A. C. M., Bassett, A. and Baulcombe, D. C. (2012) Extraordinary transgressive phenotypes of hybrid tomato are influenced by epigenetics and small silencing RNAs, *The EMBO Journal*, **31**(2), 257–266.

Song, X., Li, P., Zhai, J., Zhou, M., Ma, L., Liu, B., *et al.* (2012) Roles of DCL4 and DCL3b in rice phased small RNA biogenesis, *The Plant Journal*, **69**(3), 462–474.

Strange, R. N. and Scott, P. R. (2005) Plant disease: a threat to global food security., *Annual review of phytopathology*, **43**, 83–116.

Sunkar, R., Chinnusamy, V., Zhu, J. and Zhu, J.-K. (2007) Small RNAs as big players in plant abiotic stress responses and nutrient deprivation, *Trends in Plant Science*, **12**(7), 301–309.

Szittya, G., Silhavy, D., Molnár, A., Havelda, Z., Lovas, Á., Lakatos, L., *et al.* (2003) Low temperature inhibits RNA silencing-mediated defence by the control of siRNA generation, *EMBO Journal*, **22**(3), 633–640.

Szittya, G. (2003) Low temperature inhibits RNA silencing-mediated defence by the control of siRNA generation, *The EMBO Journal*, **22**(3), 633–640.

Taochy, C., Gursanscky, N. R., Cao, J., Fletcher, S. J., Dressel, U., Mitter, N., *et al.* (2017) A Genetic Screen for Impaired Systemic RNAi Highlights the Crucial Role of DICER-LIKE 2, *Plant Physiology*, **175**(3), 1424–1437.

Thierry, D. and Vaucheret, H. (1996) Sequence homology requirements for transcriptional silencing of 35S transgenes and post-transcriptional silencing of nitrite reductase (trans)genes by the tobacco 271 locus, *Plant Molecular Biology*.

Del Toro, F., Tenllado, F., Chung, B.-N. and Canto, T. (2014) A procedure for the transient expression of genes by agroinfiltration above the permissive threshold to study temperature-sensitive processes in plant-pathogen interactions., *Molecular plant pathology*, **15**(8), 848–57.

Vaistij, F., Jones, L. and Baulcombe, D. (2013) Spreading of RNA Targeting and DNA Methylation in RNA Silencing Requires Transcription of the Target Gene and a Putative RNA-Dependent RNA Polymerase, *The Plant Cell*, **14**(4), 857–867.

Vargason, J. M., Szittya, G., Burgyán, J. and Tanaka Hall, T. M. (2003) Size Selective Recognition of siRNA by an RNA Silencing Suppressor, *Cell*, **115**(7), 799–811.

Vaucheret, H., Vazquez, F., Crété, P. and Bartel, D. P. (2004) The action of ARGONAUTE1 in the miRNA pathway and its regulation by the miRNA pathway are crucial for plant development., *Genes & development*, **18**(10), 1187–97.

Vazquez, F., Vaucheret, H., Rajagopalan, R., Lepers, C., Gasciolli, V., Mallory, A. C., *et al.* (2004) Endogenous trans-acting siRNAs regulate the accumulation of arabidopsis mRNAs, *Molecular Cell*, **16**(1), 69–79.

Vazquez, F., Blevins, T., Ailhas, J., Boller, T. and Meins, F. (2008) Evolution of Arabidopsis MIR genes generates novel microRNA classes, *Nucleic Acids Research*, **36**(20), 6429–6438.

Voinnet, O. (2001) RNA silencing as a plant immune system against viruses, *Trends in Genetics*, 449–459.

Voinnet, O. (2005) Induction and suppression of RNA silencing: insights from viral infections, *Nature Reviews Genetics*, **6**(3), 206–220.

Voinnet, O. (2008) Use, tolerance and avoidance of amplified RNA silencing by plants, *Trends in Plant Science*, **13**(7), 317–328.

Voinnet, O. (2009) Origin, Biogenesis, and Activity of Plant MicroRNAs, *Cell*, **136**(4), 669–687.

Wakasa, Y., Kawakatsu, T., Harada, T. and Takaiwa, F. (2018) Transgene-independent heredity of RdDM-mediated transcriptional gene silencing of endogenous genes in rice, *Plant Biotechnology Journal*, 0–2.

Walsh, J. a and Jenner, C. E. (2002) Turnip mosaic virus and the quest for durable resistance., *Molecular plant pathology*, **3**(5), 289–300.

Wang, X.-B., Wu, Q., Ito, T., Cillo, F., Li, W.-X., Chen, X., *et al.* (2010) RNAi-mediated viral immunity requires amplification of virus-derived siRNAs in Arabidopsis thaliana, *Proceedings of the National Academy of Sciences*, **107**(1), 484–489.

Wang, X., Weigel, D. and Smith, L. M. (2013) Transposon Variants and Their Effects on Gene Expression in Arabidopsis, *PLoS Genetics*, **9**(2), e1003255.

Wassenegger, M., Heimes, S., Riedel, L. and Sänger, H. L. (1994) RNA-directed de novo methylation of genomic sequences in plants, *Cell*, **76**(3), 567–576.

Waterhouse, P. M. and Helliwell, C. A. (2003) Exploring plant genomes by RNA-induced gene silencing, *Nature Reviews Genetics*, **4**(1), 29–38.

Wendte, J. M. and Pikaard, C. S. (2017) The RNAs of RNA-directed DNA methylation, *Biochimica et Biophysica Acta (BBA) - Gene Regulatory Mechanisms*, **1860**(1), 140–148.

Wierzbicki, A. T., Ream, T. S., Haag, J. R. and Pikaard, C. S. (2009) RNA polymerase v transcription guides ARGONAUTE4 to chromatin, *Nature Genetics*, **41**(5), 630–634.

Wierzbicki, A. T., Cocklin, R., Mayampurath, A., Lister, R., Jordan Rowley, M., Gregory, B. D., *et al.* (2012) Spatial and functional relationships among Pol V-associated loci, Pol

IV-dependent siRNAs, and cytosine methylation in the Arabidopsis epigenome, *Genes and Development*, **26**(16), 1825–1836.

Wierzbicki, A. T., Haag, J. R. and Pikaard, C. S. (2008) Noncoding Transcription by RNA Polymerase Pol IVb/Pol V Mediates Transcriptional Silencing of Overlapping and Adjacent Genes, *Cell*, **135**(4), 635–648.

Wu, L., Zhou, H., Zhang, Q., Zhang, J., Ni, F., Liu, C., *et al.* (2010) DNA Methylation Mediated by a MicroRNA Pathway, *Molecular Cell*, **38**(3), 465–475.

Wu, L., Mao, L. and Qi, Y. (2012) Roles of DICER-LIKE and ARGONAUTE Proteins in TAS-Derived Small Interfering RNA-Triggered DNA Methylation, *Plant Physiology*, **160**(2), 990–999.

Xia, R., Zhu, H., An, Y., Beers, E. P. and Liu, Z. (2012) Apple miRNAs and tasiRNAs with novel regulatory networks, *Genome Biology*, **13**(6), R47.

Yang, D. L., Zhang, G., Tang, K., Li, J., Yang, L., Huang, H., *et al.* (2016) Dicer-independent RNA-directed DNA methylation in Arabidopsis, *Cell Research*, **26**(1), 66–82.

Yang, L., Xu, Y., Liu, Y., Meng, D., Jin, T. and Zhou, X. (2016) HC-Pro viral suppressor from tobacco vein banding mosaic virus interferes with DNA methylation and activates the salicylic acid pathway., *Virology*, **497**, 244–250.

Yang, S.-J., Carter, S. A., Cole, A. B., Cheng, N.-H. and Nelson, R. S. (2004) A natural variant of a host RNA-dependent RNA polymerase is associated with increased susceptibility to viruses by Nicotiana benthamiana, *Proceedings of the National Academy of Sciences*.

Yang, X., Xie, Y., Raja, P., Li, S., Wolf, J. N., Shen, Q., *et al.* (2011) Suppression of Methylation-Mediated Transcriptional Gene Silencing by βC1-SAHH Protein Interaction during Geminivirus-Betasatellite Infection, *PLoS Pathogens*, **7**(10), e1002329.

Ye, K., Malinina, L. and Patel, D. J. (2003) Recognition of small interfering RNA by a viral suppressor of RNA silencing, *Nature*, **426**(6968), 874–878.

Ye, R., Chen, Z., Lian, B., Rowley, M. J., Xia, N., Chai, J., *et al.* (2016) A Dicer-

Independent Route for Biogenesis of siRNAs that Direct DNA Methylation in Arabidopsis, *Molecular Cell*, **61**(2), 222–235.

Yoshikawa, M., Peragine, A., Mee, Y. P. and Poethig, R. S. (2005) A pathway for the biogenesis of trans-acting siRNAs in Arabidopsis, *Genes and Development*, **19**(18), 2164–2175.

Yuan, C., Li, C., Yan, L., Jackson, A. O., Liu, Z., Han, C., *et al.* (2011) A high throughput barley stripe mosaic virus vector for virus induced gene silencing in monocots and dicots, *PLoS ONE*, **6**(10), e26468.

Zhai, J., Jeong, D. H., de Paoli, E., Park, S., Rosen, B. D., Li, Y., *et al.* (2011) MicroRNAs as master regulators of the plant NB-LRR defense gene family via the production of phased, trans-acting siRNAs, *Genes and Development*, **25**(23), 2540–2553.

Zhai, J., Zhang, H., Arikit, S., Huang, K., Nan, G.-L., Walbot, V., *et al.* (2015) Spatiotemporally dynamic, cell-type–dependent premeiotic and meiotic phasiRNAs in maize anthers, *Proceedings of the National Academy of Sciences*, **112**(10), 3146–3151.

Zhang, C., Bradshaw, J. D., Whitham, S. A. and Hill, J. H. (2010) The Development of an Efficient Multipurpose Bean Pod Mottle Virus Viral Vector Set for Foreign Gene Expression and RNA Silencing, *Plant Physiology*, **153**(1), 52–65.

Zhang, X., Yuan, Y. R., Pei, Y., Lin, S. S., Tuschl, T., Patel, D. J., *et al.* (2006) Cucumber mosaic virus-encoded 2b suppressor inhibits Arabidopsis Argonaute1 cleavage activity to counter plant defense, *Genes and Development*, **20**(23), 3255–3268.

Zhao, J.-H., Fang, Y.-Y., Duan, C.-G., Fang, R.-X., Ding, S.-W. and Guo, H.-S. (2016) Genome-wide identification of endogenous RNA-directed DNA methylation loci associated with abundant 21-nucleotide siRNAs in Arabidopsis., *Scientific Reports*, **6**(1), 36247.

Zhong, S.-H., Liu, J.-Z., Jin, H., Lin, L., Li, Q., Chen, Y., *et al.* (2013) Warm temperatures induce transgenerational epigenetic release of RNA silencing by inhibiting siRNA biogenesis in Arabidopsis., *Proceedings of the National Academy of Sciences of the United States of America*, **110**(22), 9171–6.